STATUS OF THESIS

Title of thesis	STUDY OF HYDRODYNAMIC PROPERTIES OF SWIRLING FLUIDIZED BED

I VINOD KUMAR VENKITESWARAN

hereby allow my thesis to be placed at the Information Resource Center (IRC) of Universiti Teknologi PETRONAS (UTP) with the following conditions:

1. The thesis becomes the property of UTP
2. The IRC of UTP may make copies of the thesis for academic purposes only.
3. This thesis is classified as

☐ Confidential

☒ Non-confidential

If this thesis is confidential, please state the reason:

_____
_____
_____

The contents of the thesis will remain confidential for _____ years.

Remarks on disclosure:

_____
_____
_____

Endorsed by

_____ _____

Signature of Author Signature of Supervisor

Permanent address: Vaikom, Kerala , India.

Name of Supervisor
Assoc. Prof. Ir. Dr. Shaharin A. Sulaiman

Date : _____ Date : _____

UNIVERSITI TEKNOLOGI PETRONAS

STUDY OF HYDRODYNAMIC PROPERTIES OF SWIRLING FLUIDIZED BED

by

VINOD KUMAR VENKITESWARAN

The undersigned certify that they have read, and recommend to the Postgraduate Studies Programme for acceptance this thesis for the fulfillment of the requirements for the degree stated.

Signature: _____

Main Supervisor: Assoc. Prof. Ir. Dr. Shaharin A. Sulaiman

Signature: _____

Co-Supervisor: _____

Signature: _____

Head of Department: Assoc. Prof. Ir. Dr. Masri B Baharom

Date: _____

STUDY OF HYDRODYNAMIC PROPERTIES OF SWIRLING FLUIDIZED BED

by

VINOD KUMAR VENKITESWARAN

A Thesis

Submitted to the Postgraduate Studies Programme

as a Requirement for the Degree of

DOCTOR OF PHILOSOPHY

DEPARTMENT OF MECHANICAL ENGINEERING

UNIVERSITI TEKNOLOGI PETRONAS

BANDAR SERI ISKANDAR,

PERAK

FEBRUARY 2014

DECLARATION OF THESIS

Title of thesis | STUDY OF HYDRODYNAMIC PROPERTIES OF SWIRLING FLUIDIZED BED

I VINOD KUMAR VENKITESWARAN

hereby declare that the thesis is based on my original work except for quotations and citations which have been duly acknowledged. I also declare that it has not been previously or concurrently submitted for any other degree at UTP or other institutions.

Witnessed by

Signature of Author

Signature of Supervisor

Permanent address: Vaikom
Kerala, India

Name of Supervisor
Assoc. Prof. Ir. Dr. Shaharin A. Sulaiman

Date :

Date :

DEDICATION

I dedicate this thesis to my late Grandfather, Govinda Kammath, who held my hand when I took the first steps, but no more in this world to see me take this big step into the future.

To my family, especially to my father Venkiteswaran, Mother Geetha and my little sister Vinitha, for being so patient and filling up for me during my days away from home.

ACKNOWLEDGEMENTS

This endeavor would not have been possible without the help of a group of kind hearted and knowledgeable people, some of whom I would like to mention here.

Associate Professor Ir. Dr. Shaharin Anwar Sulaiman has been the ideal supervisor. His sage advice, insightful criticisms, and patient encouragement aided the completion of this thesis. Besides research, I had learnt from him much else in engineering and project management. I also wish to thank Associate Professor Dr. Raduan B. Razali, who offered ready help with the statistical package and taught me about statistical analysis of the data.

In addition, I would also like to thank my friends and colleagues with special mention to M. Jeevaneswary, Goo Jia Jun, Manoj Joseph Mathew, Krishna Mohan and lots of others for their whole-hearted support. At this juncture I would also appreciate everyone in the Mechanical Engineering Department for their technical support and Universiti Teknologi PETRONAS for the financial support.

This acknowledgement will not be complete without a mention of Prof. Dr. Vijay R. Raghavan whom I would like to remember with deep gratitude. He started me off on this research and continuously guided me through the grim early days. He has been my idol and model.

I also want to thank my family for their emotional support without which I could not have completed my research. Last but not least, the almighty for all his blessings.

VINOD KUMAR VENKITESWARAN

ABSTRACT

The Swirling Fluidized Bed (SFB) being a newer version of the well-known bubbling fluidized bed, a physical insight into its working, operating regimes and relationship with various aspects need to be investigated. Although some studies have been conducted on SFB in the past, a thorough understanding of the science of the process is yet to be arrived at. Since previous studies on SFB show promise of a highly effective alternative for contemporary techniques and immense potential for commercialization, a comprehensive study on the various aspects controlling the hydrodynamics of the swirling fluidized bed has been carried out.

The aspects for the study were chosen based on the available literature on conventional fluidized beds as well as swirling fluidized beds. The experimental results have shown that features of both the distributor and the bed particles have an influence on the hydrodynamics of SFB. Studies on the slug-wavy regime, hysteresis in bed pressure drop and bed expansion were also conducted.

The present investigations revealed that superficial velocity, U_{sup} is the most prominent aspect affecting the hydrodynamics of SFB followed by bed weight (W_b), diameter of the particle (d_p) and blade inclination angle (θ). Even though other aspects considered influence the hydrodynamic behavior, the effect is relatively minor. It was observed that particles of different sizes and shapes were fluidized well in SFB, which emphasizes its supremacy over contemporary techniques. The slug-wavy regime in SFB is promising and has considerable potential, especially in case of diffusion-controlled reactions and processes in the industry.

A statistical analysis of the acquired data was carried out by nonlinear regression techniques to obtain a correlation between the bed pressure drop in SFB and the

various aspects considered in the study. Different correlations were obtained for packed bed and swirling regimes. The correlation in packed bed has the laminar and turbulent components determined separately. The correlations are intended to help engineers to design a SFB reactor as per process requirement and help to control it for maximum yield.

ABSTRAK

Lapisan terbendalir berpusar (SFB) merupakan salah satu versi lapisan terbendalir yang terkini yang telah dikenali ramai, di mana permerhatian sacara fizikal bagaimana cara ia beroperasi, operasi rejim serta hubungannya dengan pelbagai aspek perlu dikaji. Walaupun banyak eksperimen telah dijalankan ke atas SFB sebelum ini, pemahaman sainstifik yang menyeluruh tentang proses operasi teknik ini masih belum dapat dirungkai dengan jayanya. Kajian-kajian yang telah dilakukan sebelum ini yang berkait rapat dengan SFB telah memperlihatkan hasil yang memberangsangkan dimana teknik ini boleh dijadikan sebagai teknik alternatif kerana ia telah terbukti lebih efektif berbanding dengan teknik-teknik yang sedia ada dan ia juga mempunyai potensi yang tinggi untuk dikomersialkan. Oleh yang demikian, satu kajian yang menyeluruh tentang aspek-aspek yang mengawal hidrodinamik SFB telah dijalankan.

Aspek-aspek yang mengawal hidrodinamik SBF bagi tujuan kajian ini telah dipilih berdasarkan hasil kajian-kajian yang telah sedia ada yang berkait dengan SBF dan juga hasil kajian yang berkait dengan lapisan terbendalir biasa. Bahawa ciri-ciri distributor dan juga ciri-ciri zarah di dalam lapisan terbendalir mempunyai pengaruh ke atas hidrodinamik SBF. Sudut kecondongan bilah (θ), halaju bendalir/ permukaan (U_{sup}), berat zarah pepejal (W_b) dan diameter zarah (dp) didapati mempunyai kesan yang lebih penting dalam operasi SFB berbanding dengan aspek-aspek lain yang dikaji. Di dalam kajian ini, keadaan bed di dalam regim slug wavy, penurunan kadar tekanan hiterisis, dan juga pengembangan bed telah diambil kira.

Hasil dari kajian ini mendedahkan bahawa halaju permukaan, U_{sup} merupakan aspek yang paling mempengaruhi hydrodinamik SFB, diikuti dengan berat bed (W_b) dan diameter zarah (dp). Selain dari aspek tersebut, aspek yang lain juga didapati mempunyai pengaruh ke atas tindak balas hidrodinamik SBF namun kesannya adalah sangat rendah. Daripada kajian ini, telah diperhatikan bahawa zarah-zarah yang berbeza saiz dan bentuk telah berjaya di apungkan dengan baik di dalam SFB, yang membuktikan kelebihan teknik ini berbanding dengan teknik-teknik komtemporari yang lain. SFB yang beroperasi di dalam rejim berombak mempunyai potensi yang

amat besar terutama bagi kes operasi yang melibatkan tikdakbalas dan proses kawalan pengembangan di dalam bidang industri.

Data yang diperoleh itu dianalisis secara statisti mengunakan teknik-teknik regresi non-linear unutuk mendapatkan satu kaitan di antara susutan atau penurunan tekanan SBF bed dengan pelbagai aspek lain yang telah dipertimbangkan di dalam kajian ini. Hubungkait tersebut telah dijalankan untuk rejim packed bed dan juga rejim swirling bed. Bagi rejim packed bed, hubungkait bagi keadaan laminar dan juga keadaan turbulent telah dijalankan secara berbeza. Ianya bertujuan membantu para jurutera supaya mereka dapat mereka bentuk satu reaktor SFB sebagaimana yang diperlukan oleh proses dan membantu untuk mengawal aspek untuk kadar hasil maksimum.

TABLE OF CONTENTS

LIST OF FIGURES

LIST OF TABLES

ABBREVIATIONS

2S	2 mm spherical particle
3S	3 mm spherical particle
4S	4 mm spherical particle
5S	5 mm spherical particle
6S	6 mm spherical particle
ANOVA	Analysis of variance
Elli	Elliptical particles
LC	Long cylindrical particle
PVC	Polyvinyl chloride
RB	Rice bead type particle
SC	Small cylindrical particle
SFB	Swirling fluidized bed
TORBED	Torroidal fluidized bed
VFB	Vortexing fluidized bed

NOMENCLATURE

A	Cross-sectional area of the bed [mm^2]
A_o	Area of opening [mm^2]
A_b	Area of the bed [mm^2]
A_{tot}	Total area of opening [mm^2]
a_1	Area of the orifice [mm^2]
C	Constant [-]
C_D	Co-efficient of discharge [-]
D_i	Inner diameter of the distributor ring [mm]
D_m	Mean diameter of the bed [mm]
D_o	Outer diameter of the distributor ring [mm]
D_p, d_p	Diameter of particle [mm]
d	Diameter of the orifices on the distributor [mm]
g	Acceleration due to gravity [m/s^2]
H_s	Static bed height [mm]

H_b	Height of bed [mm]
H_0	Height of as pour bed [mm]
M_p	Mass of particle [kg]
l	Length of fins provided on each side of the blade [mm]
L_o	Overlapping length of the blade [mm]
N	Number of blades [-]
Q	Volume flow rate of air [m^3/sec]
r	Total length of the distributor blade
r_i	Inner radius of the distributor ring [mm]
r_o	Outer radius of the distributor ring [mm]
R^2	Correaltion coeffient [-]
S	Standard deviation [-]
t	Thickness of the Vane [mm]
t_s	Slugging time [s]
U_o	Velocity of gas through orifice [m/s]
U_{mf}	Minimum fluidizing velocity [m/s]
U_{mff}	Minimum velocity of full-fluidization [m/s]
U_{msf}	Minimum velocity of swirl-fluidization mode [m/s]
U_{sup}	Superficialvelocity [m/s]
U_t	Terminal velocity of the particle [m/s]
V_p	Volume of particle [mm^3]
W_b	Bed weight [N]
W_{cf}	Centrifugal weight [N]

Greek symbols

α	Blade overlap angle [-]
Δp	Pressure drop [mm of H_2O]
Δp_b	Bed pressure drop [mm of H_2O]
Δp_d	Distributor pressure drop [mm of H_2O]
Δp_t	Total pressure drop[mm of H_2O]
ε	Packing fraction of the fluidized bed [-]

ε_s	Solid packing fraction [-]
ε_0	Packing fraction of the fixed bed [-]
θ	Inclination of the vane with the horizontal [-]
φ_d	Open-area ratio [-]
ρ_b	Density of bed [kg/m^3]
ρ_a	Density of air [kg/m^3]
ρ_p	Density of particle [kg/m^3]
ρ_o	Density of gas through the orifice [kg/m^3]
ρ_s	Density of the solid [kg/m^3]
ρ_f, ρ_m	Density of the fluidizing medium [kg/m^3]
η_m	Motor efficiency [-]
η_{fan}	Fan efficiency [-]
ω_o	Angular velocity at minimum fluidization [rad/s]

Subscripts

a	air
b	bed
d	distributor
p	particle
mf	minimum fluidiztion
min	minimum
0	packed bed

Non–dimensional groups

Ar	Archimedes number	$\frac{d_p^3 \rho_g (\rho_p - \rho_g) g)}{\mu^2}$
C_D	Coefficient of discharge	$\frac{U_{actual}}{U_{theoretical}}$
Re	Reynolds number	$\frac{\rho U D}{\mu}$

CHAPTER 1

INTRODUCTION

1.1 Chapter Overview

An overall description of fluidization and fluidized bed technologies, problem statement, objectives and scope of the work are given in this chapter. The fluidization process, its use, merits and demerits are also explained here. In view of various industrial processes involving fluidized bed and the need of using enhanced technology with higher efficiency, this research work aims to enhance the existing Swirling Fluidized Bed (SFB) technology, thereby increasing its capabilities and effectiveness. The outcomes of this work will serve as a bench mark for reactor designers as well as help in achieving higher efficiency of processes and energy savings.

1.2 Fluidization and Fluidized Beds

From an early era of industrialization, scientists have always been on the lookout for methods for improving the existing chemical or mechanical processes in their aim to bring down the production cost or improve the yield. Many such industrial processes involve an intimate interaction between solid particles (such as catalysts or reactants) and the fluid (gas or liquid). Use of the fluidized bed was seen to be the best solution as it provides high transfer rates. Hence it has been used for decades in processes such as combustion, drying, gasification, thermal and catalytic cracking, surface treatment of metals etc. [1, 2].

For a gas-solid fluidized bed system the applications can be divided into four categories as in Table 1-1 [3].

Table 1-1: Applications gas-solid fluidized bed systems [3]

Use	Example
Gas catalytic reaction	Fluid Catalytic Cracking (FCC).
Gas-phase reaction using solids as heat carriers.	Chemical vapour deposition of coatings
Gas-solid reaction, where reactants and products are a combination of gas and solids.	Combustion and gasification
Process where no chemical reactions occur.	Fluidized bed drying

Fluidization is a technique where solid particles in a bed get entrained and float in a flowing liquid or gas and the bed behaves like a liquid. When the fluid flows through the bed, it tends to apply a force on the particles, normally referred to as drag force. As the flow in the vertically upward direction increases, the drag force exerted on the particles also increases and becomes large enough to disturb the arrangement of the particles, Figure.1.1.

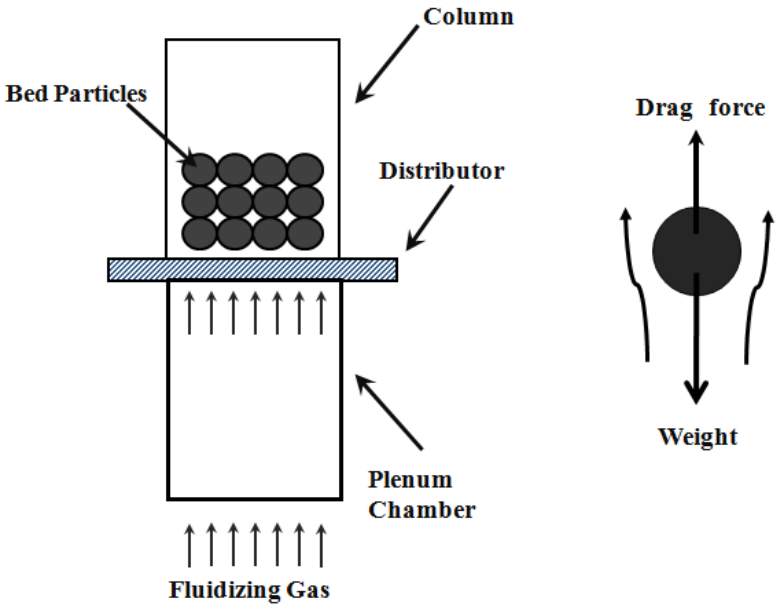

Figure 1.1: Layout of a conventional bed, depicting forces experienced by a particle in the bed

With a progressive increase in the flow rate, the drag force exerted on the particles also increases till it is sufficient to support weight of the particle acting vertically down. The solid particles effectively become weightless, possess all the degrees of freedom and behave like a liquid; hence they are said to be fluidized. Under the fluidized state, the particles exhibit properties of a liquid.

The characteristics of a fluidized bed are illustrated in Figure 1.2. For all fluidized beds the static pressure head at any height is approximately equal to the weight of bed solids per unit cross sectional area above that level. This is similar to the hydrostatic pressure in fluid mechanics. The bed readily assumes the shape of the vessel and bed surface always maintains a horizontal level, irrespective of how the bed is tilted. The solids from the bed may flow under gravity like a liquid through an orifice at the bottom or on the side of the container. A denser object will sink, while the one lighter than the bed will float (e.g. a steel ball sinks in the bed, while a light shuttlecock floats on the surface.)Particles are well mixed, and uniformity of temperature and concentration is maintained throughout the bed.

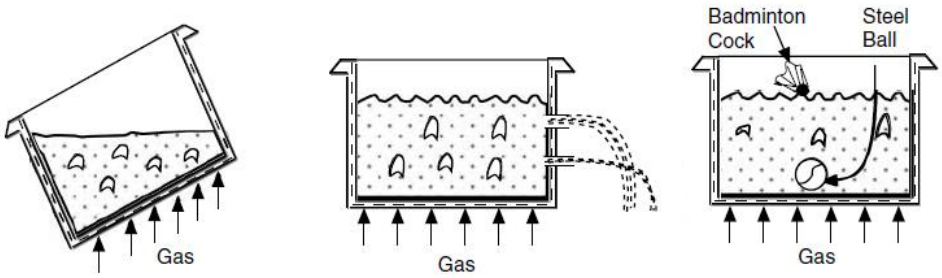

Figure 1.2: A fluidized bed demonstrates all characteristics of a liquid [1]

Even though fluidization has a lot of advantages like better solid-fluid contacting and rapid mixing of solids etc., they also have their own disadvantages. The merits and demerits of fluidized beds are recapitulated as follows:

1.2.1 Advantages of Fluidized Beds

Fluidized beds provide excellent mixing and facilitate achieving high transfer rates under isothermal operating conditions. Because of its fluid-like behavior, it facilitates

free flow of the bed between adjacent reactors. Absence of moving parts and need for smaller floor area saves cost. A continuous process coupled with high throughput is possible even without a skilled operator. Fluidized beds are suitable for large-scale operations involving heat-sensitive reaction. A batch fluidized bed reactor can be converted into a continuous reactor by multistage operations, thereby achieving the desired residence times.

1.2.2 Disadvantages of Fluidized Beds

The most important disadvantage of a fluidized bed is the difficulty in fluidizing fine-sized particles and accomplishing reactions needing a temperature gradient. Because of the complex hydrodynamics of fluidized beds, modeling and scale-up are difficult; hence highly skilled professionals in this area are needed. Occurrences like turbulent mixing, segregation, unnecessary interactions at distributor, agglomeration etc. result in undesirable outcome and affect the yield. In fluidized beds, high power consumption for pumping as well as elutriation of finer particles are unavoidable. There is a limitation on particle size range in the bed and operating velocity regime that can be utilized. Severe erosion of immersed surfaces and defluidization are common depending on the nature of reactions and materials involved.

1.2.3 Regimes of Fluidization

An increase in the gas velocity through a bed of granular solids brings about changes in the mode of gas-solid contact in many ways. With changes in gas velocity the bed moves from one state to another.

Different regimes of fluidized bed operation arranged in order of increasing velocities are shown in Figure 1.3 and are mentioned below:

- Packed (or fixed) bed.
- Bed at minimum fluidizing velocity or at incipient fluidization.
- Fluidized bed.

- Bubbling bed.
- Turbulent bed or slugging bed
- Pneumatic transport (or entrainment) usually seen in circulating fluidized bed.

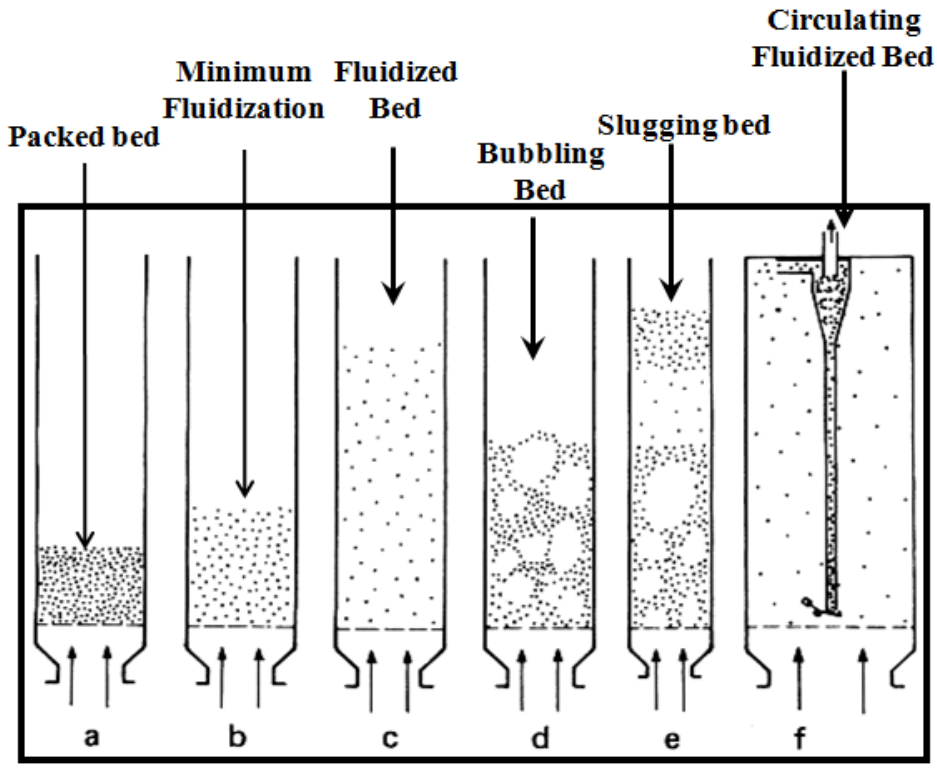

Figure 1.3: Different regimes in a conventional fluidized bed in order of increasing velocities [4, 5]

It may also achieve slugging or dense phase suspension flow under certain conditions. There have been many different types of fluidization as suggested by Gupta and Sathyamoorthy [6] with recent advancements and innovation. Some common varieties in fluidization, where the swirling fluidization is the latest addition.

With an increase in gas velocity beyond the minimum fluidization velocity (U_{mf}), the gas-solid bed starts to bubble which is known as aggregative fluidization. When the fluidizing agent is denser, such as a gas at high pressure or a liquid, or with fine and light particles, the bed undergoes a considerable degree of stable expansion, resulting in particulate fluidization. With still finer particles, it is difficult to fluidize the bed, as the inter-particle cohesive forces are then greater than the gravitational

ones. As a result particles tend to stick together, and the gas passes through the bed by blowing channels (also termed rat holes) through it.

In conventional fluidized beds, the following factors are responsible for shortcomings in operation: [6]

1. Large pressure drop across the distributor directly affects the blower and results in high power consumption.

2. The inter particle contact and particle-to-gas (fluid) interaction is rather low in a conventional fluidized bed compared to other fluidized beds. This may lead to inefficient utilization of expensive chemicals and gases involved in the process and below-par reaction kinetics.

3. Conventional beds are inefficient in handling irregular shaped particles, as the gas would bypass through the large interstices created due to the irregularities in the shape of the bed particles.

4. Bubbling is common in conventional beds. As it involves gas bypassing, it is generally undesirable.

5. Maldistribution of gas flow is common due to the occurrence of slugging and channelling in conventional beds.

Limitations of conventional fluidization have resulted in the development of new techniques such as centrifugal fluidized bed, circulating fluidized bed, vibro-fluidized bed, tapered fluidized bed, spouted fluidized bed etc. The swirling fluidized bed (SFB) is a recent effort of researchers to overcome the shortcomings of conventional fluidized bed technology. The fluid (usually a gas) enters the SFB at an angle through the inclined opening of the annular distributor resulting in two components of velocity: (i) the vertical component causes fluidization and (ii) the horizontal component caused swirling motion. Even though the swirling fluidized bed and its variants have been in the picture for a couple of decades and a commercial model of this type of bed, called TORBED [7], is utilized in chemical/ mechanical processes and marketed by Torftech Inc., the fundamental knowledge in this area has not advanced. Figure 1.5 shows a fluidized bed from Troftech being assembled on site.

The small active width of the bed, which is a major disadvantage, is noteworthy. TORBED technology is patented and few research articles are being published due to lack of knowledge in this technology. Consequently the study and development of SFB, being a similar technique, is of utmost importance and has much market potential.

Figure 1.4: TORBED, a commercial version of swirling bed, being assembled on site [7].

The SFB has many superior features over the conventional bed and other existing counterparts which are: no moving parts, uniform mixing, better quality of fluidization and lower distributor pressure drop, hence lower pumping power. Although some hydrodynamic studies on SFB have been done on this type of beds [8, 9], much about its operation is not understood well.

1.3 Problem Statement

The existing swirling fluidized bed has not been studied to an extent that the phenomenon could be completely understood and the pertinent shortcomings corrected. The most important limitation of SFB is the accumulation of bed particles at the outer wall at high fluidizing velocities, leading to gas bypass and underutilization of the fluidizing gas. Another disadvantage is the utilization of

available distributor area. In existing designs, only a small annular area is available or can be utilized, with a cone placed at the center co-axial to the bed as shown in Figure 1.6. If a distributor were to stretch across the entire bed area it would result in a dead zone at the center, leading to gas bypass, interfering with the entire fluidization process.

Four different regimes in SFB namely packed bed, slug-wavy regime, swirling regime and two-layer regime, visually observed during experiments by previous researchers are yet to be clearly explained, examined and put to commercial use. The optimal regime for a process can only be recommended once all these regimes are properly investigated.

For all fluidized bed systems, the gas distributor is an inevitable part. In the case of SFB distributor no literature or guidelines are available to design an optimal system. The existing annular spiral distributor is made of trapezoidal blades which are inclined at an angle to the horizontal. The effect of the inclination of the blades on the operation of the bed has not yet been fully established nor an optimal value suggested, hence it requires a thorough investigation. The shape of the blade, suggested by earlier researchers, also needs to be investigated. In order to overcome the shortcomings, the distributor aspects and their effect on fluidization have to be completely understood.

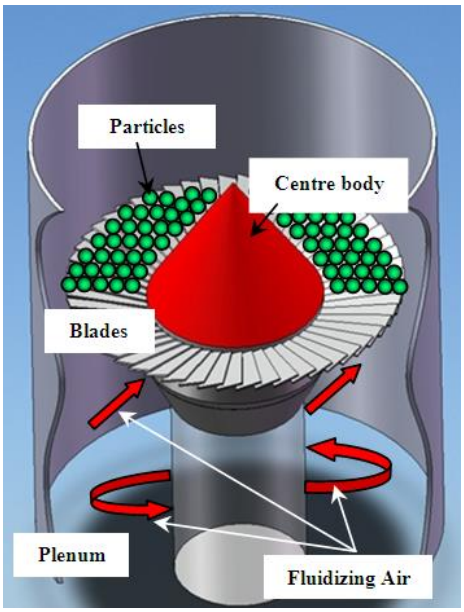

Figure 1.5: Basic configuration of swirling fluidized bed

For this, the bed behavior has to be studied under conditions of different distributor aspects and the effects should be clearly examined and quantified. The velocity of the particle at a particular flow rate of fluidizing gas should be experimentally calculated and also the trajectory of the particle in the bed should be tracked to understand the swirling characteristics. Based on this, a new distributor could be designed and tested for various configurations, thereby optimizing and enhancing the existing design of the swirling fluidized bed.

1.4 Objectives and Scope of Study

1.4.1 Objectives

This work is an endeavor to analyze the swirling fluidized bed (SFB) and enhance its performance as a whole. This involves a complete study of the hydrodynamic behavior as well as the different fluidizing regimes of the SFB. The main objective of this work is to determine the effect of different distributor and bed variables and their importance in SFB hydrodynamics. This would help in designing a SFB reactor for a desired operation and to control its operation for required results.

The main objective of the work is categorized following:

a) To study the effect of various aspects of the gas distributor, such as the blade inclination and blade overlap angle on the bed pressure drop, minimum fluidization velocity, etc.
b) To study the effect of various aspects of the particles, like shape, size and density on the same.
c) To establish a correlation of all the above mentioned variables with bed pressure drop.

1.4.2 Scope of Study

This research work identifies various aspects that affect the hydrodynamics of a swirling fluidized bed in cold bed condition. The design of the equipment was based on criterions pertaining to conventional fluidized beds and previous literature. This study mainly focuses only on Geldart D ($\rho d_p \geq 10^6$, ρ in kg/m^3 and d_p in micrometers) type particles for the following reasons; (i) most of the practical/industrial applications like drying of agricultural produce, processes involving biomass, coating and pelletization in pharmaceutical industries etc., all involve particles having sizes pertaining to Geldart D classification (ii) conventional fluidized beds cannot satisfactorily fully fluidized Geldart D particles.

1.5 Justification for the Research

Various industrial processes like refining of petroleum were revolutionized by the introduction of fluidized bed technology. Chemical processes, as they can be carried out at lower temperatures and pressures, have become safer and more efficient with the introduction of fluidized beds [1].

Figure 1.7 shows the slip velocities existing in various types of gas-solid contacting. The largest slip velocity obtained in the swirling fluidized bed which has all the features which make it suited for specialized processes like bio-crude refining, drying and gasification of biomass, combustion of biomass and bio-waste, torrefaction of biomass as well as all other processes which use the fluidized bed technique. Hence swirling fluidized bed promises a great opportunity in these applications. Even though many commercial versions of the bed are available, not much literature on its fundamental research and hydrodynamics is available and there has been no commendable improvement in the technology since its advent. In an era of energy scarcity, SFB can act as an energy producing and energy saving technology as it saves energy in terms of pumping power in industrial processes; at the same time it is used in energy producing systems like gasifiers, combustors etc. Hence fundamental

studies and research to improve the technique have viable significance which by itself rationalizes the work.

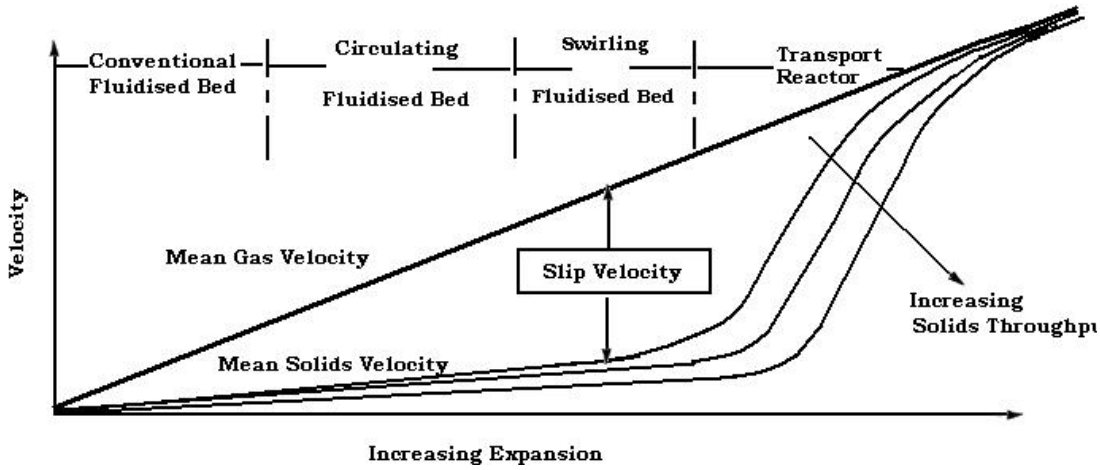

Figure 1.7: Plot showing the slip velocity in various types of fluidized beds [10]

1.6 Thesis Outline

This thesis has been arranged into six main chapters and four appendices containing subsidiary information. Chapter 1 contains general introduction, chapter 2 gives an extensive description of all the relevant literature on this work. Chapter 3 discusses in detail the design, fabrication and assembly of the experimental setup, and the materials and instruments used. The methodology followed during the experiments and in the following stages is illustrated comprehensively in chapter 4. Results are presented in chapter 5 and are discussed in detail, providing sufficient explanations for the inferences made. Conclusions from the entire work are laid out in chapter 6, with further discussions, clarifications and suggestions for future work.

CHAPTER 2

LITERATURE REVIEW

2.1 Chapter Overview

This chapter documents a review of literature related to fluidized beds and its constant improvements in the past leading to understanding of the technique and the need for its enhancement. Even though the conventional fluidized bed has been known for a long time, there is very little known about swirling fluidization and publications on it are scarce, it being a newly evolved version. The chapter starts with a brief description of evolution in fluidized bed technology from the conventional to contemporary variations with special emphasis on previous research work on swirling fluidized bed and similar technologies.

2.2 The Conventional Fluidized Bed

In conventional beds a perforated metal plate is generally used as a distributor, which distributes the fluidizing medium as well as supports the bed material in the absence of the flow. In a conventional bed with upward flowing fluid, the drag force causes the bed to expand. When the drag force on the bed particles is adequate to support the entire bed weight, the bed fluidizes. The bed pressure drop, Δp_b, in this case remains constant with respect to fluid velocity and is equivalent to the effective weight of the bed per unit area, Figure 2.1.

Determination of the velocity for minimum fluidization (U_{mf}) is important for design and efficient operation of a fluidized bed system. If the solid bed particles in the bed are of uniform size and density then U_{mf} calculation is done based on the modified Ergun equation [11]:

$$\frac{\Delta p}{L} = k_1 \frac{(1-\varepsilon)^2}{\varepsilon^3}\frac{\mu U_{mf}}{D_p^2} + k_2 \frac{(1-\varepsilon)}{\varepsilon^3}\frac{\rho_m U^2{}_{mf}}{D_p} \tag{2.1}$$

When a fluid flows through a packed bed of particles in a reactor column, there will be a drop in pressure measured across the bed. The above equation shows, quantitatively, a direct relationship between the pressure drop and the approach velocity of the fluid.

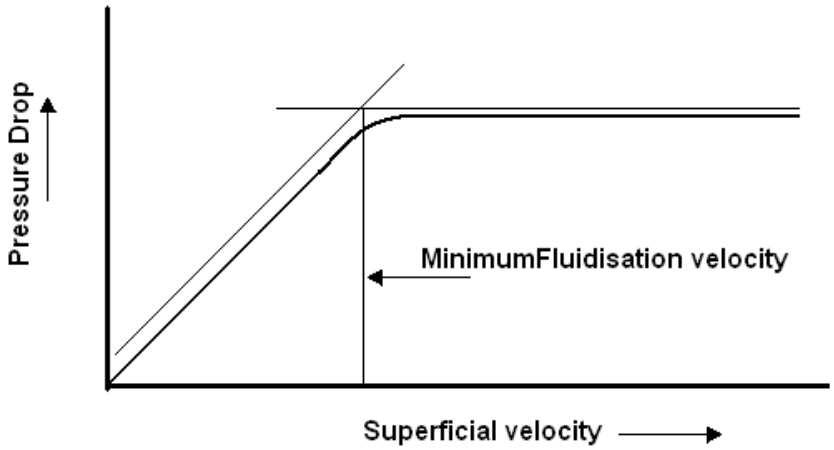

Figure 2.1: Plot of bed pressure drop against superficial velocity

Merry [12] was the first to study the effect of horizontal injection of a gas jet into a conventional fluidized bed. The primary intention was to create a swirling motion of the bed particles by entraining them in the path of the jet of gas.

Even though conventional fluidized beds have been used for various chemical and mechanical processes like gas adsorption/absorption, coating of capsules, drying, frying, pelletization, chemical reactions[1, 2] etc., their effectiveness in terms productivity is low due to the reasons summarized below:

- It has a large distributor pressure drop.
- Relatively low contact between particle-to-particle and particle-to-gas (fluid).
- Difficulty in handling particles of irregular shape.
- Bubbling, slugging and channeling which are undesirable events.

These shortcomings of the conventional fluidized bed have given rise to a number of research efforts, many of which are still in progress.

2.3 Types of Fluidized Beds

2.3.1 Centrifugal Fluidized Bed

In conventional fluidized bed, the introduction of an enormous amount of surplus aeration resulting the generation of large bubbles resulting in poor gas-solid contact. Therefore, in the case of processes that require high superficial gas velocity, the conventional bed becomes less efficient in terms of utilization of the gas.

Consequently the concept of centrifugal fluidized bed is put forth. A centrifugal fluidized bed consists of a cylindrical bucket or cylindrical vessel (column) rotating about its own axis of symmetry wherein the aeration is introduced in a radially inward direction to fluidize the bed particles. Here, unlike a conventional bed having a fixed gravitational field, the centrifugal gravity force in a centrifugal bed varies depending on the speed of rotation of the bucket and its radius. By using a strong centrifugal field which would be much greater than terrestrial gravity, the bed is able to survive a large bubble generation due to huge amount of aeration and thus the gas solid interaction at a high aeration rate is improved here [13].

Kroger *et al.* [14] proposed equations, based on the force balance at the distributor that could predict the pressure drop and radial flow distribution in a centrifugal fluidized bed and reconfirmed their theory using their own experimental results. This was seen to be true only for shallow beds. Takahashi *et al.* [15], during their study in a horizontal rotating fluidized bed with different particle densities and size distribution, reported that unlike in conventional bed, the bed pressure drop in centrifugal fluidized bed varies depending on the rotational speed. The bed pressure

drop attains a peak value at minimum fluidizing velocity, which on further increase of gas velocity tends to show a slight drop in its value.

Fan *et al.* [13] developed a new model for the determination of incipient fluidization in a centrifugal fluidized bed and also validated it with their experimental results. They concluded that the characteristics of centrifugal fluidized beds are vastly different from those of conventional fluidized beds so the known hydrodynamic relations of the conventional beds cannot be used to explain centrifugal fluidized beds. Chen [16] suggested another theoretical model based on the balancing of local momentum, to describe the fluidization occurring in a centrifugal fluidized bed. According to him, in contrast to conventional beds, the centrifugal bed fluidizes layer by layer i.e. from the inner to the outer surface, in a varying range of flow rates.

The reason for the layer-by-layer fluidization as explained by Chen [16] is due to the fact that fluid drag, centrifugal force and gas inertia, all being functions of the radius of the cylinder, will not balance each other at a particular value of flow rate/superficial velocity.

The centrifugal fluidized bed seems to have the following advantages over the conventional fluidized bed, according to Fan *et al.* [13].

a) It has a wider range of operation than that of a conventional fluidized bed. The varying radial acceleration is proportional to the rotational speed of the cylindrical bucket and overpowers gravity.
b) In systems with zero gravitational fields where the conventional bed cannot operate, the centrifugal fluidized bed would work.
c) It has better control of temperature and reaction rate compared to the conventional bed.
d) As it has a higher ‘g’ field due to its centrifugal acceleration, it shows better capture efficiency and higher throughput when used as a filter in comparison to conventional beds.
e) It needs less space due to a smaller distributor area and cylindrical shape.

In spite of all the above advantages, their complex construction is a major negative aspect. Also, due to a number of moving parts and mechanical links the efficiency will be less along with high maintenance, which would mean a higher cost. At very high rotating speeds of the cylinder there is a possibility of massing of particles towards the wall of the cylindrical bucket hence the fluid requires to be injected at very high pressure in order to fluidize the particles against the increasing centrifugal weight.

2.3.2 Circulating Fluidized Bed

In a normal fluidized bed, an increase in the air flow rate beyond the minimum fluidization value will give rise to bubbling and large pressure fluctuations. At higher gas velocities the fluctuations become more violent and particles move more vigorously. At low fluidization velocities, the bed expansion is low and bubbles coexist with the gas-particle phase. Such a condition is called a heterogeneous bubbling fluidized bed [10].

On further increase of the flow, the bed attains a homogeneity condition till a stage is reached where large bubbles are absent. This indicates the starting of turbulent phase, where the velocity approaches the transport velocity accompanied by a large amount of particle elutriation. If there is no recycling of the particulates, the bed will be empty within a short time. This condition can be referred to as fast fluidized bed or circulating fluidized bed. Both bubbling and circulating beds are depicted in Figure 2.2.

Referring to previous authors' work the circulating bed can be seen to have the following advantages:

i) Uniformity of temperature throughout the bed [17].

ii) High degree of mixing between gas and bed particles [18, 19].

iii) Very good heat transfer rates to side wall as well as towards the interior of the bed and hence its capability of taking particles or gases to bed temperature almost instantly [20-25].

iv) Excellent particle to gas contact with a high processing capacity [20, 26-28].

v) A circulating fluidized bed can easily fluidize particles with high cohesive force, which is otherwise difficult [21-25].

vi) A circulating fluidized bed can be scaled up more easily.

However, the large elutriation rate of particles in this type of bed necessitates a recirculation system and requires addition of a cyclone. This results in the circulating fluidized bed being inferior for most of the applications except for processes such as solid fuel combustion.

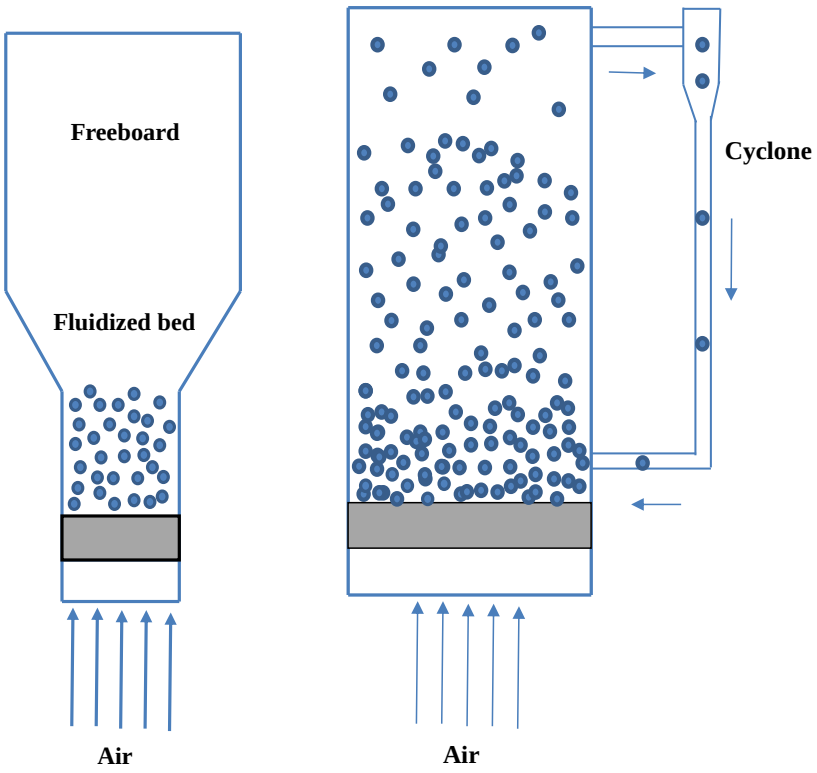

Figure 2.2: Schematic of (a) bubbling and (b) circulating fluidized bed [10]

2.3.3 Vortexing Fluidized Bed (VFB)

In another variant of the fluidized bed, as in Figure 2.3, a swirl is imparted to the fluidized bed by injecting secondary air tangentially into the freeboard. This is a concept brought forth and patented by Sowards [29], which the author refers to as the vortexing fluidized bed (VFB), and uses a perforated plate as the air distributor.

This can be used to increase the residence time of particles in the freeboard and to reduce the loss of un-burnt fines during a combustion process. According to Chyang and Hsu [30] the elutriation rates reduce with an increase in secondary air flow and they attributed the formation of a stable particle cluster suspension layer in the free board region as an explanation for increase in the residence time of bed particles.

Since the secondary air is injected in the freeboard, the effect only pertains to the circulating zone of the fluidized bed and generally applies to processes like combustion or incineration where it is necessary to create a vortex to burn off all the volatiles and other fines of waste matter or even the fuel itself.

The disadvantage of the VFB is that its utility is limited to combustion or incineration and is not universal. If air is used as the fluidizing medium, it does not involve high expense. Where the gas is hydrogen or methane for example, the excessive amounts of gas which pass through unutilized can represent a significant cost component.

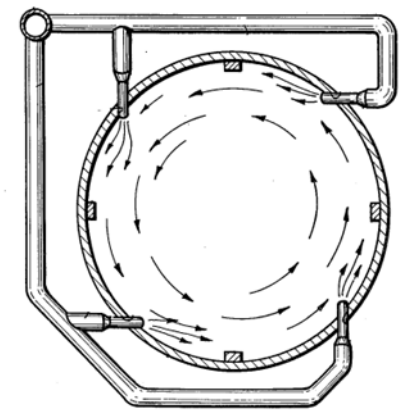

Figure 2.3: Schematic diagram of a vortexing fluidized bed [29]

2.3.4 Rotating Distributor Fluidized Bed

Another type of fluidized bed system with rotating distributor, as depicted in Figs. 2.4 (a) and (b), was proposed by Sobrino *et al.* [31]. The rotating distributor used here was a perforated plate with holes of 2 mm diameter. In order to prevent bed particles from draining down through the plate into the plenum chamber, the distributor plate was covered with a fine-wire mesh. The holes in the distributor plate were laid out in hexagonal pitch of 15 mm. A spiral pitch distributor was also utilized. To rotate the distributor, it was coupled to an AC electric motor wherein the rotational speed could be controlled using a frequency inverter.

According to them [31] the bed has following advantages

- A reduced gas flow is required to fluidize the bed,
- The fluidization state is achieved with ease and
- The bed dynamics can be controlled by adjusting the rotational speed of the distributor plate without losing the quality of fluidization, for all superficial gas velocities $U < 2U_{mf}$.

Here an important problem worth mentioning is the probable mechanical failure due to bed particles getting stuck in between the rotating distributor and static support. The particles may get crushed resulting in blocking the rotational motion of the distributor. Moreover the power input for the rotation of the distributor and high maintenance also are shortcomings of this concept.

At first sight, the concept and its working do not seem to have a significant impact on the hydrodynamics of the bed. The swirl produced by the rotation will only be there with a layer of bed particle close to the distributor and in contact with it. To create a swirl that penetrates the whole bed, the rotational velocity of the distributor should be very high. At such high velocity there is a probability of the bed particles getting worn-out because the high friction and hard nature of the perforated distributor.

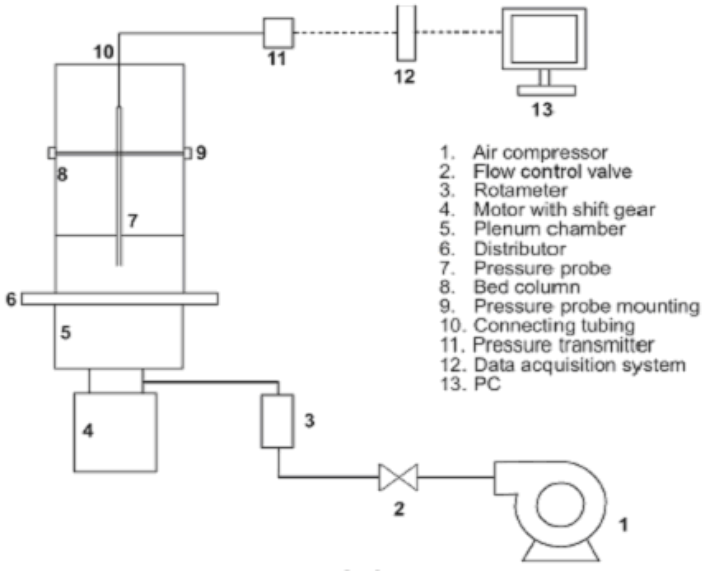

(a)

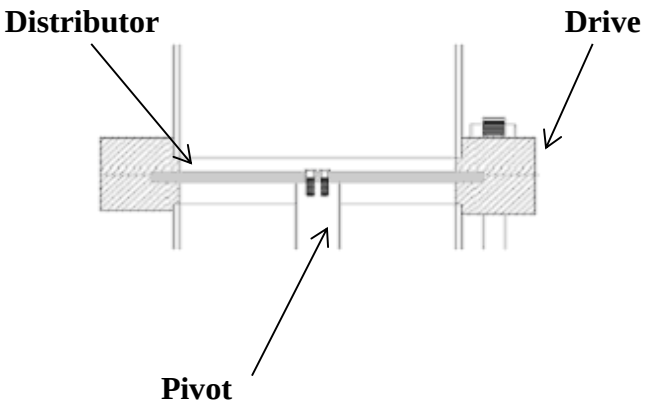

(b)

Figure 2.4: (a) Schematic diagram of the experimental fluidized bed; (b) Detail of the mechanical set-up of the distributor in the bed [31]

2.3.5 Rotating Fluidized Bed with Static Column

In rotating fluidized bed as shown Figure 2.5, another improved version of fluidized bed proposed by Broqueville [32], the rotational motion of the bed is induced by

injecting the fluidizing gas tangentially into the fluidization column using multiple gas inlet slots located on its outer periphery.

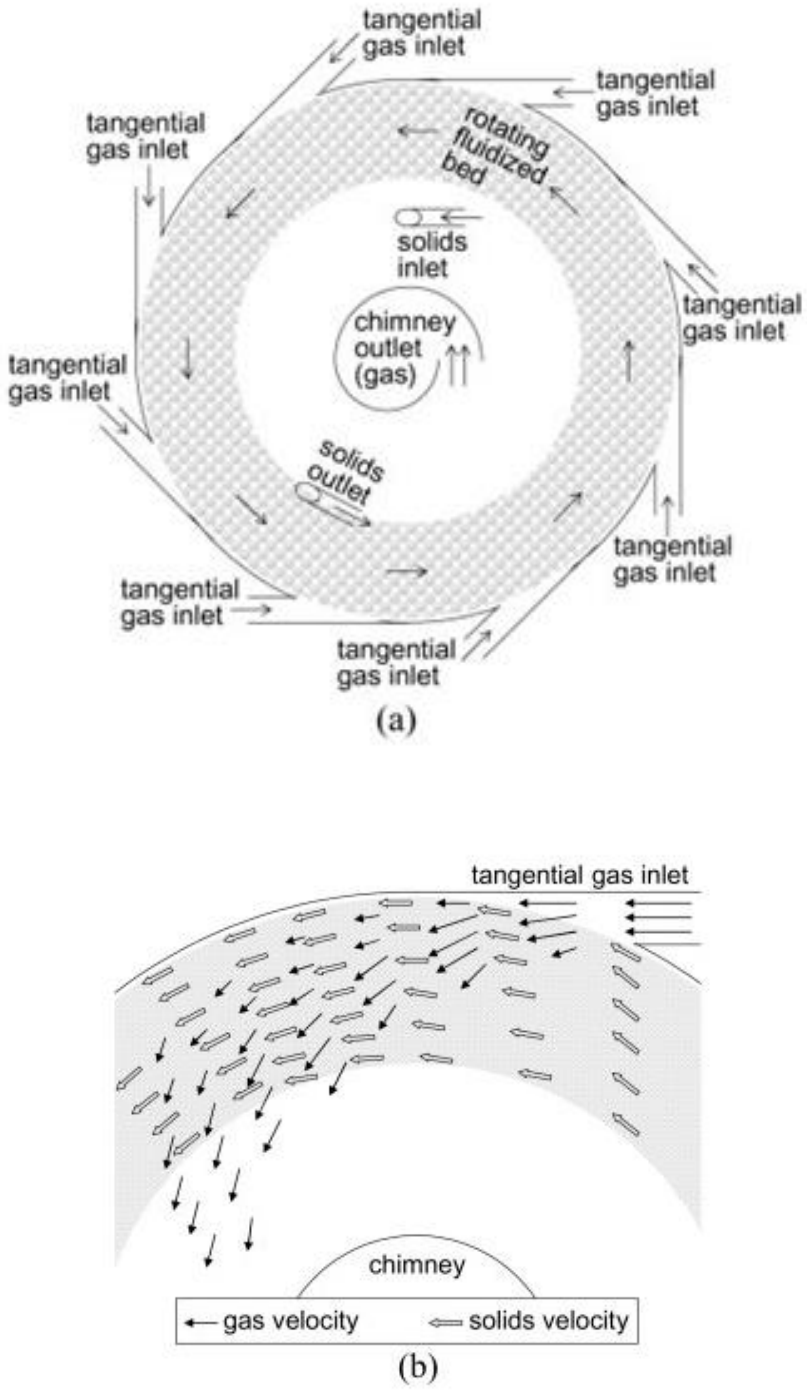

Figure 2.5:(a) 2-D section of the fluidizing chamber; (b) Behavior of the gas and particle velocities near the tangential gas inlet of the fluidizing chamber [32]

The gas–particle drag force in the tangential direction along with the shear stress governs the fluidization of the bed and the particle rotational speed. The gas–particle slip velocity in the tangential direction is anticipated to be smaller than the radial gas–particle slip velocity, except near the gas inlet. Because of the centrifugal force created by the fluid injectors, about three times the force of gravity, the particles form a rotating fluidized bed, which rotates at a certain distance from the central duct while sliding along circular wall. The particles are at least partially supported by any one stream of the fluid, which passes through the fluidized bed before being removed centrally through the discharge opening of the central duct.

In this rotating fluidized bed, it is very difficult to conclude about the quality of fluidization of particles i.e. whether there is a complete balancing of weight of the particles by an equal and opposite drag force. In addition there would be always an inward force and hence there is a possibility of particle accumulation towards the center of the fluidization chamber.

2.3.6 Toroidal Fluidized Bed (TORBED)

TORBED is a relatively new technology proposed and patented by Dodson [33]. The reactor has a gas distributor consisting of angled blades in an annular form at the reactor bottom, as shown schematically in Fig 2.6. The idea of the Toroidal fluidized bed can be seen as an extension of the centrifugal fluidized bed. For the centrifugal fluidized bed, the column rotates and creates a spiral motion in the horizontal axis, while the flow of gas creates an upward movement [16].

The pioneering study in this direction was done by Ouyang and Levenspiel [34] who proposed a spiral distributor for swirl motion as shown Figure 2.7. They evaluated and compared the characteristics of this distributor, such as pressure drop, quality of fluidization and heat transfer coefficient with that of sintered- plate distributor. The spiral distributor was fabricated with overlapping blades, shaped as sectors of a circle with an opening between the blades. They arranged the blades in such a way that the air leaving from the gap of the blades is in a direction tangential to the bed.

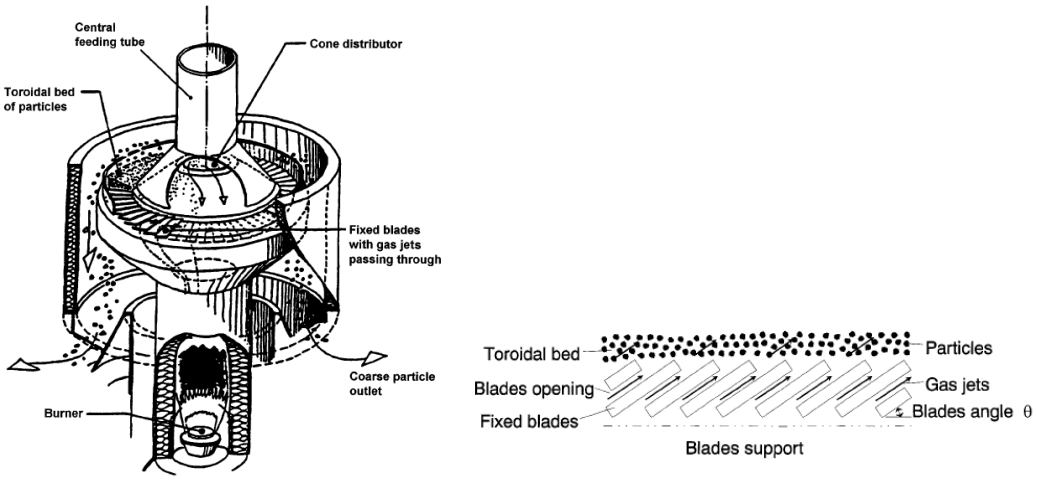

(a) (b)

Figure 2.6: (a) Configuration of a toroidal fluidized bed reactor; (b) Principle of particle movement in a toroidal fluidized bed reactor [33]

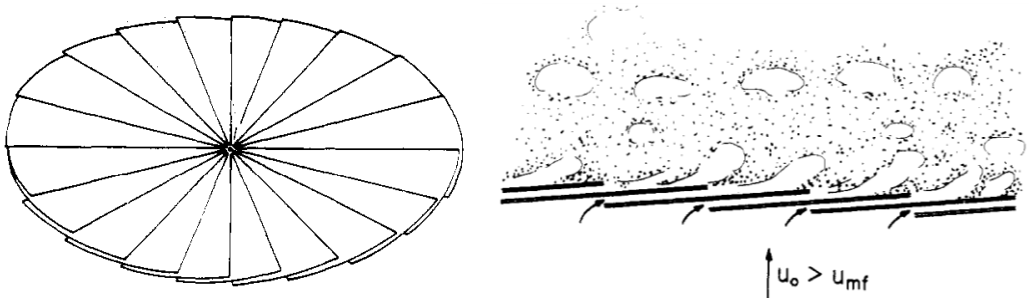

(a) (b)

Figure 2.7: (a) Spiral distributor as used by Ouyang and Levenspiel; (b) Bed behavior at the spiral distributor as used by Ouyang and Levenspiel [34]

They reported that the inclined jet from the opening between the blades imparts a swirling motion in a shallow bed while in a deep bed, the swirling motion is restricted to the lower portion of the bed and bubbling occurs in the region above the swirling region. A comparison of pressure variations across the fluidized bed with a spiral plate and a porous plate shows that, for low-density particles, the sintered plate gives better fluidization at low superficial velocity but at high superficial velocities, the performance is better in the spiral distributor. However for high-density particles, the spiral distributor seems to give a better quality of fluidization at all gas velocities. They also reported that the distributor pressure

drop across the spiral distributor is smaller than that for the sintered plate distributor.

Shu *et al.* [35] studied the hydrodynamics of a toroidal fluidized bed (TORBED), with fine particles and compared it with the performance of conventional bed. An annular ring gas distributor with blades fixed at an angle of 25^{o} with the horizontal was used for their study. They have suggested that for a shallow bed the vertical component of the gas velocity should also be considered while comparing with the minimum fluidization velocity in conventional fluidized bed.

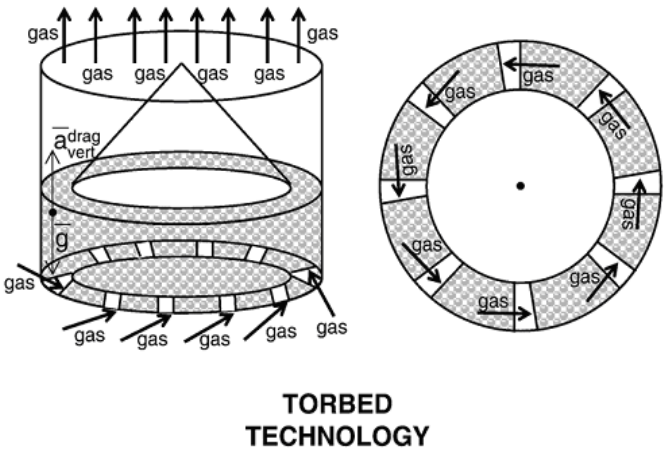

Figure 2.8: Construction of TORBED [36]

At this juncture the contrast between rotating fluidized beds in a static geometry and existing Torbed (or toroidal fluidized bed) technology can be mentioned. In a rotating fluidized bed, the fluidization gas is injected tangentially through multiple inlet slots in a distributor plate. This creates a rotating gas flow (a "tornado") on which the particles get suspended, referred to as the "tornado-effect". In a Torbed, the rotating particle bed is fluidized vertically by forcing the fluidization gas to enter via the distributor plate in to the fluidization chamber. Here, gravity is balanced by the gas–solid drag force acting vertically upwards. So the Torbed is not a true rotating fluidized bed, as there is no radial fluidization of the particles in the centrifugal field or the centrifugal force is not at all used to balance the radial gas–solid drag force which is so in the rotating fluidized bed [36].

2.3.7 Conical Swirling Fluidized Bed

Kaewklum *et al.* [37] developed a new version of swirling fluidized bed named conical swirling fluidized bed as shown in Figure 2.9. The researchers used an inclined distributor, which gives the bed a conical shape. Based on experiments conducted with an annular distributor and air supply as in Figure 2.10, they have reported that hydrodynamic regimes and characteristics in a conical swirling fluidized-bed are substantially affected by the type of air injection or swirl generator. When using annular spiral distributor, the bed exhibits four regimes (depending on the superficial air velocity): (1) fixed-bed, (2) partially fluidized-bed, (3) fully fluidized-bed with partial swirl motion, and (4) fully swirling fluidized-bed regimes. The bed characteristics (particle size and static bed height) have significant influences on major hydrodynamic characteristics of a swirling fluidized-bed, the minimum fluidization velocity (U_{mf}) and corresponding pressure drop across the bed (Δp_{mf}), as well as on the dependence of pressure drop across the bed (Δp) on air superficial velocity (U_{sup}), termed the Δp–U diagram. With coarser particles and larger static bed height, both U_{mf} and Δp_{mf} shows an increasing trend.

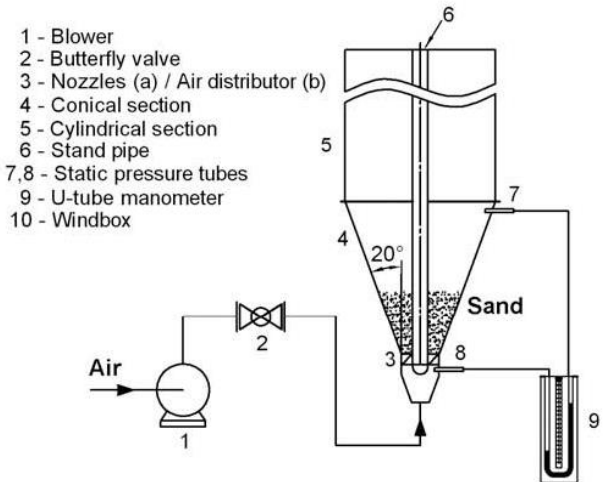

Figure 2.9: Schematic diagram of experimental rig with annular-spiral air distributor as used by Kaewklum *et al.* [37]

Even though the conical swirling fluidized bed seems to solve the problem of solids accumulation at the periphery to a small extent, it does not appear very effective as an eventual solution to the problems in swirling fluidized bed (SFB).

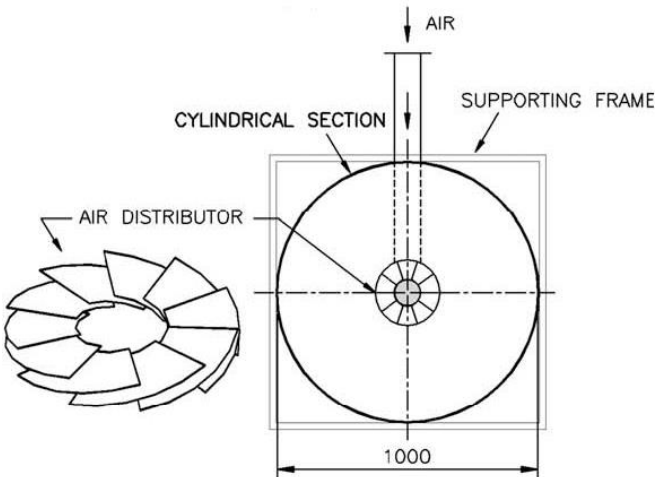

Figure 2.10: Design details of air supply of the experimental rig with annular-spiral air distributor as used by Kaewklum *et al.* [37]

2.3.8 Swirled Fluidized Bed

Kumar and Murthy [38] in a recent publication have reported their study on the hydrodynamic behavior of their swirled fluidized bed. In this study, tangentially located multiple fluid inlets at the base of a flat-bottom circular column are used to achieve the swirl flow (Figure 2.11). They also claim that this type of bed operation is distinctly different from the previous works depicted in the published literature, even though it seems to have a similarity with Soward's [29] idea.

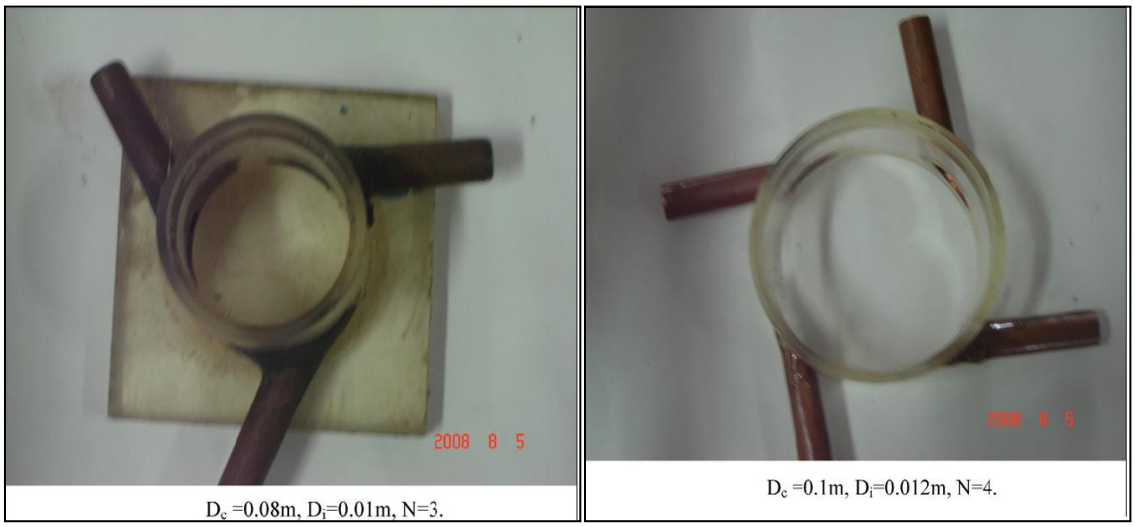

Figure 2.11: Typical column base assemblies used in swirled fluidized bed [38]

The work does not give any details of the distributor used. If there were no distributor then there is bound to be a dead zone at the base that makes the bed partially inactive. Even with a distributor, a uniform swirling motion cannot be sustained as compared to the swirling fluidized bed [39].

2.3.9 Swirling Fluidized Bed

Swirling fluidized bed (SFB) is another version of the toroidal fluidized bed (Figure 2.12), with an annular bed and inclined injection of gas through the distributor, and was first studied analytically by Sreenivasan and Raghavan [39]. The major difference between conventional fluidized beds and swirling fluidized beds is in the distributor design as shown in Figure 2.13. The fluidizing gas is injected through the distributor blades which are inclined at an angle to the horizontal, resulting in a swirling motion of the particles in a confined circular path. The gas entering the bed will have two components, horizontal and vertical. The vertical component supports fluidization while the horizontal component supports the swirling motion in the bed.

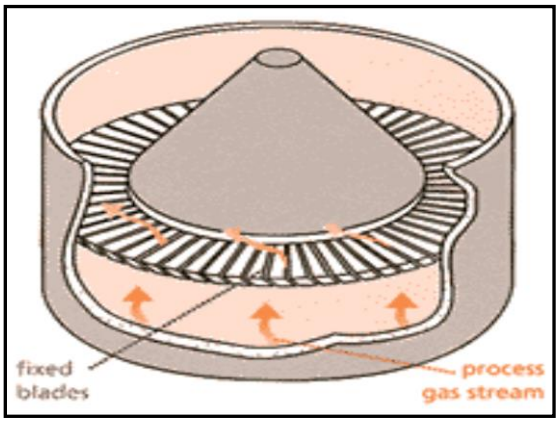

Figure 2.12: Construction of the swirling fluidized bed [39]

Sreenivasan and Raghavan [39] studied the hydrodynamic characteristics of fluidized bed with annular spiral distributors using a setup as shown in Figure 2.14. As the airflow rate is increased, they observed different kinds of bed behavior like bubbling, wave motion and swirl motion. They also observed two-layer fluidization

with a continuously swirling lower layer and a vigorously bubbling top layer. They reported that the superficial velocity required for stable swirl is higher for higher bed weight. Further, in the stable swirl zone, they noticed an increase in bed pressure drop with airflow rate and have suggested the effect of wall friction as the reason for this increase.

Vikram *et al.* [40] developed an analytical model for the prediction of hydrodynamic characteristics of a swirling fluidized bed. An annular distributor with a central cone was used for their study. According to them the swirl velocity increases linearly and bed pressure drop increases quadratically with superficial velocity. They have reported that, among the various aspects of the swirling fluidized bed, the distributor blade angle has a considerable influence on the bed characteristics such as bed pressure drop and swirl velocity while the effect of cone angle is negligible. They further reported that the swirl velocity as well as bed pressure drop decreases with an increase in blade angle. Raghavan *et al.* [41] observed that the superficial velocity and blade angle have a greater influence on the swirl characteristics than other parameters. However, large changes in blade angles can bring about a considerable variation in the bed characteristics. When gas penetrates deeper into the bed, the horizontal angular momentum of the gas is transferred to the particles. As a result, the horizontal component of gas velocity decays and the gas flow turns towards the vertical. In deep beds, a point will be reached where the gas flow direction becomes almost vertical. This results in multi-layer fluidization, with a shallow continuously swirling lower layer and a vigorously bubbling top layer [39, 40].

Sreenivasan and Raghavan [39] also reported that a considerable radial variation in the particle angular velocity is not desirable due to large energy and momentum losses caused by the inter-particle shear. This actually points to a need for a redesign of the distributor for uniform gas flow. Despite all the good qualities of the swirling fluidized bed, at very high superficial velocity the bed particles are seen to fly towards the periphery and there is an annular dead zone created at the center with gas bypassing through it. As a result, the available annular area is only partially utilized at high velocities.

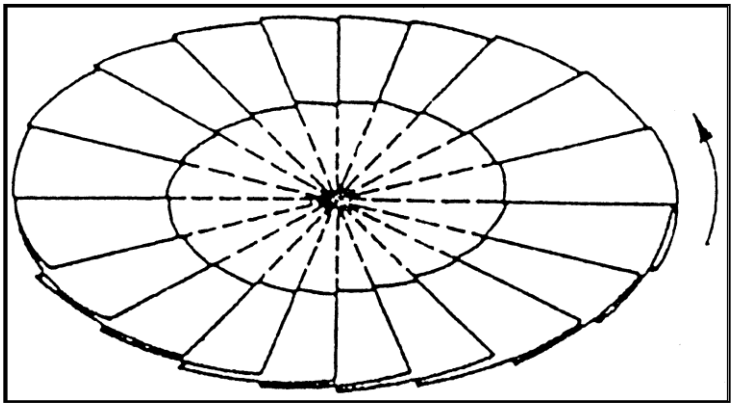

Figure 2.13: The annular spiral distributor as used by Sreenivasan and Raghavan. The airflow is in the counterclockwise direction [39]

2.4 Distributor Design

The distributor type influences the quality of fluidization [42] and has a vital role in fluidized beds. Their function is not only limited to introduction of the fluidizing gas/liquid, they also ensure good mixing between bed particles and fluid, promoting uniformity across the bed and most importantly, support the bed in the defluidized state. The desirable features of a good gas distributor may be summarized thus:

- induce a uniform and stable fluidization across the entire bed cross section
- prevent non fluidized regions on the grid
- operate for an extensive period without breaking
- reduce leakage of solids into the plenum chamber
- minimize maldistribution of the bed particles
- have enough strength to resist failure during operation
- support the weight of the static bed, and most importantly,
- have a low a pressure drop so as to minimize the power consumed.

All these requirements of a distributor may not be needed simultaneously and their relative importance depends on the application. Basically the distributors can be classified depending on the direction of gas entry to the bed. In the past,

designing of distributor was more instinctive than scientific, but recent studies have led to designs based on scientific principles.

A conventional gas fluidized bed can be divided into three zones: (i) the grid zone, (ii) bubbling bed zone and (iii) bubble erupting zone. The grid zone of a gas-solid fluidized bed is critical as any variation in this zone will in turn affect the behavior of the others zones. The grid zone at the same time is highly influenced by the gas distributor [42]. Hence the design of a distributor can affect not only the bed hydrodynamics but also thermal and species transport rates in fluidized bed operations [43].

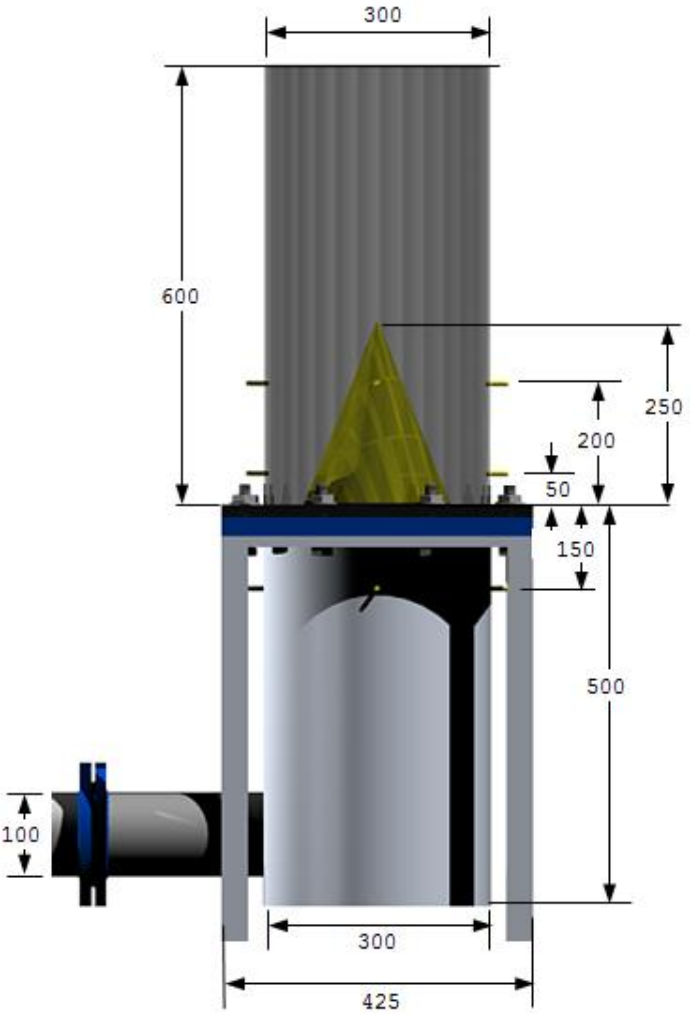

Figure 2.14: Schematic of the experimental set-up used by Sreenivasan and Raghavan [39].

An improper design of gas distributor would result in failure during operation and remains the primarily reason for most of the problems faced in fluidized bed operations [44]. A major concern in processes involving solid-fluid interaction is to accomplish rapid mixing of the solid particles and avoiding segregation of particles on the distributor; especially segregation as it may result in non- uniformity of bed properties like temperature, concentration etc. In cases which involve interactions with highly reacting, expensive gases like hydrogen etc., the distributor should be good enough to provide a uniform gas flow. The importance of a distributor is affirmed by Werther [45] as he found that it has a significant influence on the bubble flow rate, interaction area as well as transfer units in a gas fluidized bed.

2.4.1 General Considerations in Distributor Design and Factors Affecting it

The design and performance of the distributor, being an integral part, is critical to the performance of a fluidized bed. Even though over the decades there has been much development in the design of the distributor, it still remains as a challenge for the designer [44].

Properties of bed particle and fluid play an important role in the design of a successful distributor along with other design parameters like the critical pressure drop ratio, percentage area opening, geometry, dead zones, particle wear, mixing etc.

A major step in distributor design is to specify a pressure drop which should ensure satisfactory bed operation. Agarwal *et al.* [46] in their work proposed that Δp across the distributor should be about 10% of the bed pressure drop, while other researchers [47-50] suggested that the ratio of distributor to bed pressure drop ($\Delta p_d / \Delta p_b$) should be within the range of 0.02 to 1, with 0.3 as a generally used value [51].In order to appreciate how these apparently different values have come to be used, we must examine what the response of the system is to a disturbance.

From the Figure 2.15, it is understood clearly that the rate of change of distributor pressure drop with superficial velocity i.e. $d(\Delta p_d)/dU$ is the controlling

factor [51]. For a distributor, the Δp_d vs. U curve is always supra-linear, i.e., $d(\Delta p_d)/dU$ increases with the superficial velocity. It means that a distributor having a as high pressure drop will have a larger $d(\Delta p_d)/dU$ than one with a low pressure drop, at the same superficial velocity.

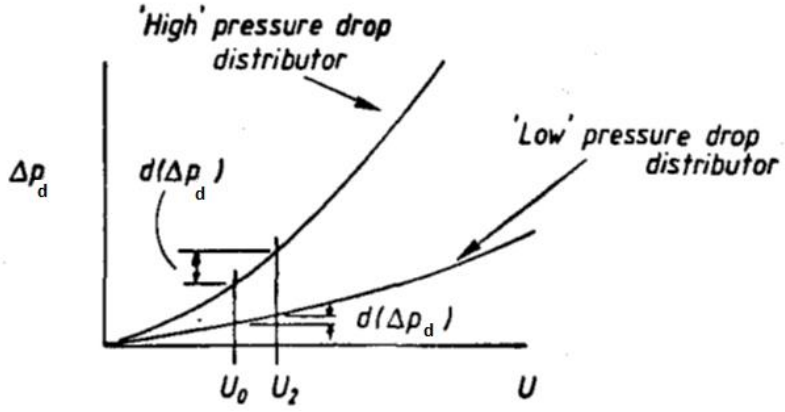

Figure 2.15: High and low pressure drop distributors [52]

In available literature, there is no general definition for fluidization stability. Nevertheless fluidization free from channelling can be considered to be uniform and relatively stable [42]. Gupta and Sathiyamoorthy [6] have discussed this aspect in detail. Researchers [53-57] over the years have tried to develop correlations with pressure ratio ($\Delta p_b/ \Delta p_d$) and velocity ratio (U/U_{mf}) to predict the stability of bed, mostly for the conventional bed. The stability conditions vary with range of superficial velocity, type of particles used, aspect ratio and other process requirements. There were even efforts to predict minimum fluidization velocityU_{mf} and critical velocity U_C which initiates complete fluidization [58-60], which were later on modified by [42, 61, 62], however complete success has been elusive.

2.4.2 Distributor Pressure Drop, Δp_d

The ratio of distributor pressure drop to bed pressure drop, as suggested in the above section, is one of the most important criterions for the distributor design. If the distributor pressure drop is too low in a fluidized bed, there will be a maldistribution of the flow, with fluidizing gas favoring the lowest pressure drop region to enter into the bed. Hence the distributor pressure drop should be large

enough to suppress any local pressure variations. The distributor pressure drop seems to be the critical factor to achieve and maintainer uniform and stable fluidization [63].

Besides the distributor type, the minimum ratio of distributor-to-bed pressure drop depends on various other factors like bed particles, bed depth, range of superficial velocity used, bed aspect ratio etc. [50]. As mentioned in the previous section, most of the successful industrial fluidized bed setups adopted distributor pressure drops based on the process involved with pressure ratio ranging from 0.02 to 0.5 [52].

Qureshi and Creasy [61] proposed an equation for overall pressure drop in a simple perforated plate distributor in the presence of a bed given by:

$$\Delta p_t = 5.33 \times 10^{-3} \left(\frac{d}{t}\right)^{1/4} U_O^2 \rho_O \tag{2.2}$$

where, d is the diameter of the orifices on the distributor, t thickness of the distributor plate, U_O velocity of gas through the orifice and ρ_O density of gas.

Saxena *et al.*[64] concluded from their experimental work that the distributor pressure drop increased with fluidizing velocity, decreased with percentage open area of the distributor and was independent of the bed weight or bed height for a given distributor type.

Chen and Cheng [65] concluded from their investigations using a perforated plate distributor that the distributor pressure drop increased in the presence of the bed particles. Otero and Munoz [66] conducted studies on the fluidization quality with bubble cap type plate distributor. They [66] reported that the particle flow back was due to the bed pulsations and this depends not only on the particle size but on the diameter and inclination of the holes in the cap as well.

Experimental investigations on multi orifice type distributors, which are extensively used in industries, revealed that the gas flow rate decides the number of operating orifices, bed height, type of bed particles and the percentage opening area of the distributor.

Based on their work, Sathyamoorthy and Rao [67] suggested an equation to determine the gas superficial velocity at which the entire orifices of the distributor become functional with uniform fluidization, given by:

$$U_{sup} = U_{mf}\,\{2.65 + 1.24\,log_{10}(\frac{U_t}{U_{mf}})$$

(2.3)

They also developed an equation for distributor pressure drop to bed pressure drop ratio ($\Delta P_d/\Delta P_b$) in terms of U_{mf} and U_{sup} :

$$\frac{\Delta p_d}{\Delta p_b} = C\,(\frac{U_{mf}}{U_{sup} - U_{mf}})^c$$

(2.4)

where the constant C is equal to 2.

The relationship was improved using experimental data as

$$\frac{\Delta p_d}{\Delta p_b} = 2.7(\frac{U_{mf}}{U_{sup} - U_{mf}})^{2.32}$$

(2.5)

In the case of multi-orifice distributors, if N is the total number of orifices on the distributor plate and *n* the number of operating orifices at any given gas flow rate, an equation for the ratio n/N was also recommended:

$$ln\,(1 - \frac{n}{N}) = -K\,(\frac{U - U_{mf}}{U_{mf}})$$

(2.6)

where K the proportionality constant is a function of the pressure drop ratio.

Sathiyamoorthy and Rao [57] used '+' and 'Y' shaped distributors for their experiments which revealed that for a given bed material the value of constant 'K'

was inversely proportional to both the bed height and the number of orifices in the distributor. It was also found that orifices near the centre of the distributor operate first and those on the outer periphery only with a subsequent increase in gas flow. The reason for such behaviour was that the resistance to the flow increases with the increase in distance of the orifice from the centre of the distributor.

Studies on multi-orifice plate distributors was also done by Whitehead *et al.* [50] to determine the minimum gas velocity at which all the orifices become operative resulting in uniform fluidization. A mathematical model to predict the number of active orifices at any given flow rate was proposed by Fakhimi *et al.* [68] in which they suggested the ratio ($\Delta P_{d,min}$ / ΔP_b) is a function of the orifice spacing, overall bed height, mean particle diameter and incipient fluidizing velocity at which all the orifices are operative.

Upadhyay [70]conducted experiments using multi-jet tuyere distributors and developed a relationship to predict the distributor pressure drop:

$$\Delta p_d = C U_O^{\,n} \tag{2.7}$$

where constants C and n would depend upon the slit width.

Investigations by Wen *et a1.* [69] on dead zone heights near the distributor plate indicated that the dead zone height depended on gas velocity, distributor type, orifice pitch and diameter along with particle size. Brik *et a1.*[71] designed a distributor with horizontal jets and inclined surfaces (HJIS), which induced sufficient mixing of the gas and the particles thereby eliminating both the heat and mass transfer problems.

2.4.3 Bed Pressure Drop, Δp_b

The pressure drop across the bed, as shown in Figure 2.16, is the most significant physical quantity measured as far as fluidized beds are concerned as it determines the quality of fluidization. An increase in bed pressure drop with increase in

superficial velocity and severe pressure drop fluctuations suggests a slugging regime whereas a decline in pressure drop indicates channelling [72].

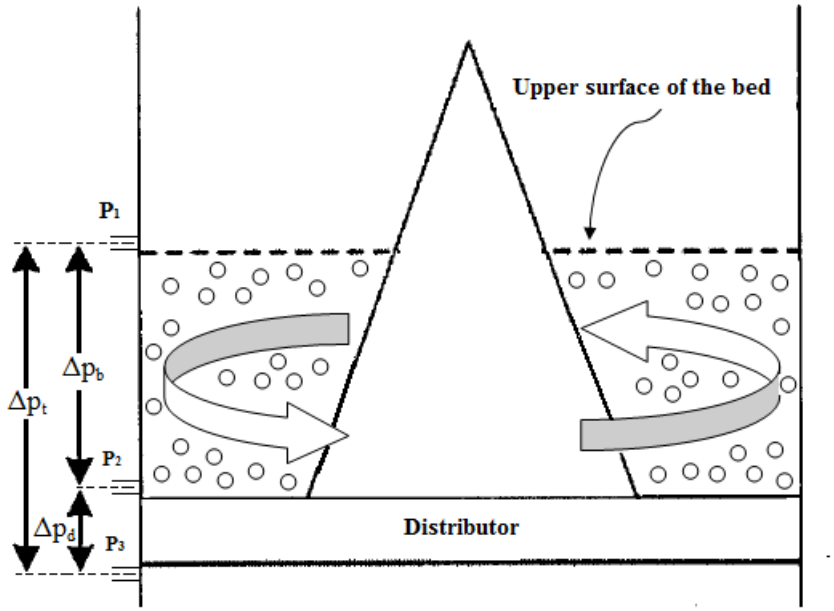

Figure 2.16: High and low pressure drop distributors

The factors affecting the bed pressure drop are the bed materials type and its weight per unit cross sectional area of the bed. De Groot *et a1*. [73] reported that for shallow beds, the bed pressure drop is equal to the value calculated on the basis of bed weight per unit area while for deeper beds, the actual bed pressure drop is lower than that calculated. Yang *et a1*. [74] developed a mathematical model and correlated it by experiments for predicting the pressure drop ratio in shallow fluidized beds. Static bed pressure drop represents the total weight of the fluidized particles divided by the cross sectional area of the bed. The relationship for pressure drop ratio, PR is given by

$$PR = \frac{Bed\ pressure\ drop}{Static\ bed\ pressure\ drop} = \frac{\Delta p_b}{\{\rho_p(l-\varepsilon_s)H_s\}} \tag{2.8}$$

The pressure drop ratio was seen to be increasing with increasing particle size for deeper beds. As for shallow beds of fine particles, the pressure drop ratio was observed to be independent of superficial gas velocity.

Sathiyamoorthy *et al.* [67] conducted experiments using two types of multi-orifice distributors and three types of bed materials and concluded that aspect ratio has a significant effect on the quality of fluidization. Aspect ratio (R) is defined as the ratio of bed height (H) to the diameter of the bed (D) with the bed height usually taken at the minimum fluidizing velocity. The bed is usually designated as a deep bed if the aspect ratio is more than 1 and shallow bed when the aspect ratio less than or equal to unity. They further observed that there exists a critical value of aspect ratio where the quality of fluidization is maximum, which is influenced by the operating velocity and the type of the distributor used.

Investigations on the variation of bed pressure drop with superficial velocity were conducted by [64, 75-77]. The influence of various parameters such as type of the distributor, bed geometry, particle size and size distribution, bed temperature and bed pressure was studied. It was concluded that at all superficial velocities greater than the minimum fluidizing velocity, the bed pressure drop remained constant. Gelperin *et al.* [78] proposed the following relation based on his studies on centrifugal fluidized bed to determine the maximum bed pressure drop, usually occurring at minimum fluidizing velocity.

$$\Delta p_{bmax} = \frac{W_O \omega_O{}^2}{2\pi r l} \tag{2.9}$$

where W_o is the bed weight at minimum fluidization

Kroger *et al.* [14] developed a mathematical equation for predicting the bed pressure drop in rotating fluidized beds and observed during their work that fluidization commenced at the lower edge of the bed where the inner diameter of the vortex, R_I has its smallest value and centrifugal forces are smaller. It was also pointed out that fluidization occurred earlier in a deep rotating bed than in a shallow

rotating bed as the r_i is small for a larger bed mass. Takahashi *et al.* [15] in experiments with a bed rotating about an axis horizontally, conclude that the experimental values of maximum bed pressure drop closely agreed with the calculated values.

Upadhyay *et al.* [70] noticed that there is 15-20% reduction in bed pressure drop compared to the static bed pressure and was mainly due to partial fluidization with 15-20% of the bed remaining unfluidized. Bouratoua *et al.* [79] suggested that the dip in pressure drop after minimum fluidizing velocity is due to the presence of an additional force along the walls, the wall friction exerted on particles flowing down along the walls, which compensates the up flow of particles in the wake of bubbles there by supporting the fluidized particles.

Sreenivasan and Raghavan [39] studied the swirling fluidized bed and developed the following mathematical model to predict the bed pressure drop and validated it with experiments on a swirling fluidized bed using two different sizes of spherical particles.

$$\Delta p_b = \frac{kM_b}{am} + \psi\omega^2 \tag{2.10}$$

where a is area of the bed, ψ is a constant, k is the fraction of the bed weight supported by fluidising gas, ω angular velocity m and is the mass flow rate between a pair of blades and M_b is mass of the bed.

Ellias *et al.* [80] conducted studies on the bed hydrodynamics of gas solid turbulent fluidized beds with the help of pressure transducers, optical probes and capacitance probes and concluded that the superficial velocity, at which the turbulent flow regime occurs, depended on the aspect ratio. Mohanty *et al.* [81] studied the effect of different types of promoters: co-axial rod, disk and blade on bed fluctuation and expansion in a gas-solid fluidized bed with varying distributor open areas. It was found that bed fluctuation ratio was more affected by mass velocity than static bed height, particle density and size. Also the fluctuation ratio

increased with increasing static bed height until about twice the minimum fluidizing velocity but reduced at higher velocities.

In their study on hydrodynamic characteristics of sand conical beds Kaewklum and Kuprianov [82] suggested that there were three different bed modes; (a) fixed-bed mode (where $U_{sup} < U_{mf}$), (b) partially fluidized-bed mode ($U_{mf} \leq U_{sup} < U_{mff}$) and (c) fully fluidized-bed mode(at $U_{sup} \geq U_{mff}$).They also formulated equation for each zone.

For packed bed mode

$$\Delta p = Ah\,(r_0/r_1)\,U_0 + Bh\left\{\frac{[r_0(r_0^2 + r_0r_1 + r_1^2)]}{3r_1^3}\right\}U_0^2 + \frac{1}{2(u_0^2/\varepsilon_0)^2}\left[\left(\frac{r_0}{r_1}\right)^4 - 1\right]\rho_f \tag{2.11}$$

where

$$A = 150\left[\frac{(1-\varepsilon_o)}{\varepsilon_o^3}\right]\left[\frac{\mu_f}{(\Phi_s d_p)^2}\right]$$

and

$$B = 1.75\left[\frac{(1-\varepsilon_o)}{\varepsilon_o^3}\right]\left[\frac{\rho_f}{\Phi_s d_p}\right]$$

From Figure 2.17 if the bed radius at the air distributor, r_0, is given, the top radius, r_1, is readily determined from geometrical consideration (using r_0, h and θ).

For partially fluidized-bed mode

$$\Delta p = A(h-h_b)\left(\frac{{r_0}^2}{r_1 \times r_b}\right)U_0 + B(h-h_b)\left\{\frac{[{r_0}^4(r_b^2 + r_br_1 + r_1^2)]}{3r_1^3r_b^3}\right\}U_0^2 + (1-\varepsilon)(\rho_s - \rho_f)gh_b + 1/2\,U_0^2 \times [(1/\varepsilon_0)^2(r_0/r_1)^4 - (1/\varepsilon)^2]\rho_f \tag{2.12}$$

For fully fluidized-bed mode, the pressure drop Δp will be equivalent to pressure drop at minimum fluidization, Δp_{mff} and will remain constant.

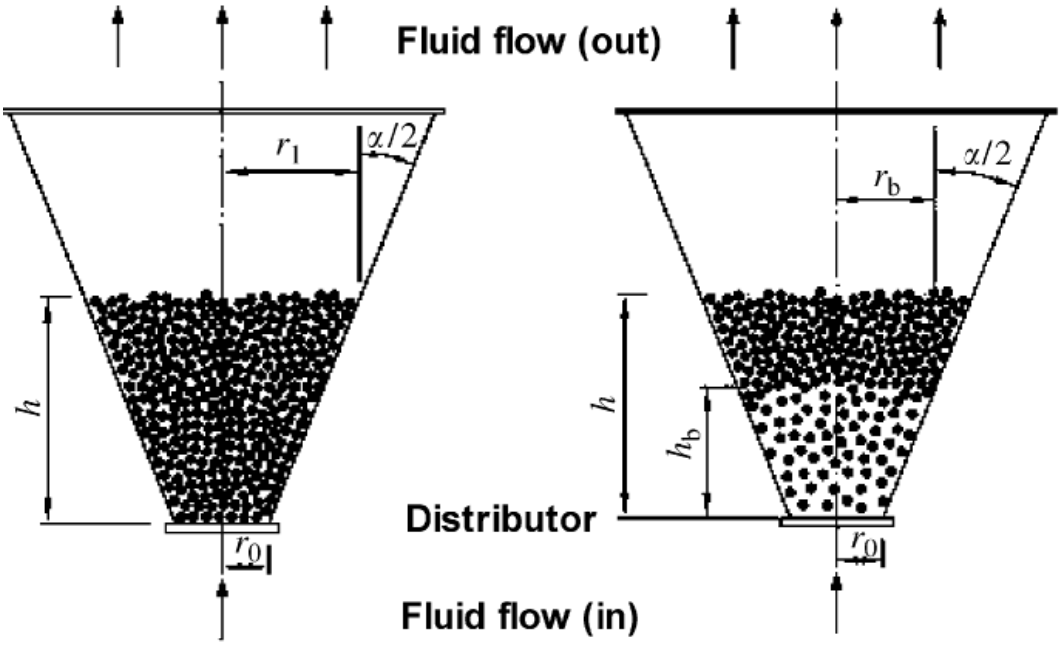

Figure 2.17: Sand conical beds in (a) fixed and (b) partially fluidized state [82].

2.4.4 Minimum Fluidizing Velocity, U_{mf}

Minimum fluidizing velocity (U_{mf}) can be determined from the plot of bed pressure drop versus superficial velocity. When the fluidizing gas flows through a bed of particles in the packed bed region, initially the bed pressure drop increases linearly with increase in superficial velocity and reaches a maximum. At this point the bed gets fluidized and is referred to as incipient fluidization. In the fluidized region any further increase in superficial velocity would not bring a change in the bed pressure drop. Then the intersection point of the inclined fixed bed regime and the horizontal fluidized bed regime is the minimum fluidization velocity. Evaluation of minimum fluidization velocity is a necessary step in the design and operation of fluidized beds.

Kunii and Levenspeil [10] have demonstrated the development of equation for U_{mf} from Ergun equation (2.1), rearranging the quantities and substituting values at incipient condition

we have

$$(\rho_p - \rho_f)g = 150\frac{(1-\varepsilon)^2}{{\phi_s}^2\varepsilon^3}\frac{\mu U_{mf}}{D_p^2} + 1.75\frac{(1-\varepsilon)}{\phi_s\varepsilon^3}\frac{\rho_p {U_{mf}}^2}{D_p} \tag{2.13}$$

The above quadratic equation can be written as equation

$$K_1 Re_{p,mf}^2 + K_2 Re_{p,mf} = Ar \tag{2.14}$$

For small particles with $Re_{p,mf} < 20$

$$U_{mf} = \frac{D_p^2(\rho_p - \rho_f)g}{150\mu}\frac{{\phi_s}^2\varepsilon^3}{(1-\varepsilon)^2} \tag{2.15}$$

For large particles with $Re_{p,mf} > 1000$

$${U_{mf}}^2 = \frac{\phi_s\varepsilon^3}{1.75(1-\varepsilon)}\frac{D_p}{\rho_p} \tag{2.16}$$

Wen and Yu [83] suggested the following expression to predict the minimum fluidizing velocity in conventional fluidized beds.

$$\frac{d_p U_{mf}\rho_g}{\mu} = \{(33.7)^2 + 0.0408 d_p^3\rho_g\frac{(\rho_p - \rho_g)g}{\mu^2}\}^{0.5} - 33.7 \tag{2.17}$$

Experimental investigations in hot fluidized bed by Botteril *et al.* [75] revealed that minimum fluidizing velocity decreases with increase in the operating temperature for group B materials whereas for Group D materials, the minimum fluidizing velocity increased with increase in operating temperature. Nakamura *et*

al. [77] conducted experimental investigations to study the variation of minimum fluidizing velocity with temperature and pressure in a conventional bed. They observed that the minimum fluidization velocity decreased progressively with pressure in the low pressure region however decline was more rapid in the high pressure region. Also the minimum fluidization velocity showed an inconsistent behaviour with variation of temperature for different sizes of particles.

The variation of U_{mf} with particle density and size is an interesting aspect to be investigated and is summarized in Table 2-1. The references are taken from [84].

Table 2-1: Summary of various correlations for U_{mf} in terms of density and particle diameter [84]

S. No.	Author	Exponent of density, ρ	Exponent of particle diameter, d_p
1.	Davies and Richardson	1	2
2.	Frantz	1	2
3.	Pillai and Raja Rao	1	2
4.	Rowe and Henwood	1	2
5.	Doichev and Akhmanov	1	1.84
6.	Miller and Logwinuk	0.9	2
7.	Leva *et al.*	0.94	1.82
8.	Bena	0.9	1.0
9.	Wen and Yu	-0.5	0.5
10.	Goroskho	-0.5	0.5
11.	Riba *et al.*	0.7	1.98

Another set of formulas with the following form is also proposed. The general dependency seems to be like that of Goroshko. The general formula developed by Wen and Yu is given below

$$Re_{mf} = [(A^2) + B \times Ar]^{0.5} - A \tag{2.18}$$

Various efforts made to realize the constants A and B are summarized in Table 2-2.

Table 2-2: Summary of various correlations for U_{mf} in terms of Archimedes number [84]

S. No.	Author	Value of A	Value of B
i.	Wen and Yu	33.7	0.0408
ii.	Saxena and Vogel	25.28	0.0571
iii.	Babu *et al.*	25.25	0.0651
iv.	Richardson and Da St. Jeronimo	25.7	0.0365
v.	Thonglimp	31.6	0.042
vi.	Bourgeois and Grenier	25.46	0.0382
vii.	Chitester *et al.*	28.7	0.0494

Shu *et al.* [35] conducted hydrodynamic studies on a toroidal fluidized bed reactor with a distributor consisting of blades inclined at an angle of 25° to 30° to the horizontal held in an annular ring. They observed that there was no significant variation between a toroidal fluidized bed and a conventional fluidized bed in the matter of transition from fixed bed to minimum fluidization and suggested an equation for evaluating the minimum fluidizing velocity in a TORBED as follows

$$U_{mf,TORBED} = \frac{U_{mf}}{Sin\theta} \tag{2.19}$$

Sreenivasan and Raghavan [39] in their studies on swirling fluidized bed observed that the minimum bubbling velocity values compare well with the calculated minimum fluidisation velocity obtained from a correlation suggested by Chitester *et al.* [85] for coarse particles in a conventional bed:

$$Re_{p,mf} = [(28.7)^2 + 0.0494\ Ar]^{0.5} - 28.7 \tag{2.20}$$

Moreno *et al.* [86] noted that in a vibrofluidzed bed the minimum fluidization velocity was reduced up to three times compared to those in a non-vibrated bed based on their experimental study. Sobrino *et al.* [31] while performing

experiments to study the influence of rotational speed of the distributor plate on the hydrodynamics of the fluidized bed found that the minimum fluidizing velocity decreased with increase in rotational speed.

Kaewklum *et al.* [87] studied tangential and axial air entries into the plenum of the conical swirling fluidized bed and developed a correlation for the annular spiral distributor:

$$U_{mf} = \frac{0.06\,\mu/}{(d_p/\rho_f)} \left\{\frac{\left[\rho_f d_p^3 \left(\rho_s - \rho_f\right)\right] g}{\mu^2 \left(\frac{h}{D_O}\right)^{1.67}}\right\} \tag{2.21}$$

Kaewklum and Kuprianov [37] in their work on conical swirling fluidized-bed combustor revealed that with increasing d_p, U_{mf} increased to some extent creating an increase of Δp_{mf} and other hydrodynamic characteristics, U_{mff} and U_{msf}. Also for all d_p, the variation of pressure drop with respect to U in the fully swirling-fluidized condition is same, showing same pressure drop at similar bed heights.

Faizal *et al.* [88] in their work on swirling fluidized bed concluded that the sequence of flow regimes in swirling fluidized bed are packed bed, minimum fluidization, swirling regime, two-layer regime and finally elutriation or transport regime, with deep beds forming partially fluidized regime and two-layer beds. They also suggested the following.

a) The hydrodynamics of swirling fluidized bed is entirely different from a conventional fluidized bed

b) Larger particles have lower pressure drop and larger overlap angle imposes additional pressure drop,

c) Particle size and bed weight were found to be the most important variables that influenced the bed behaviour. Even though blade geometry had an effect on the bed behaviour, it was relatively small.

Mohideen *et al.* [89] suggested that radial inclination, i.e., sloping of distributor blades in a swirling fluidized bed (SFB) affects the bed hydrodynamics, reduces both distributor and bed pressure drops significantly with no variation in minimum fluidization velocity U_{mf}. They also noted that the radial inclination of distributor blades prolonged the swirling regime, avoiding the formation of the two-layer bed regime in deep beds. Radially inclined distributor is also seen to reduce distributor pressure drop and total pressure drop, especially for the smaller particles.

2.4.5 Variants of Distributors used in Fluidized Beds

Fluid Distributors for fluidized bed can be classified based on their design and construction and advancement in features. Figures 2.18 and 2.19 show some of the distributors commonly used.

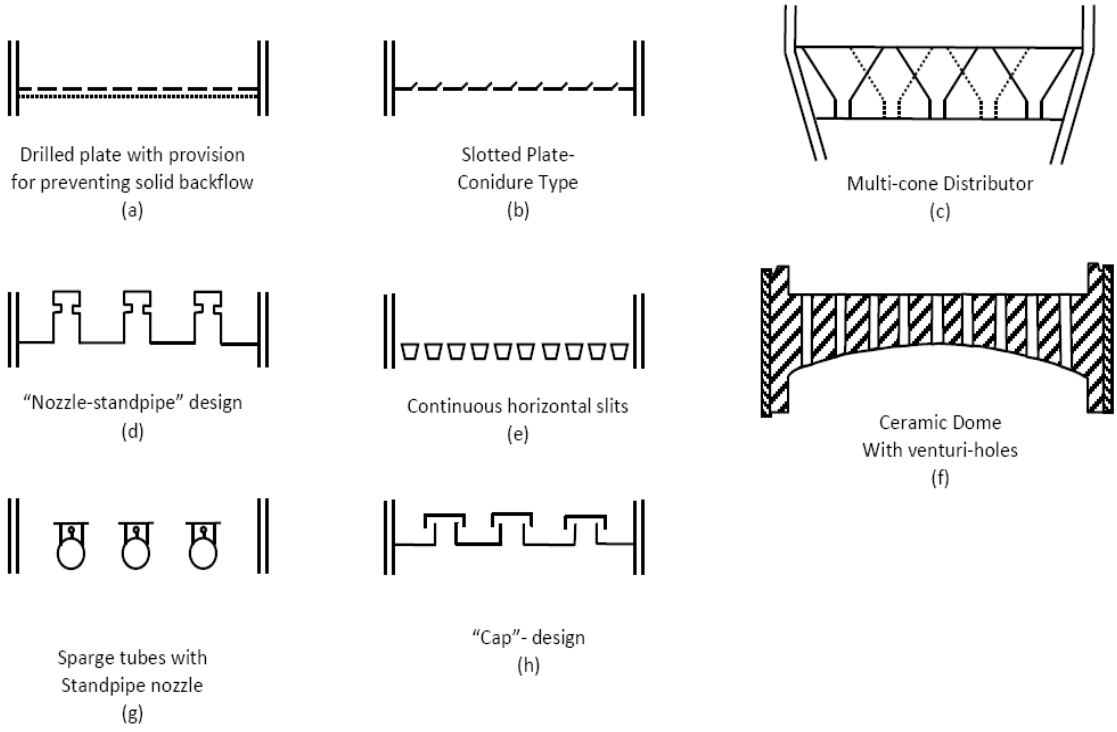

Figure 2.18: Examples of distributors in common use [44]

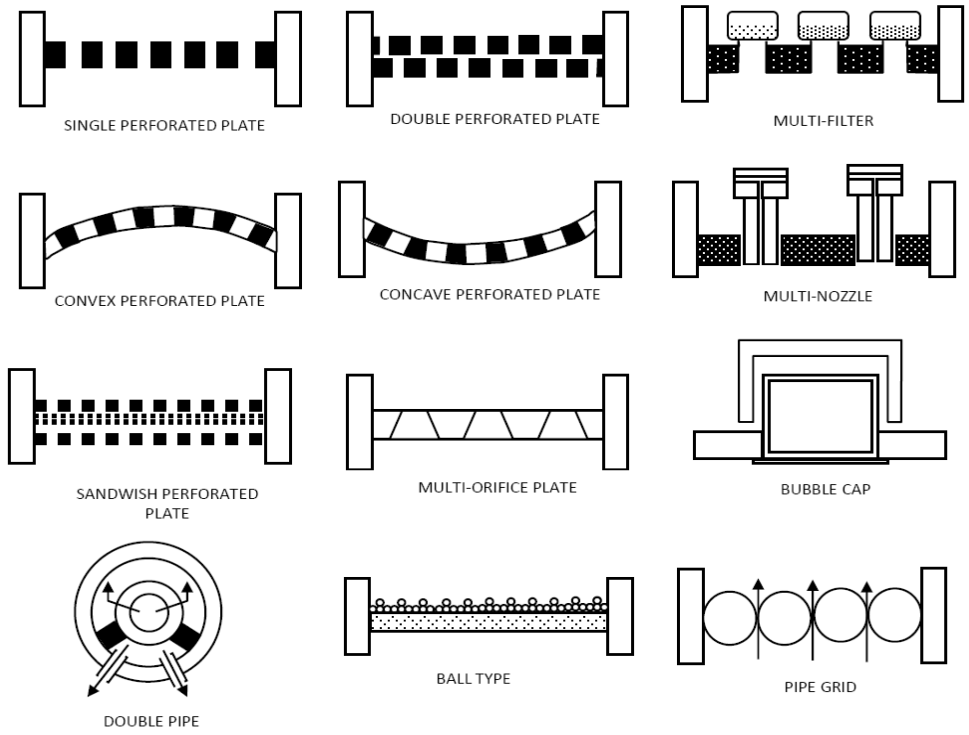

Figure 2.19: Examples of distributors in common use [44].

2.4.5.1 Various Perforated Plate Distributors

According the studies of Sathiyamoorthy and Masayuki [42], using two different types of multi orifice distributors (Table 2-3), the critical aspect ratio for highest quality of fluidization is most influenced by the distributor type. They also found that for a multi-orifice distributor, pressure drop approaches the behavior of a porous plate in empty bed condition and does not change a great deal at operating velocities much above the minimum fluidization velocity when coarse and dense materials are used as bed material. Distributor type was also found to have a remarkable influence on shallow beds.

Wormsbecker *et al.*[90] investigated three different distributors to establish the effect of distributor design on the hydrodynamics of a fluidized bed dryer, that were are shown in Figure. 2.20 and Figure. 2.21 with more details. The first one of these was a Dutch Weave mesh distributor with triangular shaped openings having base and height dimensions of about 25 and 90 μm, respectively. The percentage area of opening was estimated to be about 15 %. The perforated plate distributor had 256

holes of 2.7 mm diameter on a 7.5 mm square pitch, with a resultant open area of 9.5%. The punched plate distributor with hooded openings, each of 5.75 mm by 1 mm, where the openings were oriented along a pitch circles with 3 mm between adjacent rows. This orientation is designed to produce a swirling effect in the bed. This had a calculated open area of 9.6%.

Table 2-3: Details of multi orifice distributors [42]

Distributor type	Number of orifices, N	Orifice diameter d_O (mm)	Free area, Φ (%)	Orifice spacing in a triangular array(mm)	Plate thickness, t (mm)	Plate thickness at the orifice, t_O (mm)
A	121	0.95	0.273	16.6	6.1	0.8
B	325	0.8	0.52	10	5.0	0.8

In this study researchers found that the punched plate distributor needs shorter drying times than the other two. The positive influence of the punched plate may be more evident with larger bed loads i.e. larger bed depths.

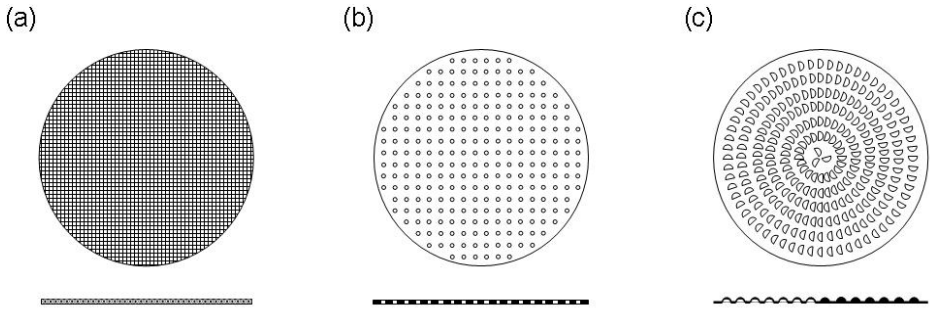

Figure 2.20: Distributor designs (a) Dutch weave mesh; (b) Perforated plate; (c) Punched plate [90]

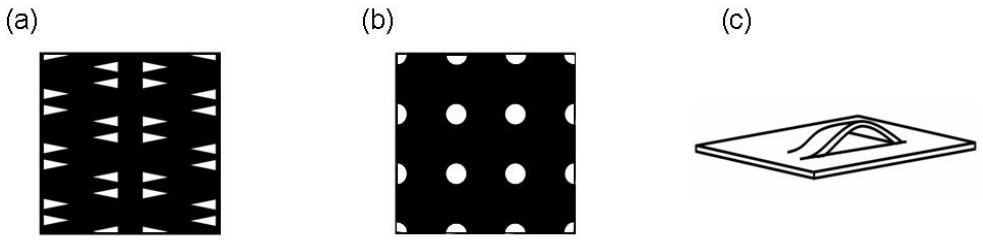

Figure 2.21: Details of distributor designs (a) Dutch weave mesh; (b) Perforated plate; (c) Punched plate [90]

Sobrino *et al.* [31] used distributors as shown in Figure 2.22 for their rotating distributor fluidized bed. One of them has a uniform pitch another one is with a spiral pitch, both having circular holes of 2 mm diameter.

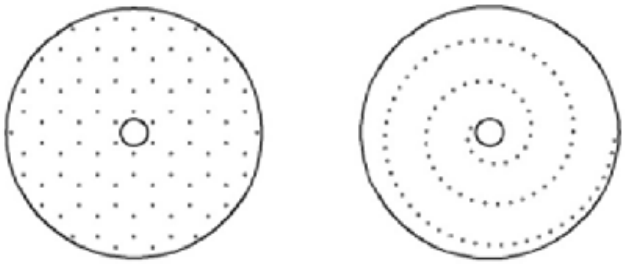

Figure 2.22: (a) Uniform pitch distributor (b) Spiral pitch distributor [31]

The uniform pitch distributor looks much similar to one used in a conventional bed and will have similar disadvantages also. Whereas in case of spiral distributors the pressure drop across the distributor is likely to be very high and may also lead to uneven fluidization and a lot of dead spaces.

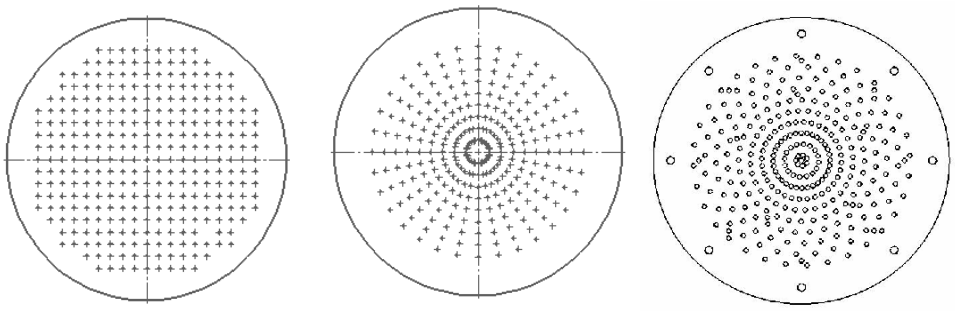

Figure 2.23: Distributor design, (a) square pitch distributor (SPD), (b) circular pitch distributor (CPD) and (c) semi-circular pitch distributor (SCPD) [91]

In another work by Batcha *et al.* [91] three different types of perforated plate type distributor were used, these were made by drilling 4mm diameter holes on a 5 mm thick Perspex plates. The estimated fraction of open area (FOA) of all these distributors was about 13%. The same FOA is important to ensure that equal comparison was being made during testing. Each distributor differs in terms of pattern and pitch. These distributors are designated as the square-pitch distributor (SPD), circular pitch distributor (CPD) and semi-circular pitch distributor (SCPD). Though the distributor plates are 260 mm in diameter, the effective area for

fluidization was limited to 200 mm, in accordance to column diameter which encloses the bed. Figure 2.23 shows the distributor configurations.

Researches in this particular work evaluated the performances of three perforated type gas distributor in terms of pressure drop and quality of fluidization with Geldart type-D particles. Although the three distributors, (a) Square Pitch Distributor (SPD) (b) Circular Pitch Distributor (CPD) and (c) Semi- Circular Pitch Distributor (SCPD) differ in their design and construction, they have same opening area. From the study conducted it was found that SPD had better performance than the other two distributors.

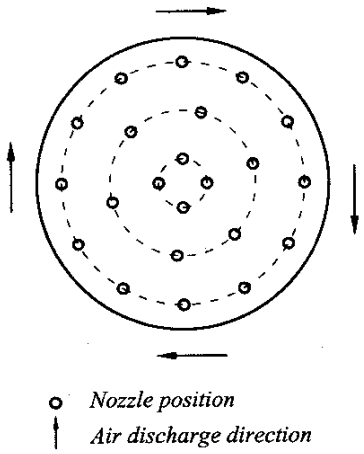

Figure 2.24: A Schematic diagram of the fluidized-bed [92]

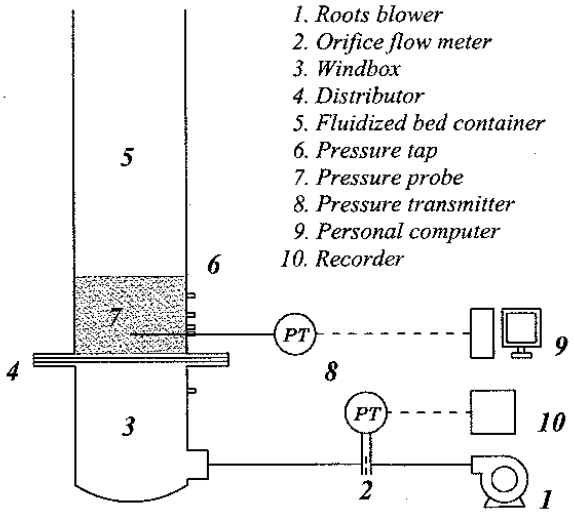

Figure 2.25: Illustration of the multi-horizontal nozzle distributor (top-view) [92]

In their study Chyang *et al.* [92] investigated the influence of a swirling fluidizing pattern on the fluidization characteristics and elutriation of fines as well. The swirl fluidizing pattern of a multi-horizontal nozzle distributor and that of a conventional distributor with axial fluidizing pattern of perforated plate in a gas-solid fluidized bed were compared.

The schematic of the apparatus is shown in Figure 2.24. The nozzles were arranged in three concentric circles with discharges all of them in clockwise direction, Figure 2.25, was used. Three different tubes of inside diameter 4.3, 6.8 and 9.8 mm were used for the nozzles providing open-area ratios of 0.5, 1.2 and 2.5% respectively. For comparison, three perforated plates, as in Table 2.2, based on the same open-area ratio were employed.

The multi-horizontal nozzle distributor generated an innovative swirling fluidizing which improved both the fluidization quality as well as reduced the elutriation. Chyang *et al*. [91] concluded that by modifying the fluidizing pattern it is possible to improve the fluidization quality and elutriation reduction without the need of any auxiliary equipment.

Table 2-4: Details of the distributors used by Chyang *et al.* [92]

Distributor A		Distributor B	
Type	multi-horizontal nozzle distributor	Type	perforated plate
Nozzle diameter mm	4.3, 6.8, 9.8	Orifice diameter [mm]	0.9, 1.4. 2.0
Distributor Arrangement	22 horizontal nozzles arranged in three concentric circles with all discharge exits directed clockwise	Distributor Arrangement	535 holes drilled on a triangular pitch of 11. 8 mm
Open-area ratio $.\varphi_d$	0, 5, 1.2, 2.5	Open-area ratio $.\varphi_d$	0, 5, 1.2, 2.5

The idea to produce an improved swirl was novel, but nozzles can disturb the flow and mixing of particles at the lower bed heights and need continuous cleaning of the nozzles as it may be clogged by the dust and fines or the particles itself.

Furthermore the pressure drop across the distributor has to be measured and compared with the conventional in order to confirm its superiority.

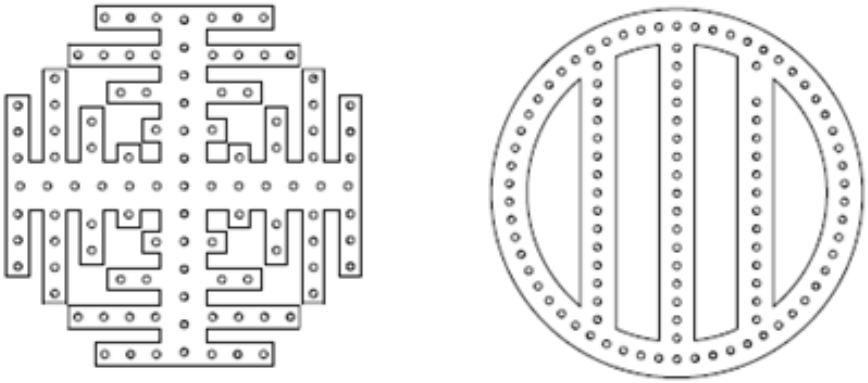

Figure 2.26: Branched pipe distributor and circular pipe distributor [92]

Wang *et al*. [93] in their work used branched pipe distributor and circle pipe distributor in the circulating fluidized bed system as shown in Figure 2.26. The distributors are made of stainless steel pipe and equipped with nozzles of diameter 2 mm.

They concluded that the solid concentration in the dense phase area is directly proportional to r/R (ratio of standpipe diameter to distributor diameter) and initial bed height, while inversely to axial distance and superficial gas velocity. As for the effect of distributor shape, the solid particles were well distributed in case of branched pipe distributor with 5% porosity.

2.4.5.2 Various Annular distributors with blades/Vanes

Dodson [33] patented TORBED consisting of a gas distributor with angled blades in an annular distributor in Figure 2.27. The spiral distributor consisted of overlapping blades, shaped as sectors of a circle with an opening between the blades. Sreenivasan and Raghavan [39] proposed a swirling fluidized bed (SFB) similar to the toroidal fluidized bed, with an annular bed and inclined injection of gas through the distributor.

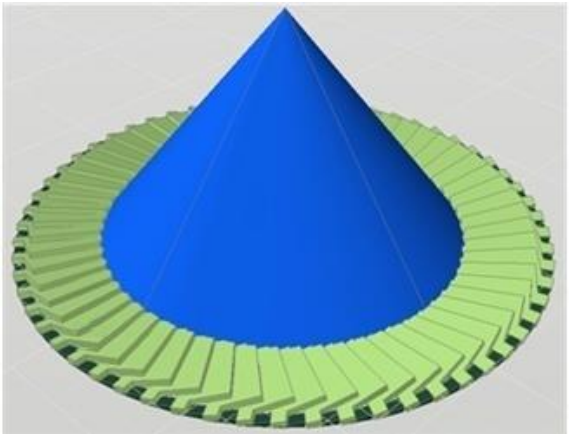

Figure 2.27: Annular spiral distributor

The annular spiral distributor consists of blades that are truncated sectors of a circle with each blade inclined at an angle to the horizontal. A hollow metallic cone was placed at the centre of the bed to avoid particle accumulation and dead zone.

Kumar *et al.* [94] in their work investigated three different types of distributors: Type-1distributor with inclined blades in a single row, fabricated by inserting the blades in a slotted ring at an angle to the horizontal as shown in Figure 2.28.The openings between the blades were trapezoidal in shape and the total area of opening was 5692.5 mm^2, utilizing about 15% of the distributor area.

The Type-2 perforated plate distributor with inclined holes was made by drilling a Perspex plate of 25 mm thickness. All the inclined holes were on the same circular pitch as shown in Fig 2.28. There were 502 such holes each of inner diameter 5 mm providing an opening area of 9818 mm^2. In this case, the open area was about 10% of the total distributor area.

The Type-3 distributor with three rows of inclined blades was fabricated with blades in three rows as in Figure 2.28. Sixty blades were provided at the outer row, forty five blades in the middle row and in the inner row there were thirty blades. The total area of opening was 5105 mm^2. This works out to about 13% of the distributor area.

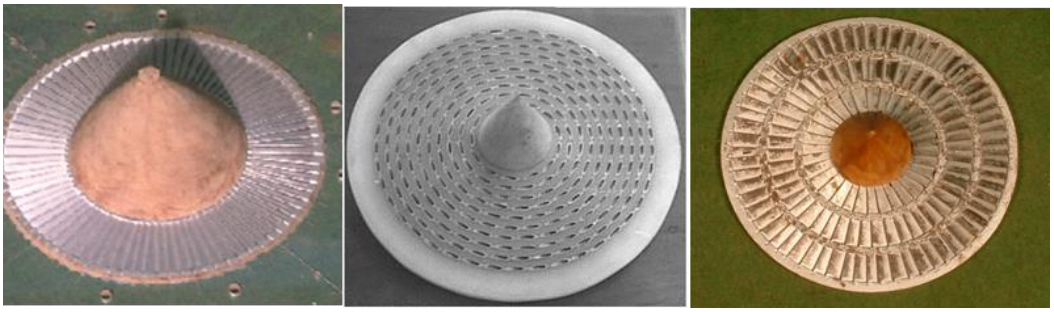

(a) (b) (c)

Figure 2.28: Type 1, Type 2 and Type 3 distributors [92]

The open area was the least for Type 2 and the maximum for type 1. Accordingly, the distributor pressure drop was highest for Type 2. Unlike the conventional fluidized bed, where the stability of operation of the bed depended on the distributor pressure drop, the advantageous feature of the swirling bed is that its successful operation did not critically depend on the distributor pressure drop. However, the Type 3 distributor offers flexibility in matching the mean gas velocity to the bed radius. Thus the gas flow is more uniform in Type 3.

2.4.6 Summary

The above literature study connected with different types of fluidized beds shows that each variant has its own merits and shortcomings. Some of them, such as the rotating distributor are mechanically too complex. Others such as the conical bed or swirling by means of lateral gas injection are only suitable for custom applications. The annular swirling fluidized bed (SFB) with inclined injection of gas has been chosen here for comprehensive investigation as it reveals the potential for application in a variety of industrial processes and deserves further development. The studies hitherto on SFB have not led to a complete understanding of the physics and the interrelationship between various operating parameters. Inherent questions on underutilization of annular distributor area, ideal distributor design, accumulation of bed particles at the periphery at high superficial velocities, lack of

knowledge on different regimes of operation and their characteristics, and effect of various aspects on the hydrodynamics of the bed still remain.

All this points to a gap in knowledge that needs to be resolved in order to apply the swirling fluidized bed and to further expand its utilization. Among the large number of unknowns in this promising technology, the present research aims to investigate the individual aspects of the fundamental problem in detail, namely the hydrodynamics of the SFB for the Type 1 (annular spiral) distributor, with the objective of exploiting the potential for improvement and widespread application of swirling fluidized bed.

The Type 1 distributor is selected for more intensive study as it combines the advantages of ease of fabrication, flexibility in varying the distributor parameters and potential for scaling up. Furthermore, it has the lowest pressure drop of the three types available. The tables below summarize the most important and relevant results.

CHAPTER 3

DESIGN OF EXPERIMENTAL SETUP AND METHODOLOGY

3.1 Chapter Overview

This chapter discusses the design and fabrication of the experimental setup along with the distributor, with explanation of the rationale for the design. The distributor is an essential part of a fluidized bed and the swirling fluidized bed is no different. In this work a flexible design of annular distributor is used, and the design and fabrication details of the same are explained in detail in this chapter. The experimental setup used was designed, fabricated and assembled in accordance with fluid mechanics fundamentals as well as Malaysian design standards. This chapter also explains the methodology followed in the entire work in order to achieve the objectives and also briefly discuss the instrumentation used for measurement of various parameters during the work.

3.2 Design Calculations for the SFB Setup

The first step in the design of a fluidized bed setup is the calculation of minimum fluidization velocity and from there, the flow rate and pumping power required. Swirling fluidized bed being a newer version of fluidized bed, correlations or equations are not available in the literature for calculation of minimum fluidization velocity. However, it can be recognized that in the packed bed state, the inter-particle friction is such that the freedom of motion required for swirling cannot be attained; the particles need to be physically separate before swirling can occur. This condition of particle separation occurs exactly at minimum fluidization. Thus in the packed bed and up to incipient fluidization, the SFB is similar to a conventional bed

and equations pertaining to minimum fluidization velocity in conventional fluidized beds apply for the basic design calculations.

The minimum fluidization velocity is considered one of the most important factors to design the swirling fluidized bed, and it can be calculated from the equation suggested by Wen and Yu [83].

From the equation (2.18), it is observed that diameter of the particles and their density are two variables which control the minimum fluidization velocity. Hence, for design of the swirling fluidized bed setup, taking the maximum diameter of the particles to be 0.001 m (10 mm) and nominal density of the particles as 1000 kg/m^3, the minimum fluidization velocity (U_{mf}) will be equal to 1.77 m/s (Appendix A). A factor of 2 is chosen to determine the blower capacity so as to include the uncertainty in velocity prediction and in blower specifications. Hence the maximum velocity that can be applied to the particles by the system is calculated to be 3.54 m/s. Based on previous work [39] the outer and inner diameters of the bed are chosen as300mm and 200mm respectively and the distributor area is 0.13 m^2. Based on these values the maximum flow rate is calculated to be 0.46 m^3/sec and the blower is specified for this flow rate.

As for the static pressure rise of the blower, taking into consideration all the pressure losses in the pipe elements from the blower up to the distributor and the bed, the Δp value is calculated. For a chosen pipe diameter of 0.10 m and 6 m length, the friction factor f for PVC pipes selected from Moody's chart corresponding to a Reynolds number based on a pipe diameter of 100 mm is 41,400 is 0.016 and the pressure loss along the line is calculated to be 24 Pa. A reasonable value of 200 Pa and 150 Pa is assumed for pressure drop across the plenum chamber and the distributor respectively[8, 9]. For calculation of pressure drop across the bed, the maximum bed height is assumed to be 200 mm and the bulk density to be 70% of the particle density. The Δp across bed is calculated as ≈ 1400 Pa. Hence the total pressure drop Δp_{total} is calculated as 1750 Pa = 175 mm of water. These are conservative values, intended to ensure that the system will operate satisfactorily.

The blower power was calculated from the Δp_{total} and flow rate determined earlier. After considering the motor efficiency and fan efficiency, the power was estimated to be 2.3 kW ≈ 3.1hp. Based on the calculations, a blower of 5hp (next standard power rating available close to the calculated value) with a flow rate of 1600 m^3/hr. was chosen.

3.2.1 Fabrication and Assembly of Experimental Setup

The experimental setup (Figure 3.1) consists of a blower to supply air at the required flow rate, controlled by a motor controller. PVC piping connects the blower outlet to the plenum chamber, with an orifice meter appropriately fitted in between. The length of piping was calculated as per Malaysian design standards, taking into consideration the losses that could occur due to the inclusion of flanges, bends and orifice plate. The piping was supported by adjustable supports which were custom made. Butterfly valves were inserted in the pipe line for further control of the airflow.

Figure 3.1: Blower and blower stand

The distributor support made of Bakelite and the cylindrical fluidizing column made of Perspex rest above the plenum chamber. The Perspex cylinder is joined to a Perspex flange which is then secured along with the Bakelite base and rubber gaskets to the plenum chamber flange.

The blower shown in Figure 3.2 is supported by a frame made of mild steel and grouted to the floor with bolts with a rubber gasket in between in order to isolate the blower vibrations from the flooring.

3.2.1.1 Design and fabrication of the plenum chamber

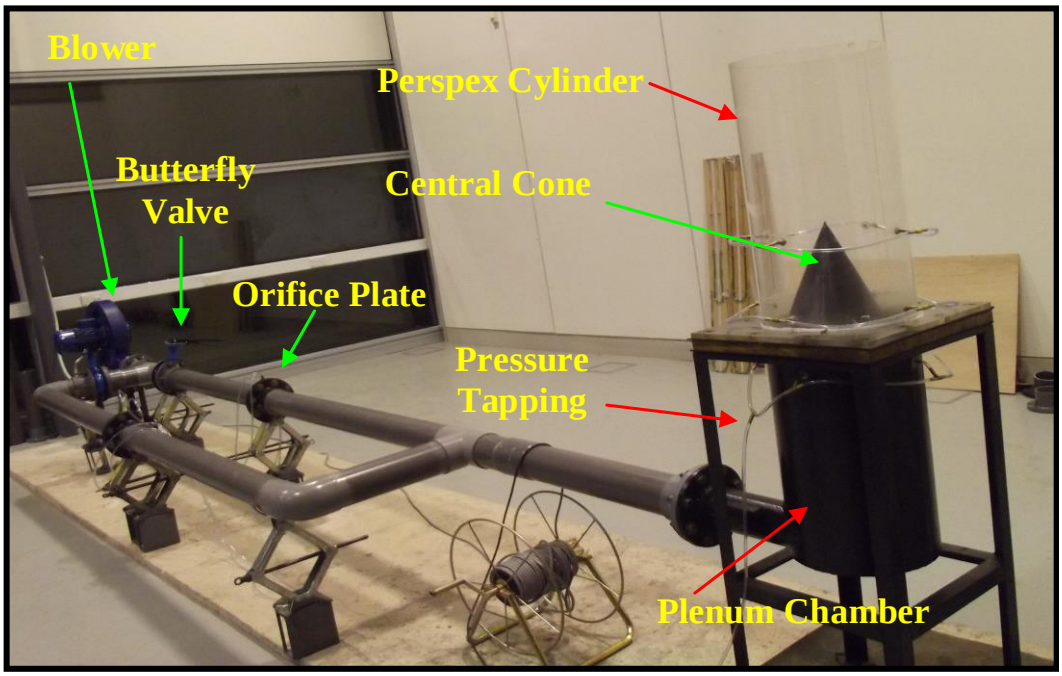

Figure 3.2: Swirling fluidized bed experimental set up

The plenum chamber or wind box is an important part of any fluidized bed as shown in Figure 3.3. The main function of the plenum chamber is to reduce the fluctuations in the air flow and provide a smooth flow towards the distributor of the fluidized bed.

The plenum chamber height was chosen as 500 mm, in order to smoothen the flow and provide a steady up-flow into the fluidized bed through the distributor. The entry of air into the plenum chamber is also important as discussed by Othman *et al.* [95] as they studied the effects of different entries into the plenum chamber of the SFB. Based on the above work, the plenum chamber entry was designed to be tangential, with an anti-clockwise rotation of flow and without any center body.

The plenum chamber was fabricated in 3 mm mild steel sheet with inner diameter of 300 mm. The entry pipe diameter was 100 mm with a flange connection to the plenum chamber. The upper part of the plenum chamber was a square-shaped flange 425×425 mm and 15 mm thickness with 12 equally spaced 10 mm holes, drilled.

The plenum chamber was attached to a stand with an overall height of 900 mm and four legs to support the weight. Inside the chamber a cylinder of 8mm thickness with a diameter of 205 mm is welded coaxially using three metal rods of 4 mm diameter to the inner wall at a depth of 70 mm from the plenum chamber flange. This is to support the central hub on which the distributor inner rings will rest. The purpose of the plenum chamber stand, as shown in Figure 3.4, was to keep the plenum chamber inlet flange in-line with the air flow line and to protect the base of the chamber.

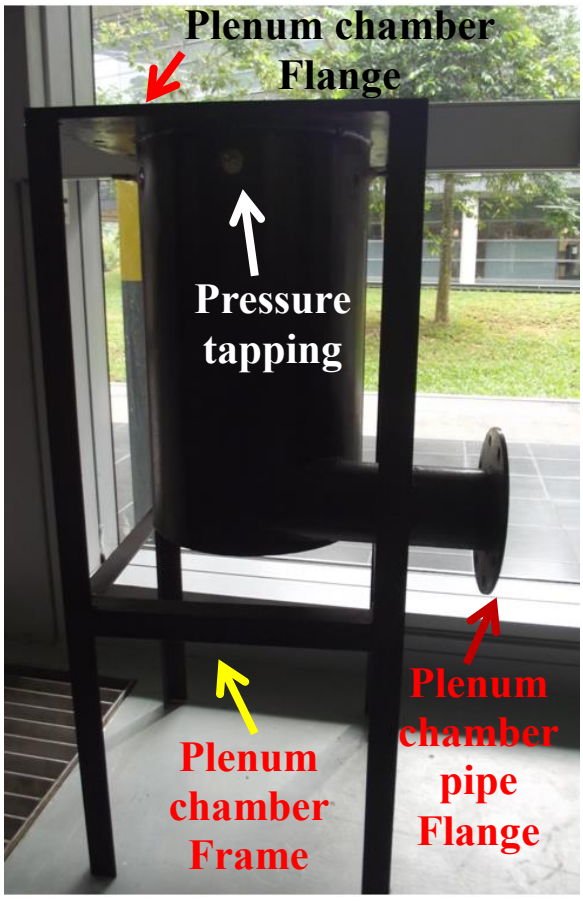

Figure 3.3: Plenum chamber

3.2.1.2 Fabrication of Bed Column

The bed column is made up of a Perspex cylinder of 300 mm inner diameter, 5 mm thick and 600 mm long. The column is attached to a 12.5 mm thick square Perspex flange of 425 × 425 mm, with 12 holes of 12.5 mm diameter drilled to secure it with the Bakelite and plenum chamber flange.

A piezometric ring made of 4 mm inner diameter flexible hose connecting 4 tappings, is attached at two points on the column as shown Figure 3.5.This is to measure the pressure difference across the points during the experiment. Scales with 1mm graduations are attached to the Perspex wall at three points, equidistant from each other. A cone fabricated from mild steel with height 250 mm and base diameter 200 mm , is attached to the center of the bed in order to avoid a dead zone at the center.

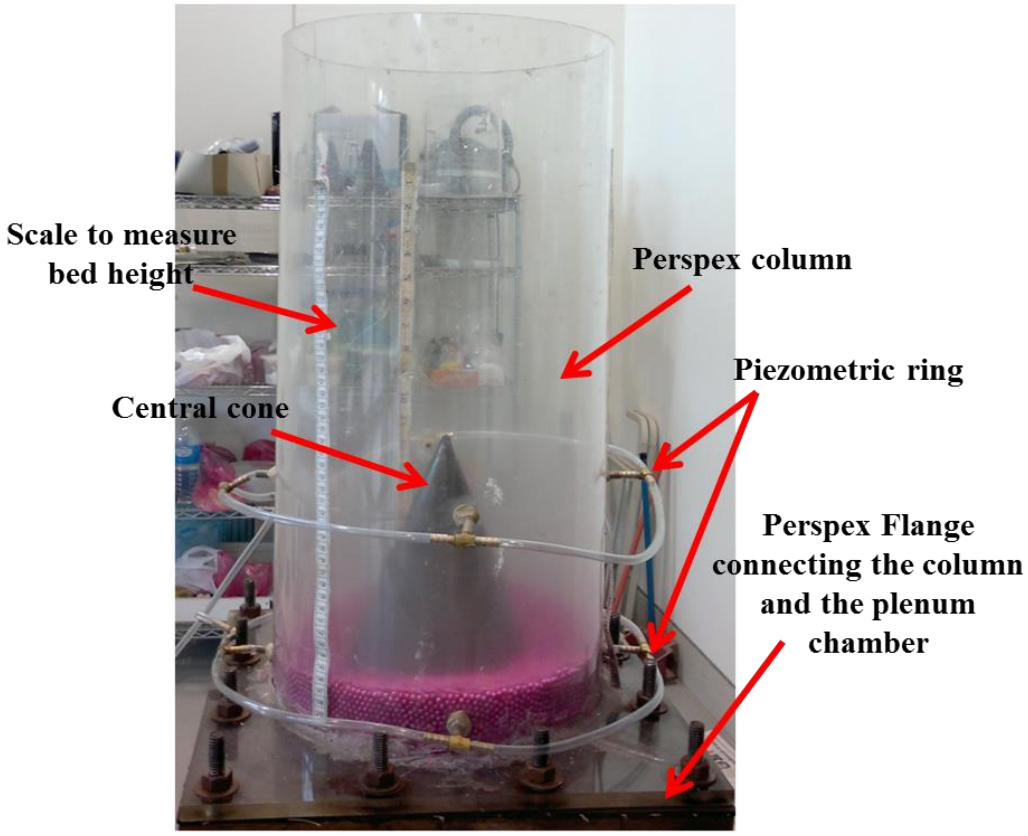

Figure 3.4: Perspex bed column

3.2.1.3 Design of the Flow Line and Orifice plate

3.2.1.3.1 Design of Orifice Plate

To measure the flow of air from the blower to the plenum chamber, orifice plates are used. The prime motive of using orifice plates is that they measure flow rates to a fair accuracy without disturbing the flow. Compared to other flow measuring devices it is easy to design and fabricate, and moreover it is inexpensive.

The orifice plate was designed based on Malaysian standards [96]. There were two orifice plates, designed for high flow and low flow respectively placed in parallel. Two mild steel flanges, one on each side of the orifice plate were also designed and fabricated so as to facilitate the attachment of orifice plate to the flow line. The flanges are designed with a 10 mm groove (OD 139 mm, ID 129 mm)with 8mm depth connected to a 2 mm hole drilled at the periphery of the flanges to which pressure taps were attached so as to communicate the pressure variations to the measuring device. Detailed drawing provided in appendix D

Table 3-1: Design details of the orifice plate

Aspect	**Value**
d / D ratio	0.513 (low flow); 0.62(high flow)
D, diameter of pipe	100 mm
Outer diameter of orifice	256 mm
Thickness of the plate	4 mm
Taper angle	50^{o}
Material	ASTM A36

Six 12.5 mm bolts, 5mm long, secured the orifice plate between two flanges with two rubber gaskets, one on each side of the plate, to prevent any leakage. A taper angle of 50^{o} was selected based on the design standards.

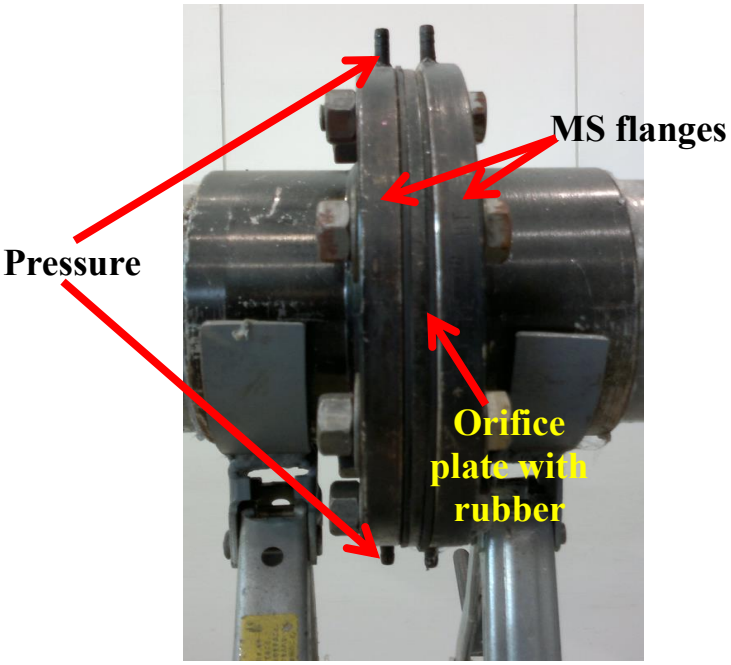

Figure 3.5: Orifice meter assembly

The orifice plate was assembled with the flanges with rubber gaskets in between as shown in Figure 3.5.

3.2.1.3.2 Design of Flow Line

The flow line with overall length of 6 m includes blower flange with attachment, bellows to isolate vibration, butterfly valves and orifice plate assembly. The flow line is designed abiding to the Malaysian standards. The orifice plates are positioned at 8D (800 mm) upstream and 15D (1500 mm) downstream from any disturbance-causing attachments, like bend, elbow, joint, valve etc. in order to maintain the accuracy. The flow pipe is made of PVC of 100 mm inner diameter and 7.25 mm wall thickness. The parts of the piping are connected to each other using PVC flanges (except for orifice meter) with an inner diameter of 115 mm, OD of 256 and 100 mm long, having 8 bolt holes each, 12.5 mm in diameter.

The entire flow line is supported with adjustable custom-made supports as shown in Figure 3.6. These supports are made out of readily available car jacks.

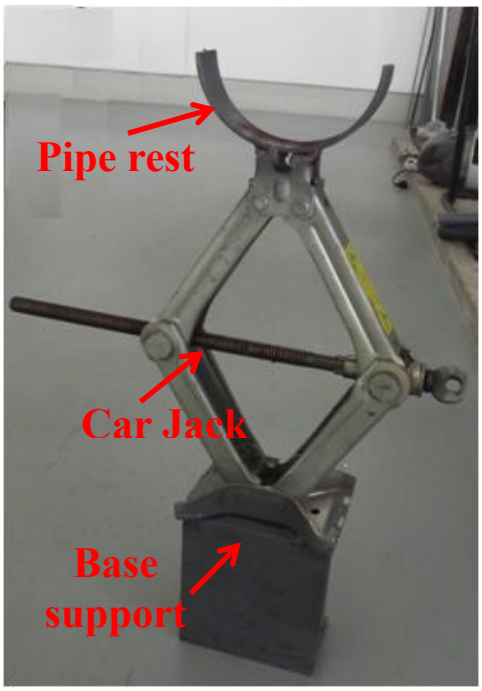

Figure 3.6: Pipe support

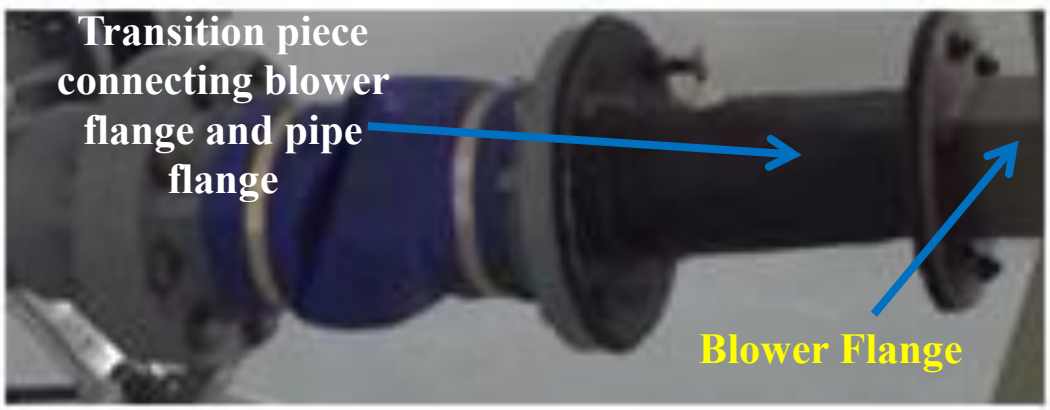

Figure 3.7: Blower flange and attachment

The blower flange is attached to the circular piping with a transition piece as the blower opening is square shaped. The transition piece has an opening of 72 mm square on the blower side and develops into a 100 mm circular opening on the downstream side. It was fabricated in mild steel and was attached to a PVC flange as shown in Figure 3.7. A bellow made of rubberized tarpaulin cloth, as shown in

Figure 3.8 is connected between blower flange and the piping flange, to avoid vibrations from being transmitted to the piping.

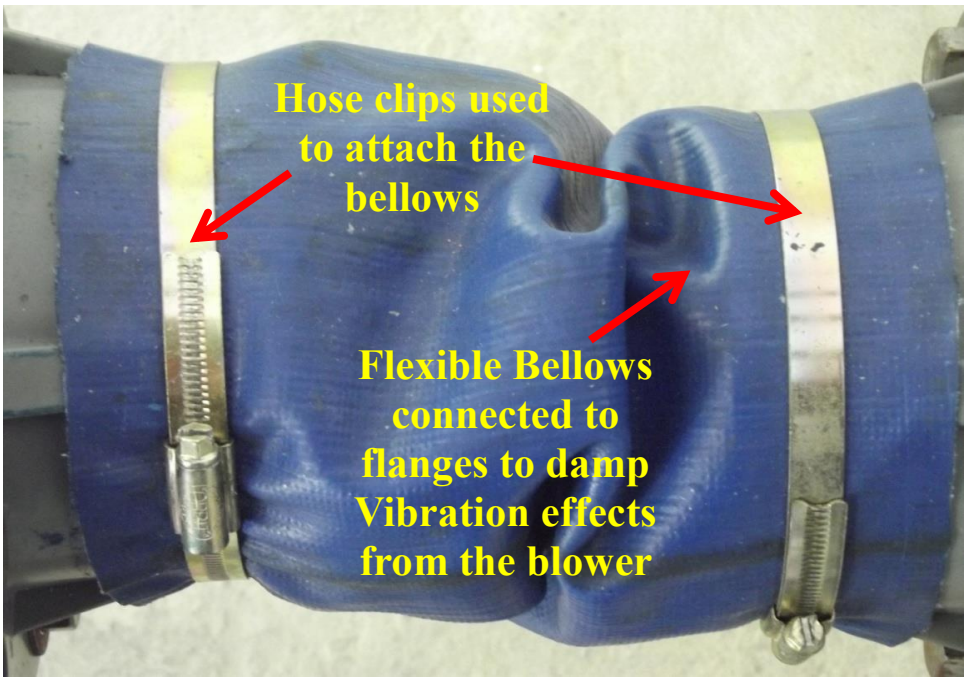

Figure 3.8: Flexible joint using bellows to isolate vibrations

3.2.2 Design and fabrication of the distributor

The annular spiral distributor for the swirling fluidized bed has been designed as per the work of Sreenivasan and Raghavan [39], Figure 3.9. In his work Paulose [97] also used a similar distributor as shown in Figure 3.10, fabricated using same technique, mostly hand made by a skilled technician. This was usually fabricated out of Perspex or mild steel. But most of these distributors lacked consistency and uniformity. The distance between the blades and their inclination with the horizontal were inconsistent. The most important problem about these distributors was that they were not flexible. For any change in blade width or blade inclination, the entire distributor had to be re-fabricated. Not only does this increase the cost but it also increases the complexity of handling the SFB processes and makes it difficult to modify the existing system.

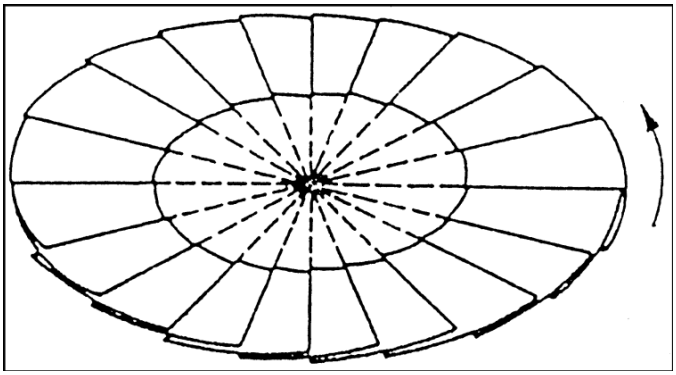

Figure 3.9: The annular spiral distributor as used by Sreenivasan and Raghavan [39]

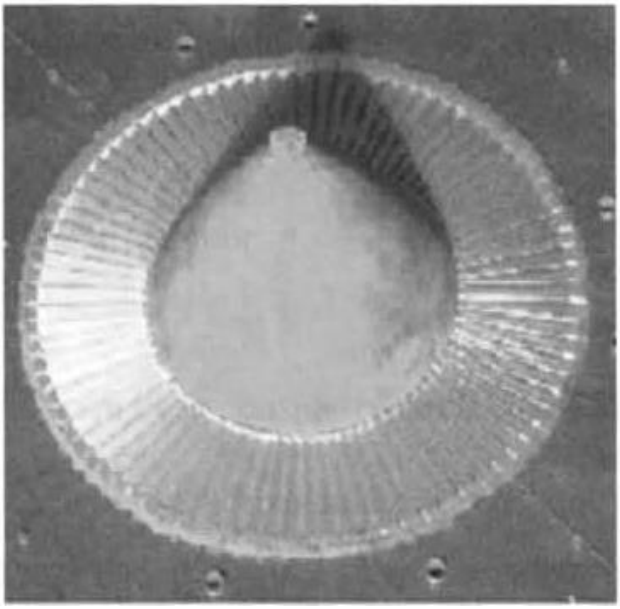

Figure 3.10: The distributor as used by Paulose [97]

To make the distributor easier to use, the flexible annular spiral distributor was designed. The design is based on the previously used annular spiral distributor but making it more flexible and easy to fabricate and use. The whole distributor was split into parts and designed separately. There are four rings, two outer and two inner, with sets of blades of different overlap angles. The rings were machined with 60 steps of the required angle of inclination, as the distributor was meant to have 60 blades. The outer rings, one at the top and other at the bottom, were with outer diameter 320 mm and 300 mm inner diameter, flush with the column inner diameter. The thickness of each ring was 10 mm.

The inner set of rings, top and bottom, are similarly machined and are of outer diameter 200 mm and inner diameter 180 mm.The outer ring is supported by the distributor flange with bottom ring sitting in the slot cutting the flange made of Bakelite. As for the inner ring, it is supported by a central hub, made of aluminum and machined. The blades are arranged on the slots cut on the rings and are secured in position by the top ring.

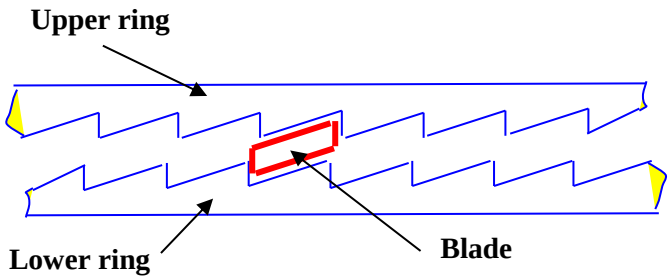

Figure 3.11: Section view describing assembly of blades and distributor rings

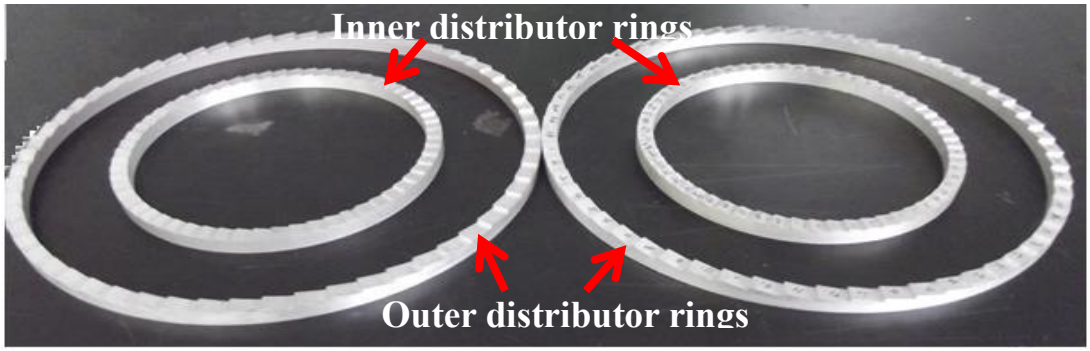

Figure 3.12: Outer and inner rings of annular spiral distributor realized

Figure 3.13: Central hub of annular spiral distributor realized

The set of inner and outer distributor rings fabricated in aluminum is shown in Figure 3.12; meanwhile Figure 3.13 shows the central hub fabricated also from aluminum.

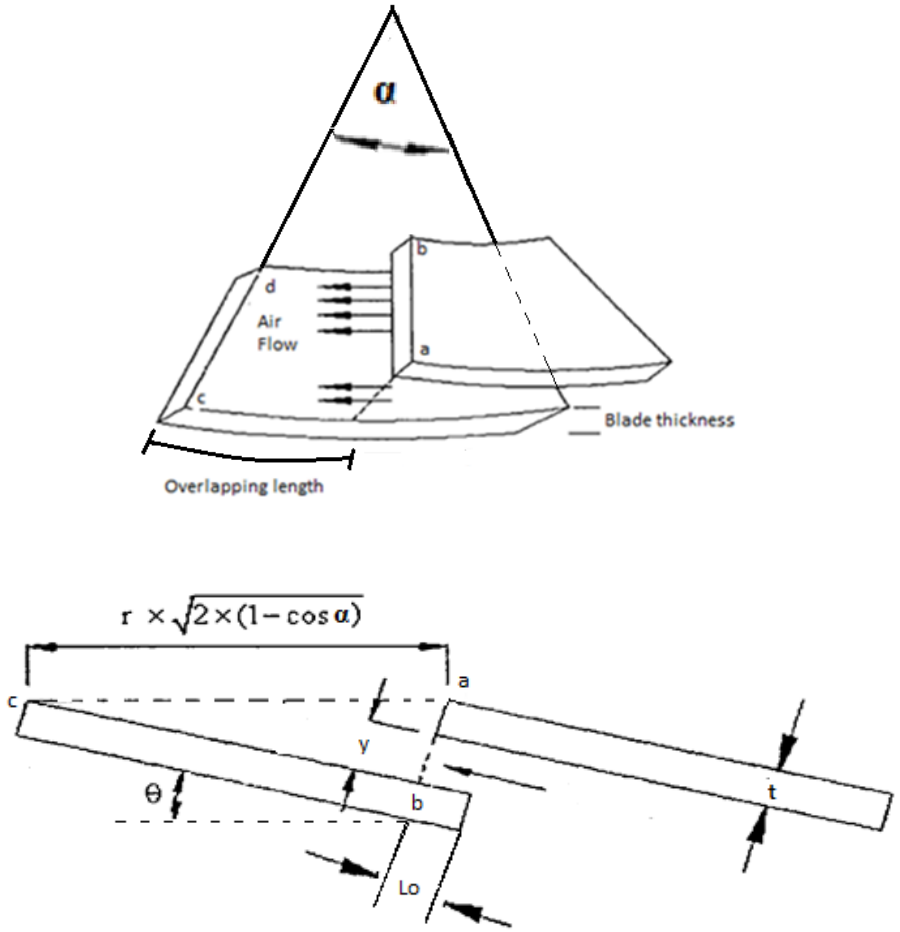

Figure 3.14: Detailed blade drawing depicting design parameters [95]

An annular spiral distributor of swirling fluidized bed consists of overlapping blades with a trapezoidal shape opening between consecutive blades, thereby forming an annulus between the outer and inner radii of the distributor. The blades are designed based on literature [8, 97] but modified as the blades used in previous studies were in the shape of truncated sectors. In this work the blades are in a trapezoidal shape with extended fin on each side for seating the blade on the distributor rings. The design process basically consists of determination length and width of the blade for given set of parameters like inclination angle (θ), overlap

angle (α) and number of blades. From Figure 3.14 considering points 'a' and 'c' on top edge of two adjacent blades at radius r, the distance between these two points is given by the relation

$$ac = r \times \sqrt{2 \times (1 - cos\alpha)} \tag{3.1}$$

where r is the radius and α is the angle of overlap.

The gap between the blades (y) at radius r, is given by

$$y = r \times \sqrt{2 \times (1 - cos\alpha)} \times sin\,\theta - t \tag{3.2}$$

where t is the thickness of the blade

Area of opening,

$$\text{Ao} = \frac{(y_i + y_O)}{2}(r_O - r_i)$$

$$= [\frac{\sqrt{2 \times (1 - cos\alpha)}}{2} \times sin\,\theta \times ({r_O}^2 - {r_i}^2) - t \times (r_O - r_i)] \tag{3.3}$$

where r_O and r_i are outer and inner radii respectively.
If n is the total number of blades used in the distributor then total area of opening

$$\text{A}_{\text{to}} = n \times [\frac{\sqrt{2 \times (1 - cos\alpha)}}{2} \times sin\,\theta \times ({r_O}^2 - {r_i}^2) - t \times (r_O - r_i)] \tag{3.4}$$

The annular bed area, $\text{A}_\text{b} = \pi({r_O}^2 - {r_i}^2)$ (3.5)

Hence Percentage area of opening

$$= \frac{n \times [\frac{\sqrt{2 \times (1 - cos\alpha)}}{2} \times sin\,\theta \times ({r_O}^2 - {r_i}^2) - t \times (r_O - r_i)]}{\pi({r_O}^2 - {r_i}^2)} \tag{3.6}$$

Length of blade, $r = (r_o - r_i) + 2l$ (3.7)

where l is the length of fins provided on each side of the blade to seat it as shown in Figure 3.15.

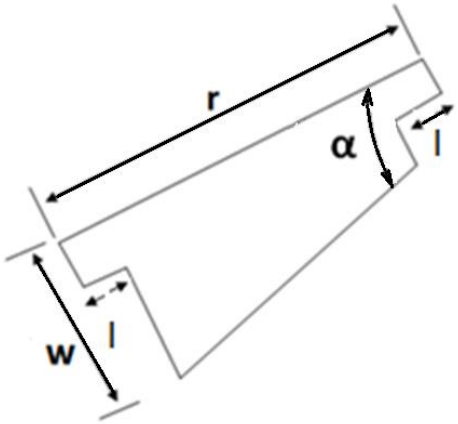

Figure 3.15: Trapezoidal shaped blade used in the work

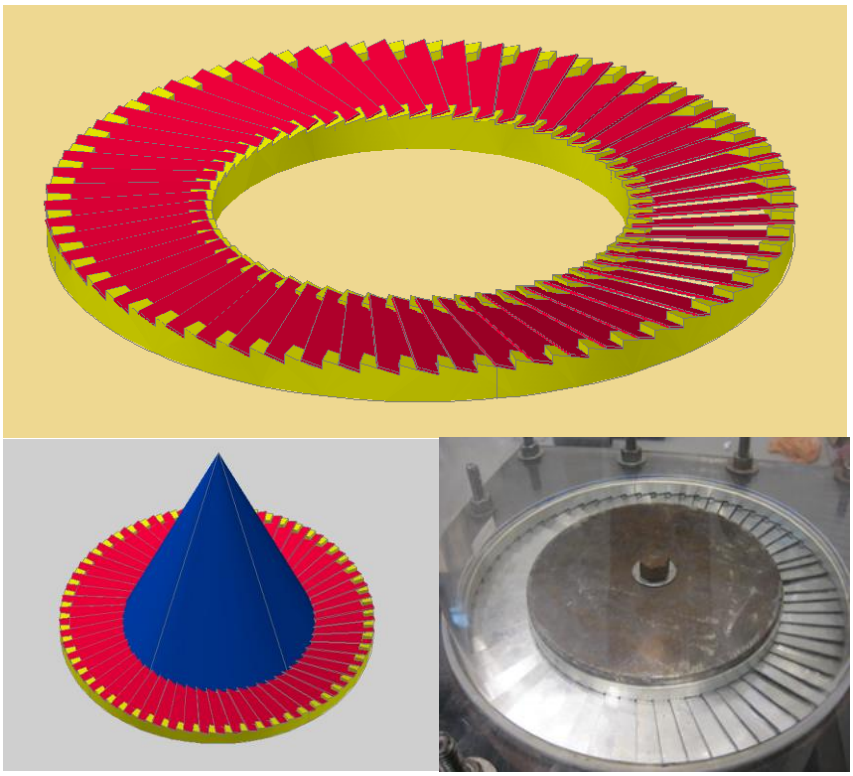

Figure 3.16: Annular spiral distributor

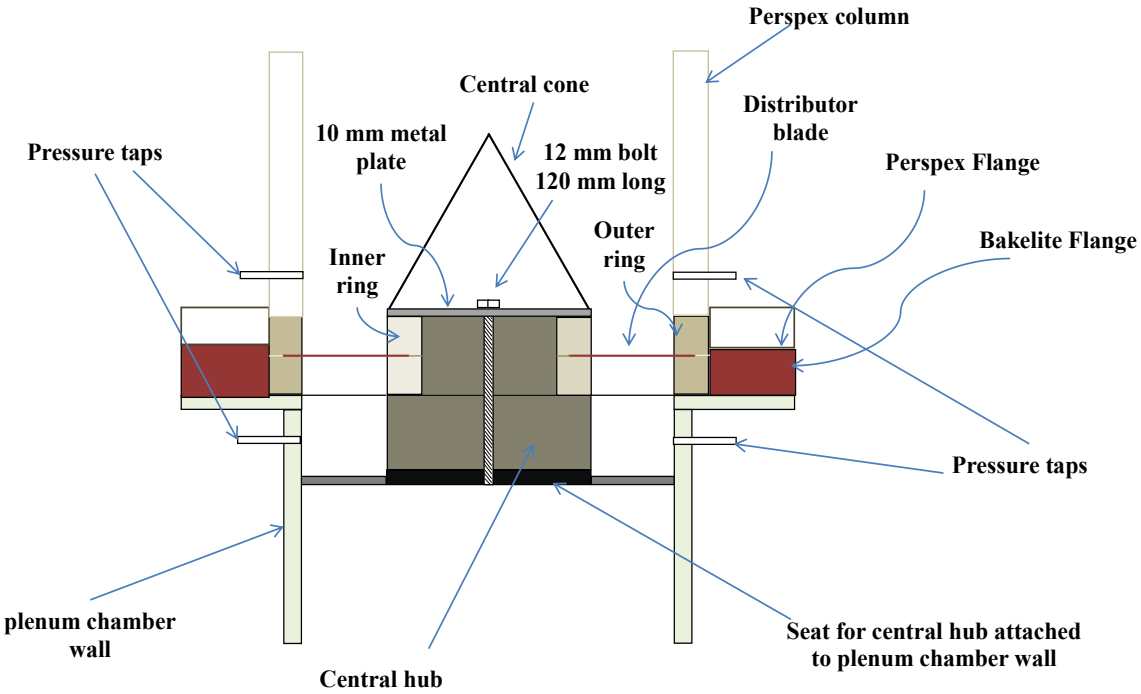

Figure 3.17: A cross sectional view of the SFB setup

The blades are fabricated from 1mm thick aluminum sheet using wire-cut machine. Four different sets of blades, with blade overlap angles varying from 9^o to 18^o are fabricated. A 5 mm thick mild steel sheet of 200 mm diameter and 12.5 mm hole at the center was used to keep the inner rings secured with a 120 mm long 12 mm bolt.

Figure 3.16 shows the assembly of blades over the distributor rings of an annular spiral distributor with the cone attached at the center. Figure 3.17 illustrates a cross sectional view of the entire SFB assembly, with all important components duly labeled. This gives an absolute clarity to the idea of the SFB with flexible annular distributor, its components and their assembly.

3.3 Experimental Methodology

During the work a standard procedure was followed for determining the physical properties of the bed particles used in the experiments. Each of them is explained in detail in the following segment. The method followed in recording the variation of

physical parameters during the experiment and the calculations used thereafter is also depicted in the subsequent section.

3.3.1 Physical Properties of the Particles

Different types of particles were used during the experiment as bed particles. Most of them were rigid polystyrene beads purchased from market based on their size and shape. To specify the bed material physical properties like mean particle size (chiefly diameter of the bead), particle density and bed voidage are to be determined.

3.3.1.1 Particle Shape and Size

Four different shapes of particles were used, spherical, elliptical, long and short cylindrical as well as rice bead type, designated respectively as S, ELIP, LC, SC and RB, shown Figures 3.18 and 3.19 . The dimensions of the particles were measured using a screw gauge by randomly picking a significant sample size from each lot to give a statistically significant average. In the case of cylindrical particles (SC/LC), the base diameter and the length of randomly chosen particles were measured and the L/D ratio was chosen as the distinguishing characteristic.

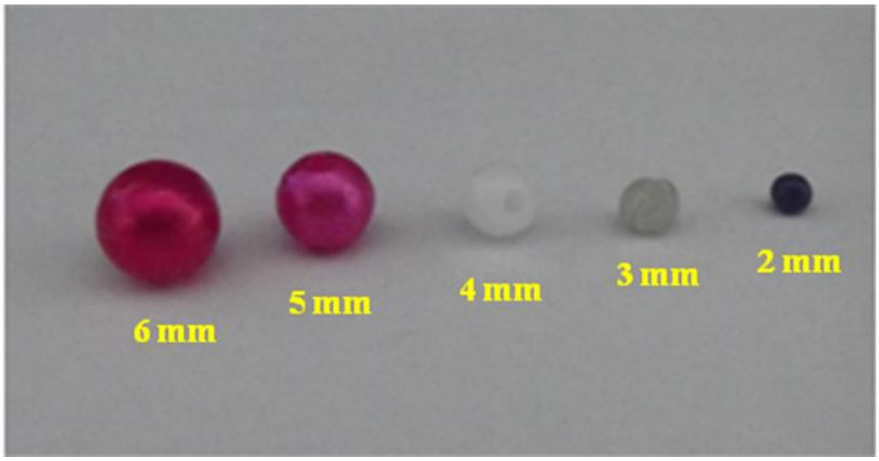

Figure 3.18: Spherical particles used in the experiments

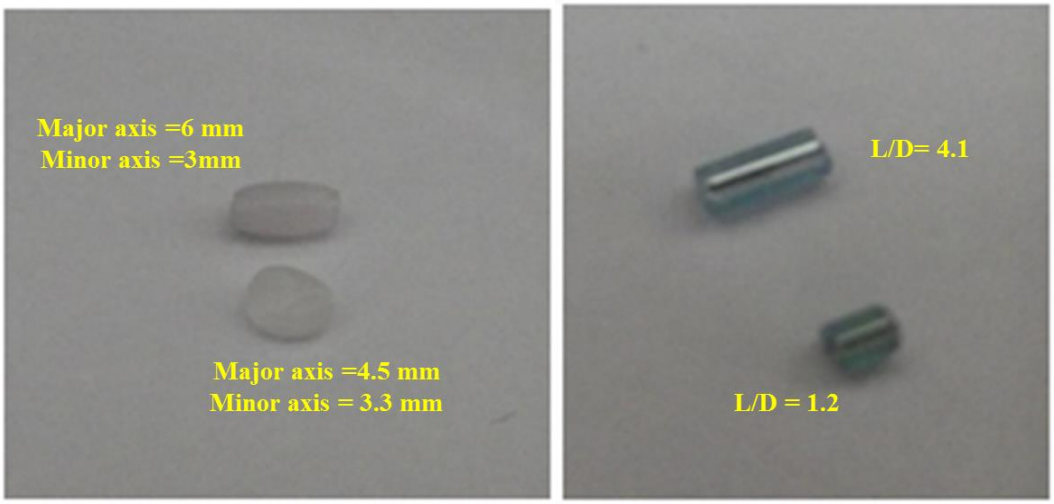

Figure 3.19: Non-spherical particles used in the experiments

3.3.1.2 Particle Density

The particle density was determined using a standard pycnometer. Mass measurement was done using a digital weighing machine with a resolution of 0.2 g

The procedure followed during the determination of density of bed particles was as follows:

The pycnometer was weighed in the digital weighing machine. Then it was filled with particles and again weighed. Distilled water was added to it and the weight was again taken. Then water and the particles were removed from it and filled with distilled water and weighed. The particle density was calculated as explained in Appendix E.

3.3.1.3 Bed Density

Bed density can be determined from the above experiment using the equation given below:

Bed Density, ρ_b = Mass of particles in the container / volume of the container

= Mass of particles (M_p) in the pycnometer / Volume of pycnometer(V_{py})

$$\rho_b = (M_{py+p} - M_{py}) / \{(M_{py+w} - M_{py}) / \rho_w\} \quad (3.8)$$

3.3.1.4 Bed Voidage

The bed voidage (ε) can be calculated from the relation

$$\varepsilon = 1 - (\rho_b / \rho_p) \quad (3.9)$$

3.3.1.5 Particle Specification

The physical properties of various particles used as bed materials determined during the work is tabulated in Table 3-2

3.3.2 Physical Properties of Bed

Physical quantities of the bed such as distributor pressure drop, bed pressure drop, superficial velocity, minimum fluidization and bed height were measured. The method of measurement and the equations used are explained in detail in the following sections.

3.3.2.1 Distributor Pressure Drop, Δp_d

Distributor pressure drop being an important factor that influences the quality of fluidization, its determination is decisive. The energy consumed in a fluidization process is directly proportional to distributor pressure drop. Saxena [62] in his work states that distributor pressure drop increases with increasing superficial velocity. Distributor pressure drop can be determined by observing the pressure difference across the distributor in an empty bed.

Table 3-2: Physical properties of various particles

Type of particles	Density of particle, kg/ m^3	Bulk Density of bed ρ_b, kg/m^3	Bed voidage	Size of particle	Material
2S	2306.67	1384	0.40	2 mm	Glass
3S	969.23	504	0.48	3 mm	Plastic
4S	857.14	480	0.44	4 mm	Plastic
5S	945.21	552	0.42	5 mm	Plastic
6S	971.43	544	0.44	6 mm	Plastic
RB	923.08	480	0.48	6 mm (major axis) 3 mm (minor axis)	Plastic
Elli	884.62	552	0.38	4.5 mm (major axis) 3.3 mm (minor axis)	Plastic
LC	2215.38	1152	0.48	Diameter = 1.8 mm L/D = 4.1	Glass
SC	2109.59	1232	0.42	Diameter = 1.6 mm L/D = 1.2	Glass

The distributor was seated in the flanges between the plenum chamber and bed column and secured in position using 12 bolts of 12 mm diameter. Rubber gaskets of 3 mm thickness were provided on either side of the distributor flange to make the interfaces leak-proof.

For determination of the distributor pressure drop a calibrated digital manometer Model EJA110A, Yokogawa make, with resolution of 0.01 mm water was used. The manometer was connected to three pressure tappings P_1, P_2 and P_3, through a piezometric ring, provided on the set up. P_1 and P_2 are on the Perspex

cylinder wall and P_3 is on the plenum chamber wall just below the distributor plane as shown in Figure 3.20.

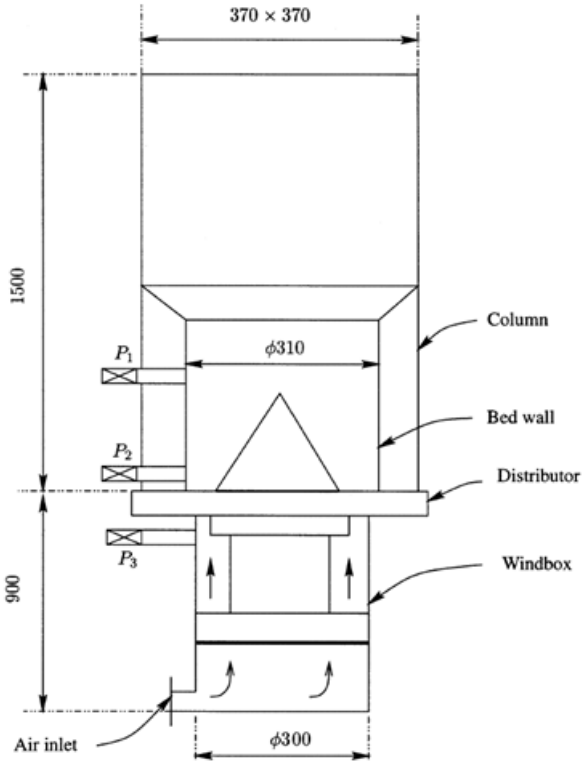

Figure 3.20: Sketch of swirling fluidised bed showing location of pressure taps

The distributor pressure drop, ($P_3 - P_2$), was measured with an empty bed at different airflow rates, for different blade overlap angles and blade inclinations. The airflow rate, measured using an orifice meter, was varied progressively using a speed controller connected to the blower motor. For each value of the flow rate (orifice meter pressure drop, Δp_o), the distributor pressure drop (Δp_d) was determined.

3.3.2.2 Superficial Velocity, U_{sup}

The superficial velocity is defined as the volume flow rate divided by the free cross sectional area before the distributor. It is always used as the reference velocity in packed beds, fluidized beds, pebble bed reactors, multiphase systems etc. The

choice of superficial velocity as the reference velocity in SFB is justified on the basis of the following argument: the correct velocity to correlate the hydrodynamics will be the upward percolation velocity of the gas through the bed. This velocity will be equal to the superficial velocity divided by ε, the bed voidage. As the bed voidage is not known a priori, it is a sensible choice to take the superficial velocity, which is unambiguously defined, as the reference. Taking the passage area of the blades to calculate the reference velocity is unsuitable as it varies with inclination, overlap, shape, length and number of blades.

To find the superficial velocity, the air flow rate through the bed has to be calculated. The flow rate of air, Q was calculated by the equation

$$Q = C_D \left[\frac{\left(\sqrt{2g\Delta P_o}\right) \times a_1}{\sqrt{1 - \left(\frac{d}{D}\right)^4}} \right] \tag{3.10}$$

where (d/D) is ratio of orifice diameter to pipe diameter.

$$Q = 0.668 \left[\frac{\left(\sqrt{2 \times 9.81 \times \Delta P_o}\right) \times 0.0031754}{\sqrt{1 - (0.620)^4}} \right] \tag{3.11}$$

The superficial velocity was then calculated from the volume flow rate by the equation

$$U_{sup} = \frac{4 \times Q}{\pi[(D_O^2) - (D_I^2)]} \tag{3.12}$$

where D_I and D_O are the inner and outer diameters of the annular spiral distributor.

The experiment was repeated for different combinations of the distributors. The pressure drop across the orifice plate as well as the distributor and the bed is measured using a manometer with an uncertainty of ± 0.01% and hence a similar margin could be expected in all the readings taken during this work.

3.3.2.3 Bed Pressure Drop, Δp_b

Variation of bed pressure drop with superficial velocity is one of the important characteristics of a fluidized bed that helps to assess the quality of fluidization. The bed pressure drop can be determined by observing the pressure difference across the loaded bed and deducting the distributor pressure drop from it.

Bed pressure drop, Δp_b = Total pressure drop (Δp_t) – Distributor Pressure drop (Δp_d) (3.13)

Referring to Figure 3.20 the distributor pressure drop ($P_3 - P_2$) is measured with an empty bed and in the case of a bed loaded with known weight of bed particles the total bed pressure drop, the pressure difference ($P_3 - P_1$), is measured for various air flow rates.

Hence the net bed pressure drop, $\Delta p_b = [(P_3 - P_1) - (P_3 - P_2)]$ (3.14)

3.3.2.4 Minimum Fluidizing Velocity, U_{mf}

Minimum fluidizing velocity, U_{mf} of fluidized beds, a vital parameter in the study, depends on various aspects of the distributor as well as the physical properties of the bed particles used. Hence U_{mf} has to be determined in each case examined during the study.

The bed was loaded with a known weight of bed particles and the experiment was repeated at regular increments of the air flow rate by adjusting the variable drive controller connected to the blower motor. The following observations are made for every experiment.

1. Orifice meter reading (pressure drop across orifice meter Δp_o from manometer)

2. Mean pressure drop across the distributor as well as the bed provided by pressure tappings P_1, P_2 and P_3 (manometer readings)

Superficial velocity and Δp_b were calculated using Eqs. (3.12) and (3.14) respectively.

The experiment was repeated for different combinations of distributor characteristics by varying the bed particles and their bed weight. A graph of Δp_b versus U_{sup} was plotted and the minimum fluidizing velocity (U_{mf}) was determined from the plot.

3.3.2.5 Bed Height, H_b

To measure the bed height and bed expansion, three vertical scales were symmetrically attached to the outer periphery of the Perspex column. The scales had graduations in mm. Exact measurement of the bed height was not possible during the slugging regime, high speed swirling regime and two-layer bubbling regime.

3.3.2.6 Identification of Different Fluidizing Regimes in Swirling Fluidized Bed

As superficial velocity increases, the state of the bed changes from packed bed to minimum fluidization, then to slug-wavy bed, followed by swirling bed and vigorously bubbling bed with a lower swirling layer. When beds are deep, a two-layer regime may also exist. To understand the bed behaviour under different modes, it is important to identify and classify the regimes.

In this work nine different bed materials were used and in each case, bed weight from 500g to 2000g with successive increments of 500g was loaded into the bed. The behaviour of the bed was studied for different flow rates which were varied from low velocities till the maximum operating velocity, i.e., elutriation velocity. The orifice meter pressure drop as well as the pressure drop across the bed were

measured and tabulated. The superficial velocity at which the fluidization starts (minimum fluidizing velocity, U_{mf}), initiation of slugging mode and swirl regime are noted along with other observations by visual inspection.

3.3.3 Error Analysis

A detailed error analysis is provided below;

The functional dependence of measured variables is as follows:

$$\Delta p = f(Usup, dp, \theta, Wb, \alpha, \mu gas, \rho p, \rho gas) \quad (3.15)$$

A non-dimensionalization of the above functional dependence yields:

$2\Delta p/\rho U2$, Re, $\theta/90$, $\alpha/90$, $\rho p/\rho gas$ and Wb/g

Taking the functionality

$$2\Delta p/\rho U2 = f(Usup, dp, \theta, Wb, \alpha, ,\mu gas, \rho p, \rho gas) \quad (3.16)$$

The error relationship will be as follows. Since error can be either (+) or (-), the maximum error is:

$$[d(\Delta p)/\Delta p] = 2[dU_\infty/ U_\infty] + [d\theta/\theta] + [d\alpha/\alpha] + [d(d_p)/d_p] + [dWb/Wb] + [d\rho gas/\rho gas] + [d\rho p/ \rho p] \quad (3.17)$$

Given below are the measured quantities along with their error and machining allowances in fabrication of components.

For velocity U_∞ the error will involve calibration / design error and the manometer error. Design error based on to the Malaysian standards and error analysis done by Zaki [104] the maximum error would be ± 1%. Uncertainty in pressure p will be due the manometer error. Since the differential pressure is directly measured error in Δp will be 0.5% (as stated in manometer specifications).Bed weight involves error in weighing. The minimum weighed is 500 g and the weighing machine has a least count of 0.2 g. Therefore the error is (0.2/500) x 100 = 0.04%.

Angle measurements depend on the machining accuracy of the CNC machine. Since angle is a ratio of two length quantities, the error is 2 (dL/L). The same is applicable for the overlap angle α also. The CNC machine was capable of 1 micron accuracy, and the graduations on the machine are in mm; therefore that error (dL/L) is (0.001mm/1mm) x 100% = 0.1%.

Density of gas is obtained from property tables [105], which is quite accurate. It can be estimated as < 0.1% which is quite small compared to the others. The density of particles involves both weight and volume measurement. The graduated jar used had graduations with minimum of 1 ml and the volume used was 250 ml to fill the vessel, then the % error is (1/250) x 100 = 0.4%.

Hence the total % error = 0.01% + 2 × (0.01% + 1%) + 0.1% + 0.1% + 1% + 0.04 % + (0.1% + 0.04 + 0.4%) = 3.81 % (3.18)

Therefore the percentage total error = 3.81 % ≈ ±3.8% cumulative error

CHAPTER 4

RESULTS AND DISCUSSION

4.1 Chapter Overview

This chapter reports the results obtained from the experiments and discusses their physical significance and the possible explanations for the observed phenomena. The basic idea of the work, as explained under Objectives, is to investigate the various hydrodynamical aspects of the swirling fluidized bed.

Various aspects affecting the hydrodynamics of the swirling fluidized bed discussed in this work are as follows:

1) Velocity of fluidizing medium (air), U_{sup}
2) Distributor blade inclination angle, θ
3) Distributor blade overlap angle, α
4) Size of the particle, d_p
5) Shape of the particle
6) Bed weight, W_b
7) Density of particle, ρ_p

The hydrodynamic parameters investigated during the work are

i) Distributor pressure drop, Δp_d

ii) Bed pressure drop, Δp_b

iii) Minimum fluidization velocity, U_{mf}

iv) Bed height, H_B

The sizes and shapes of particles given Table 3-2.

Other features of different regimes of the swirling fluidized bed which were measured and presented for discussion during the work are

a) The time taken for one slugging cycle, T_s

b) Hysteresis occurring during increase and decrease of air flow.

4.2 Pressure Drop across Distributor, Δp_d

The distributor pressure drop, being a major parameter influencing the fluidization quality and energy consumption, has immense significance in the hydrodynamic study of fluidized beds. In short, a higher distributor pressure drop leads to higher energy consumption. For a conventional fluidized bed, Agarwal *et al*. [44] observed that a minimum distributor pressure drop of 350 mm of water is required for uniform fluidization in a shallow bed and that any value lower than this may result in maldistribution of the fluidizing medium in the bed. In contrast, Sreenivasan and Raghavan [39] showed that in the case of a swirling fluidized bed, uniform fluidization can be achieved with a much lower distributor pressure drop, which is a unique advantage of SFB.

The distributor pressure drop can be determined by measuring the pressure difference across the distributor in an empty bed. The detailed procedure for the determination of distributor pressure drop is explained in section 3.5.2.1.

To understand the interplay of forces determining the hydrodynamic behavior of the bed, it is expedient to consider a free-body diagram of forces acting on a mass of particles in the swirling fluidized bed as in Figure 4.1:

Here we consider the (r, θ, z) system of co-ordinates.

It is known in mechanics that forces normal to a surface produce a tangential frictional force, such as the resistive force on a block sliding down an inclined plane.

In the swirling fluidized bed, the outward centrifugal force acting horizontally normal to the column wall produces two reaction forces, one a horizontal tangential force opposing the swirling of the bed, that is responsible for limiting the swirling velocity, and another orthogonal force acting downward, restraining the bed expansion. This may be represented simply by a free-body diagram of forces:

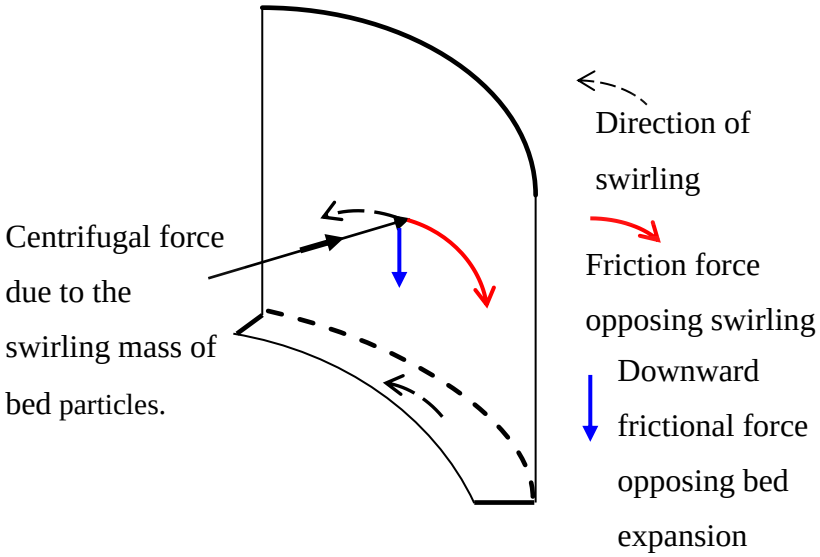

Figure 4.1: Free body diagram of forces acting on the swirling fluidized bed

In the fluidized bed, there is a downward force due to the net weight of the particles. For stable operation of the bed, this force has to be zero according to the second law of motion:

F = ma, where the forces and acceleration are in the vertical (z) direction.

The other forces in z direction are the downward friction at the wall and the upward force due to pressure drop of the gas.

Similarly, in the θ direction, the angular momentum transferred by the gas to the particles is dissipated against the friction of the particles at the wall.

As for the r direction, the centrifugal force of the particles due to their rotation is balanced by the inward centripetal force which is produced as a result of the weight of a given height of the bed acting on the lower portion of the bed and producing an orthogonal reaction force.

This balance condition in (r, θ, z) exists in the normal stable operation of the bed. The free body diagram above helps us to explain the experimental results and to give a physical interpretation and will be frequently called into context in this chapter.

4.3 Influence of Various Aspects on Pressure Drop across the Distributor, Δp_d

Among various aspects investigated in the work, only two were observed have an influence on the distributor pressure drop, namely, distributor blade inclination angle, θ and distributor blade overlap angle, α.

4.3.1 Influence of Blade Inclination on Δp_d

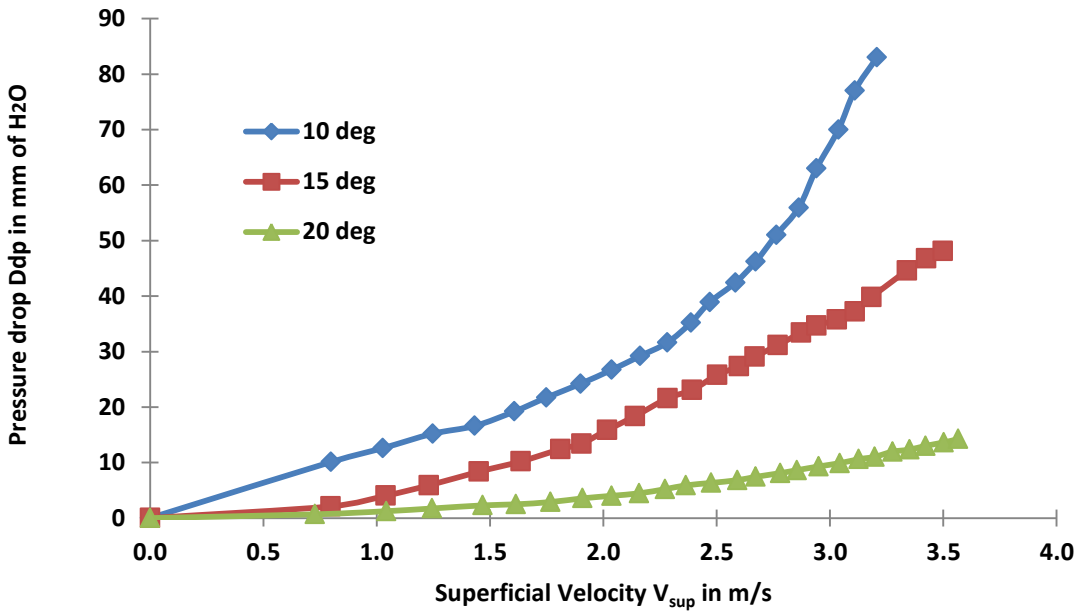

Figure 4.2: Distributor pressure drop versus superficial velocity at different blade inclinations

Figure 4.2 shows the variation of distributor pressure drop with superficial velocity for the three different blade inclinations of 10^o, 15^o and 20^o respectively. All the three plots show the expected supra-linear trend and serve as standardization of the apparatus and instrumentation.

The inclination of 20^o has the least resistance and hence the pressure drop is the lowest compared to other two. The reason for this can be explained as follows

The percentage opening area is least for 10^o and highest for 20^o. This is illustrated in Fig. 4.3 below and shown by means of calculation:

Mean length of opening, $L_O = \{(\pi D_m/60) - t\} \times \sin\theta$

Percentage opening area, $A_O = \{4 \times L_O \times 60 \times (r-2l) / \pi (D_o^2 - D_i^2)\} \times 100$

a) for 10^o inclination

Mean length of opening, $L_O = \{(\pi \times 250/60) - 1\} \times \sin 10 = 2.1$ mm

Percentage opening area, $A_O = \{4 \times 2.1 \times 60 \times 100 / \pi (300^2 - 200^2)\} \times 100$

$= 32.1\%$

similarly

b) for 15^o inclination

Percentage opening area, $A_O = 47.8\%$

c) for 20^o inclination

Percentage opening area, $A_O = 63.2\%$

It is evident from the above calculation that the percentage opening area of 20^o is more than that of 10^o and 15^o and hence clarifies the trend of having the least distributor pressure drop.

From Figure 4.3 it can be understood that with an increase in angle of inclination θ, the opening L_O increases and consequently the area of opening also increases. The pressure drop is inversely proportional to the area of opening as inferred from Figure 4.2.

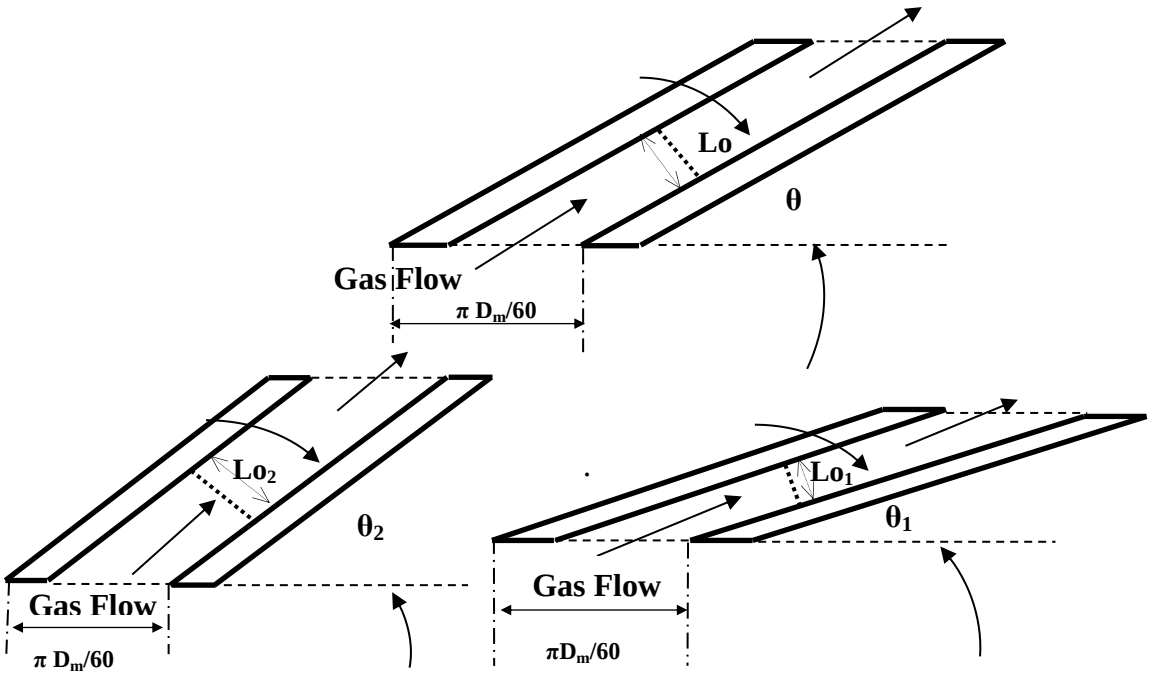

Figure 4.3: Illustration of blade inclination angle and blade opening, where $\theta_2 > \theta_1$

4.3.2 Influence Blade Overlap Angle on Δp_d

A larger overlap angle implies a larger blade width and a longer path of flow between the blades as shown in Figure 4.4. The overlap angle, rather than the overlap length, has been chosen to characterize blade overlap since the overlap length varies from the inner to the outer radius, while the angle is a constant value. In correlating the hydrodynamics, the overlap angle is used as the representative value.

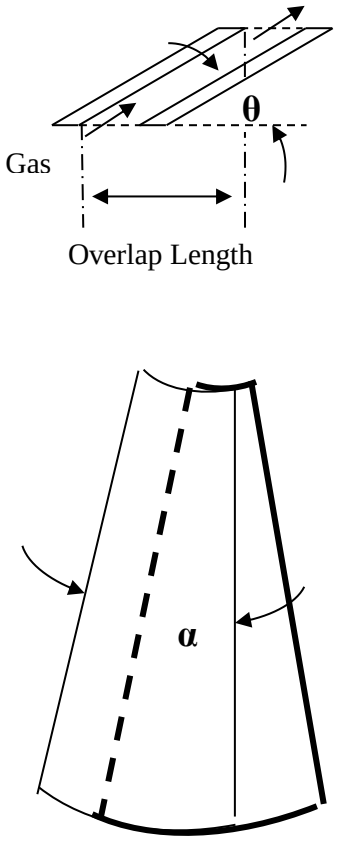

Figure 4.4: Sketch describing blade overlap length and blade overlap angle

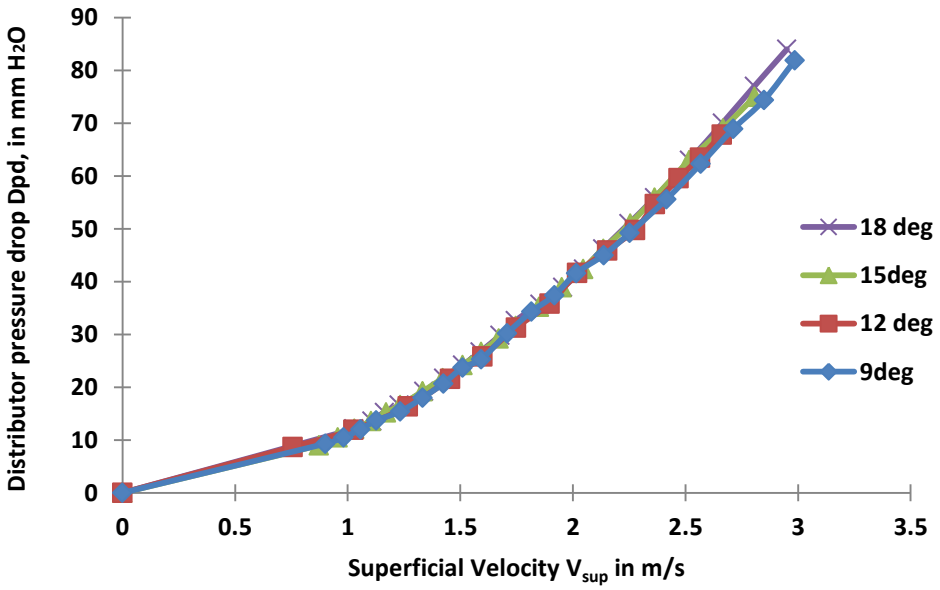

Figure 4.5: Distributor pressure drop versus superficial velocity at different blade overlap angles

Figure 4.5 shows the variation of distributor pressure drop with superficial velocity for the four different blade overlap angles of 9^o, 12^o, 15^o and 18^o. As

anticipated, the pressure drop is least for 9^o and maximum for 18^o, though the lines lie very close. This confirms the observation by Batcha *et al.* [98] that the influence of angle of overlap, α, on the distributor pressure drop of SFB is quite small. Even though the difference between the plots is small, the distinct trend is that pressure drop increases with an increase in blade overlap angle. Based on the well-known relationship between pressure drop and length of the fluid flow path, the observation in the plot is justified. The friction over the longer blades would offer more resistance to the flow and hence increase the pressure drop.

4.4 Pressure Drop across the Bed, Δp_b

The bed pressure drop is another significant aspect of fluidized beds which influences the quality of fluidization, In shallow beds, too low a pressure drop causes channeling. In deep beds ($H_b/D > 1$), the resultant high pressure drop causes slugging. This explains the relationship between Δp_b and quality of fluidization. In swirling fluidized beds, the swirling is most vigorous at the distributor. As the gas travels upwards, the swirl motion decays due to friction and there is a reduction in pressure gradient. In SFB, the relationship between Δp_b and quality of fluidization does not appear to have been studied and calls for investigating Δp_b in detail as a function of several variables.

4.5 Influence of Various Parameters on Δp_b

The different parameters that were seen to affect the bed pressure in SFB are as follows

1. Velocity of fluidizing medium (air), U_{sup}

   It is the velocity with which the fluidizing medium approaches the bed. Also referred to as superficial velocity, it is a major parameter that influences bed behavior. Different regimes of the bed are demarcated based on the velocity of the fluidizing medium.

2. Distributor blade inclination angle, θ

   Inclination angle θ is described as the angle at which the distributor blades are inclined to the horizontal as shown in Figure 4.3. The inclination influences the direction of the air jet emerging from the distributor thereby affecting both swirling as well as fluidization.

3. Distributor blade overlap angle, α

   It is the subtended angle of a single blade and decides the width of the blade. The blade overlap angle has considerable influence on the flow development in the blade passage. Consequently it affects velocity profile of the fluid emerging out of the distributor into the bed. From Figure 4.4, it is obvious that the blade overlap length varies from the inner to the outer radius and cannot serve as a characteristic dimension, while the overlap angle is more suitable as it is a unique value.

4. Size of the particle, d_p

   In this work, both spherical and non-spherical particles were used. The size d_p refers to the diameter of the spherical particles. In this section, the hydrodynamic performance of the bed is studied for the spherical particles on the basis of d_p.

5. Shape of the particle

   Particles of different shapes are used in this work, as set out in Table 3-2 and explained in detail under section 4.5.5. A single criterion for comparing particles of all shapes and sizes is not available. However in certain cases L/D ratio is used as a basis of comparison.

6. Bed weight, W_b

   It is the weight of the particles over the distributor which is primarily responsible for the bed pressure drop. For a bed of given particle size,

the higher the bed weight, the higher is the bed height and the resistance to flow, resulting in higher bed pressure drop.

7. Density of particles, ρ_p

   This is an aspect which has a major influence on fluidization. The higher the density the higher will be the bed weight and hence requires a higher velocity to provide the larger drag force needed for force balance at the expense of a larger pressure drop. Hence the density of the particles also has an effect on the minimum fluidization velocity.

   The most common materials in which beads are available in the market are a variety of plastics with a density close to that of water. The other common material is silica or glass, with a specific gravity close to 2.5. To find a material with both density and size specified is not feasible. Therefore, the study was done only for two density ranges, 850-970 kg/ m^3 and 2100-2300 kg/ m^3 kg/ m^3 as shown in Table 3-2.

4.5.1 Influence of Velocity of Fluidizing Medium on Δp_b

A typical plot of bed pressure drop with respect to superficial air velocity obtained from the experiments on swirling fluidized bed is depicted in Figure 4.6 for the following parameters: 4 mm spherical particles, inclination angle of 15^o, overlap angle of 18^o, bed weight of 2 kg and density of 857 kg/m^3, indicated in the legend thus: 4S-15-18-2-857. This representation is consistently used hereafter.

In the graph it can be seen that with an increase in superficial velocity the bed pressure drop follows a linear trend initially and at the point of minimum fluidization, ≈ 1.1 m/sec, it experiences a slight drop and then stabilizes. The linear variation is on account of the laminar nature of the flow at low velocities through the packed bed of 4 mm particles. In the packed state, the particles are in mutual contact and get physically separated at incipient fluidization. The extra energy required to lift the particles apart manifests as a ‘hump’ in the curve. Soon after

this, once the inter-particle contact disappears, the resistance offered by the bed decreases and is seen as a drop in Δp_b. Thereafter the pressure drop remains almost constant over the velocity range of 1.1 m/s to about 2 m/s, signifying the slug-wavy regime. Beyond this velocity, the entire bed swirls and the curve is supra-linear, suggesting an increased wall friction due to contact with the swirling particles that extends till the elutriation velocity U_t.

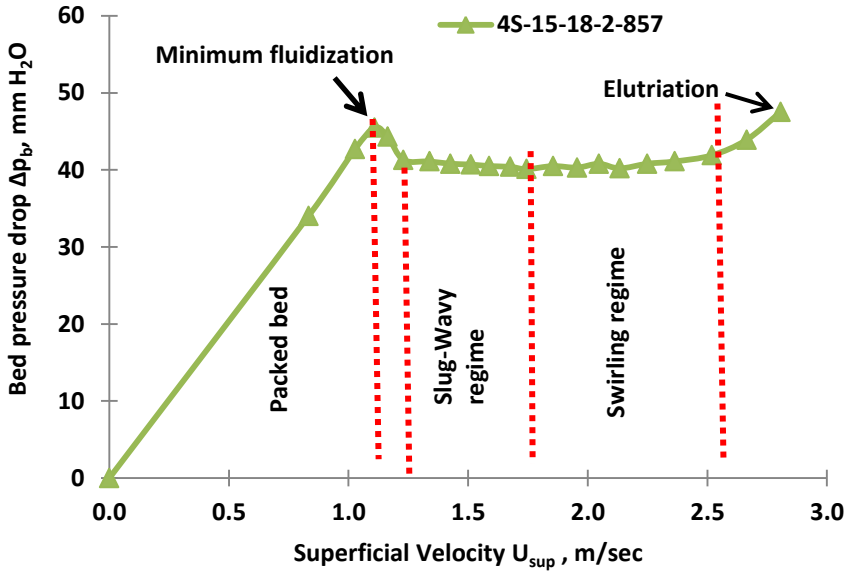

Figure 4.6: Plot of bed pressure drop versus superficial velocity

4.5.2 Influence of Blade Inclination Angle on Δp_b

Figure 4.7 shows the variation of Δp_b with respect to different blade inclination angles. A close observation would show that the bed pressure drop increases with decreasing blade inclination angle. The reason for this is that, with an increasing blade inclination angle, the percentage area of opening of the distributor increases, as discussed in section 4.3.1. As the percentage opening area increases, both resistance at the distributor and distributor pressure drop decrease, which has a bearing on the 'hump' as well as the slug-wavy regime. For 10^o angle, the vertical component of gas velocity is smaller and a greater effort is required to separate the particles, while at higher angles, the hump is not as prominent.

It is also observed from the graph that except for 10^o blade angle, the plots have an extended zone of constancy of Δp_b, suggestive of the slug-wavy regime. For the 10^o case, there is little slugging. The swirling starts soon after incipience and is observed in the form of the supra-linear curve which is a characteristic of the swirling regime. These inferences on the slug-wavy regime have been confirmed visually as reported in forthcoming sections. It is concluded that for reactors requiring a slug-wavy regime, a larger blade angle should be chosen

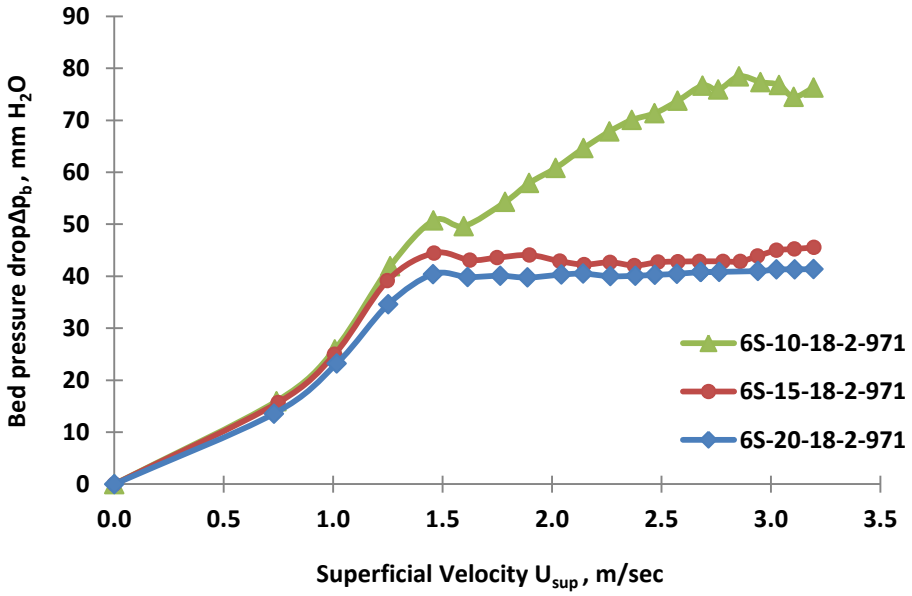

Figure 4.7: Bed pressure drop versus superficial velocity at various distributor blade inclination angles

4.5.3 Influence of Blade Overlap Angle on Δp_b

Figure 4.8 shows how the bed pressure drop would vary with increase in blade overlap angle. Four overlap angles of 9^o to 18^owere employed. As described in section 4.3.2, there is not much variation in the distributor pressure drop with an increase of blade overlap angle. But when it comes to variation in bed pressure drop, the blade overlap angle has an impact, which is quite evident from the plot.

The case of 18^o clearly shows the change in the nature of bed behavior. The wavy regime is shortened and an early onset of vigorous swirling is seen.

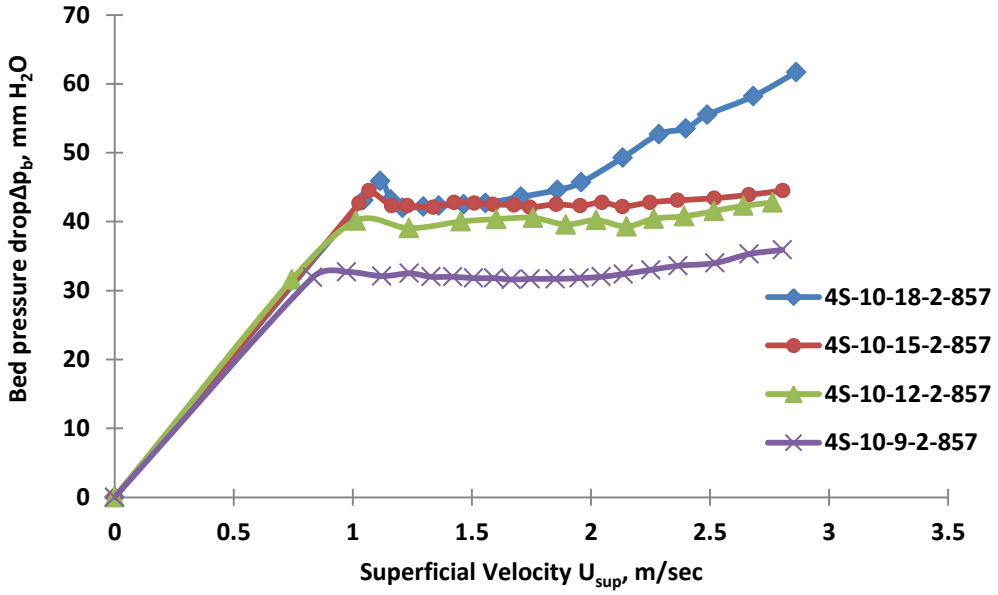

Figure 4.8: Bed pressure drop versus superficial velocity at various distributor blade overlap angles

The angle of overlap governs the velocity pattern at the distributor outlet. A smaller overlap angle would mean a smaller flow development length and an underdeveloped flow with a lower maximum velocity at the distributor outlet. With an increase in blade overlap angle, the gas entry angle into the bed is lower, the horizontal component of gas velocity is greater, hence the horizontal momentum is larger and consequently, the bed swirls more vigorously. This gives rise to higher friction components, such as gas-particle, gas-wall, particle-particle, particle-wall and particle-distributor. As the area of wall and distributor are much smaller than the surface area of particles, it is reasonable to neglect the friction components of gas-wall and gas-distributor in comparison with gas-particle. The larger Δp_b can be attributed to the lower gas entry angle into the bed due to the flow development in the blade passage. Thus the bed pressure drop is lowest in the case of 9^o and increases with increased overlap as illustrated in Figure 4.9.

For bed particles, the velocity of the fluidizing medium is not the only consideration. A longer overlap is desired to discourage leakage of bed particles. For a given number of blades, a longer blade overlap is the main consideration for limiting the drainage of particles into the plenum chamber when the bed is

defluidized. It also has the following additional effects: longer flow development length, lower inclination of gas velocity at inlet to the bed, higher bed pressure drop, change in minimum fluidizing velocity and change in the slug-wavy regime. Therefore, a proper consideration of the interplay of all these factors is necessary for the design of the SFB distributor.

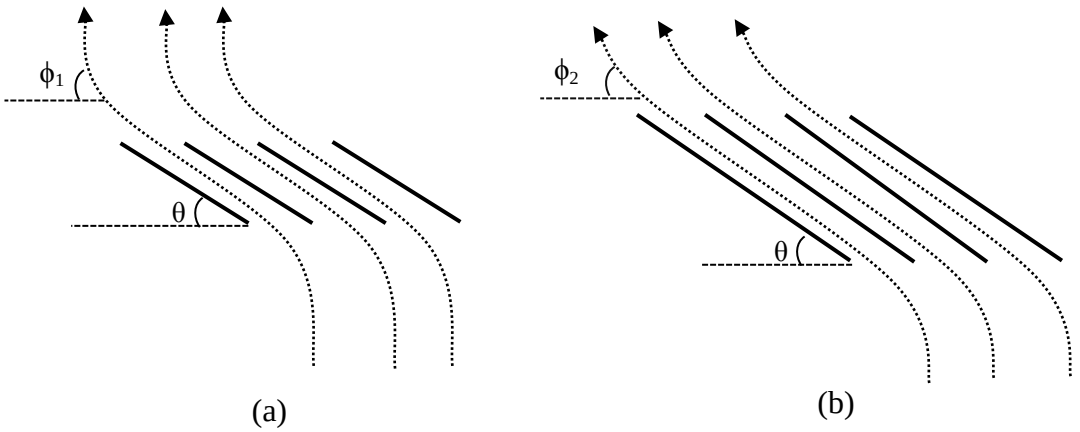

Figure 4.9 : Fluidizing gas direction after passing through the distributor of variable overlap angles (a) shorter overlap (b) longer overlap

4.5.4 Influence of Particle Size on Δp_b

Figure 4.10 depicts the effect of particle size on Δp_b. We can see that the 2 mm particle bed is the first to fluidize even though it is the densest among the particles used in the study and the 6 mm particle is the last to fluidize though its density is lower as depicted in Table 4-1. For 2 and 3 mm particles, the packed bed region is linear indicating laminar flow in the interstices. As per the first seven correlations by various authors for laminar flow as listed by Wu and Baeyens [84], the functionality at minimum fluidization is ρd_p^2 that has been derived from a force balance at minimum fluidization. It shows that the effect of d_p is more dominant than the effect of particle density. This is confirmed from the values of the ρd_p^2 product given in Table 4-1. For 2 and 3 mm particles, the closeness of the ρd_p^2 values confirms the closeness of the Δp_b values at incipience**.** In the packed bed region for 5 and 6 mm particles, the parabolic nature of the curve indicates turbulent behavior. The flow through the packed can be treated as flow through a

capillary (Hagen–Poiseuille flow) as suggested by Ergun [8].When the diameter of the particles increases, the interstitial spaces are larger which leads to a larger Reynolds number. If it is sufficiently large, turbulent flow can result. This emphasizes the fact that diameter is the correct length basis for definition of Re in a particulate bed. For 2 and 3 mm particles, after incipient fluidization the bed pressure drop is invariant for a certain range of gas velocities indicating a slug-wavy regime which is the partial swirling regime. As for 4 mm, after the minimum fluidization point the bed pressure drop is invariant for a short velocity range corresponding to the slug-wavy regime and later the behavior shifts to a parabolic one as it enters the fully swirling zone. The crossing of the 3S and 4S lines is due to the fact that the density of 4S beads is about 10% less than that of 3S. For 5 mm and 6 mm particles, after incipient fluidization the bed enters the fully swirling regime straightaway without slugging, which is also confirmed by visual observation. The trend is supra-linear on account of the fact that the centrifugal force during swirling is proportional to U_{sup}^2.

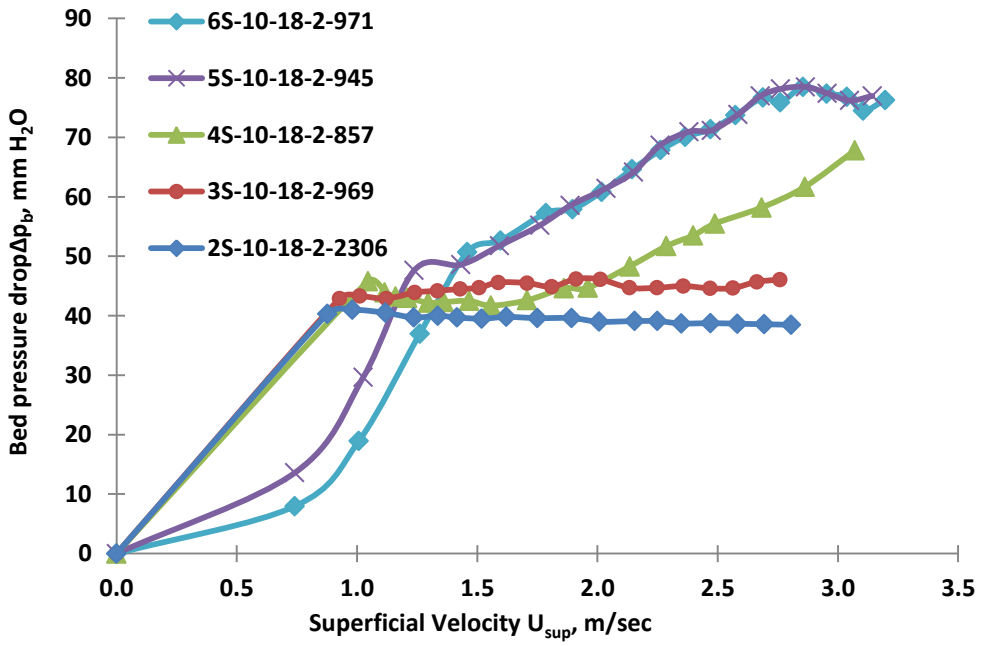

Figure 4.10: Bed pressure drop versus superficial velocity for various sizes of spherical bed particles

Figure 4.11 depicts the dependency of Δp_b at minimum fluidization on particle diameter. It is seen that Δp_b is linear with d_p. This result may be interpreted as follows. At the minimum fluidization condition, the bed weight is balanced by the drag force which determines the pressure drop. The drag force consists of both viscous drag and pressure drag components. Viscous drag is proportional to the gas-particle interface area while pressure drag is proportional to the projected area, both of which are functions of d_p^2. As the particle diameter is increased, the number of particles in the same volume gets reduced. The general rule is that as the particle diameter increases by a factor of n, the number of particles reduces as 1/n.

The drag force $F_d \propto N \times d_p^2$, where N is the number of particles.

But $N \propto 1/d_p$. Therefore, $F_d \propto d_p$.

This relationship between F_d and d_p is manifested in Figure 4.11 as a linear relationship between Δp_b and d_p.

Table 4-1: Details of different particles used in the study

Particle type	Density in kg/m^3	$\rho d_p^2 \times 10^{-10}$
Low density beads		
4 mm Spherical (4S)	857.1	1.37
Elliptical (Elip), dia = 3.3 mm, L/D = 1.36	884.6	0.96
Rice Bead (RB), dia = 3 mm, L/D = 2	923.1	0.83
5 mm Spherical (5S)	945.2	2.36
3 mm Spherical (3S)	969.2	0.87
6 mm Spherical (6S)	971.4	3.49
High density beads		
Short Cylindrical (SC), dia = 1.6 mm, L/D = 1.2	2109.6	0.54
Long Cylindrical (LC), dia = 1.8 mm, L/D = 4.1	2215.4	0.72
2 mm Spherical (2S)	2306.7	0.92

The most important conclusion from Figure 4.11 is that a swirling fluidized bed can effectively fluidize large particles of Geldart type D ($\rho d_p \geq 10^6$, ρ in kg/m^3 and d_p in micrometers). As per Geldart [99], type D particles cannot be fluidized in a conventional fluidized bed. Efforts to fluidize it will result in spouts or spurts of gas issuing through the bed. The spouted bed is an example of poor fluidization.

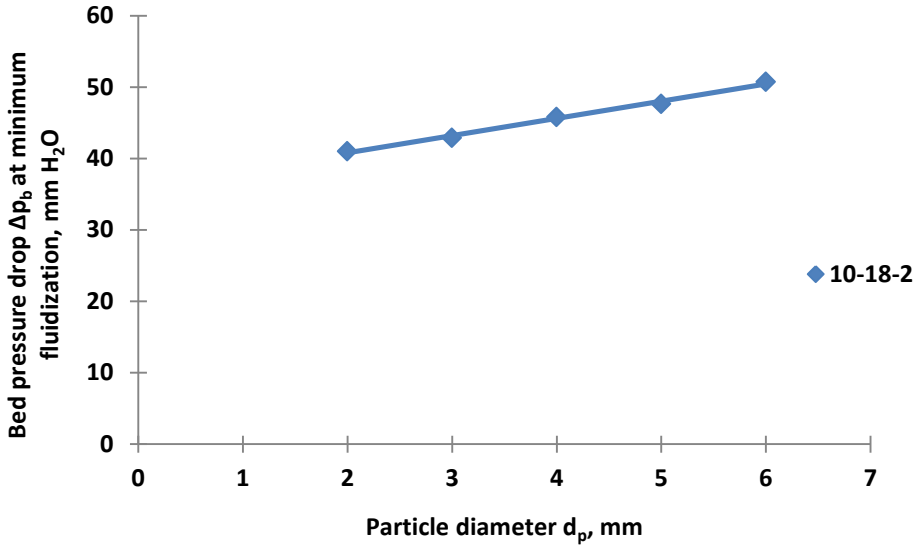

Figure 4.11: Bed pressure drop at minimum fluidization versus particle diameter

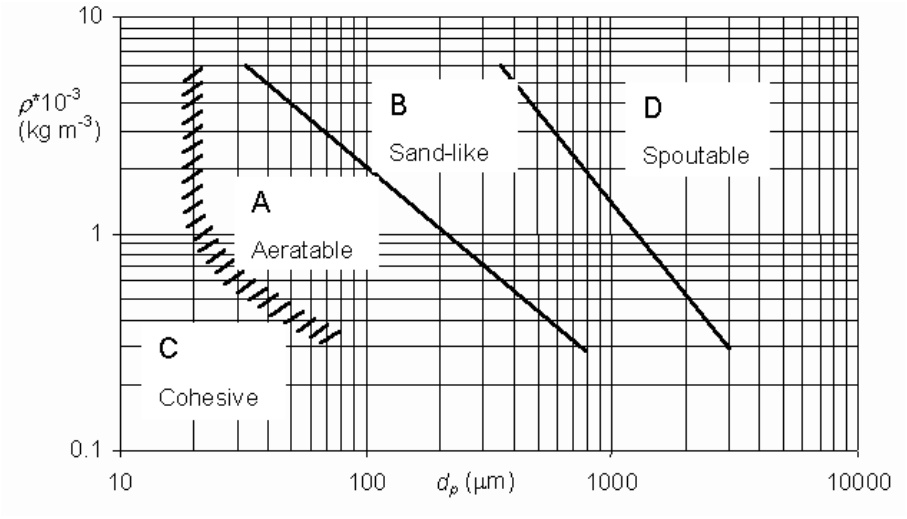

Figure 4.12: Geldart classification of particles [99]

4.5.5 Influence of Particle Shape on Δp_b

The influence of particle shape on bed pressure drop in a swirling fluidized bed is depicted Figure 4.13. Four different shapes of particles, apart from five different sizes of spherical ones, were used in the work. Of the nine types of particles, six belonged to one range of densities while three others had over twice that density as given in Table 3-2. It can be seen that both types of cylindrical particles fluidize late and have a higher pressure drop. In the SFB, it has been observed that the axis of

the cylinders is predominantly transverse to the direction of the flow. This counterintuitive result can be explained by the fact that the cylindrical particles get rearranged horizontally in a direction transverse to the flow of the fluidizing gas. Bejan's [100] constructal theory of natural systems explains this observation. This is a natural behavior of cylindrical particles to assume a direction in which they will experience less drag so as to get fluidized. This is similar to logs floating downstream in a river.

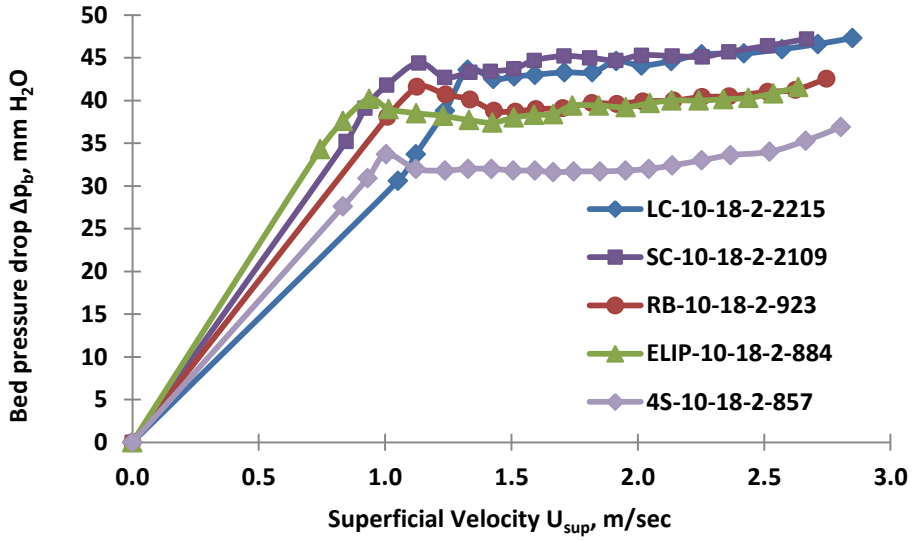

Figure 4.13: Bed pressure drop versus superficial velocity

The rice bead (RB) particle fluidizes after the elliptical and spherical particles respectively. The RB particle with a major axis 6 mm and minor axis 3 mm behaves intermediate to spherical and cylindrical particle. The elliptical particle is the first to fluidize mainly due to its lower density. The cylindrical particles could be compared with spherical particles by defining a suitable equivalent diameter. However, it is difficult to apply a sphericity criterion here because of their large deviation from a spherical shape.

An interesting observation is that all the particles irrespective of shape were well-fluidized in the SFB. Geldart [99] has also stated that highly non-spherical particles, such as wheat grains, cannot be fluidized but only spouted. This behavior is similar to the spouting of Geldart type D particles, i.e., larger and denser particles, as stated in section 4.5.4. In SFB, the quality of fluidization of non-

spherical particles is superior to contemporary techniques. Further, it appears a good idea to replace spherical particles, such as catalysts, by cylindrical ones as they offer a larger surface area and require a smaller gas velocity for fluidization.

4.5.6 Influence of Bed Weight on Δp_b

Figure 4.14 shows the effect of bed loading on bed pressure drop for 4 mm spherical particles. As anticipated, the higher the bed weight, the higher will be the resistance to the gas flow and therefore, the larger the bed pressure drop. Due to the conical center body, the cross sectional area of the bed increases continuously along the gas flow. Thus, equal increments in bed weight do not yield equal increases in bed height. Hence there is a reduction in the increments in Δp_b as bed weight increases.

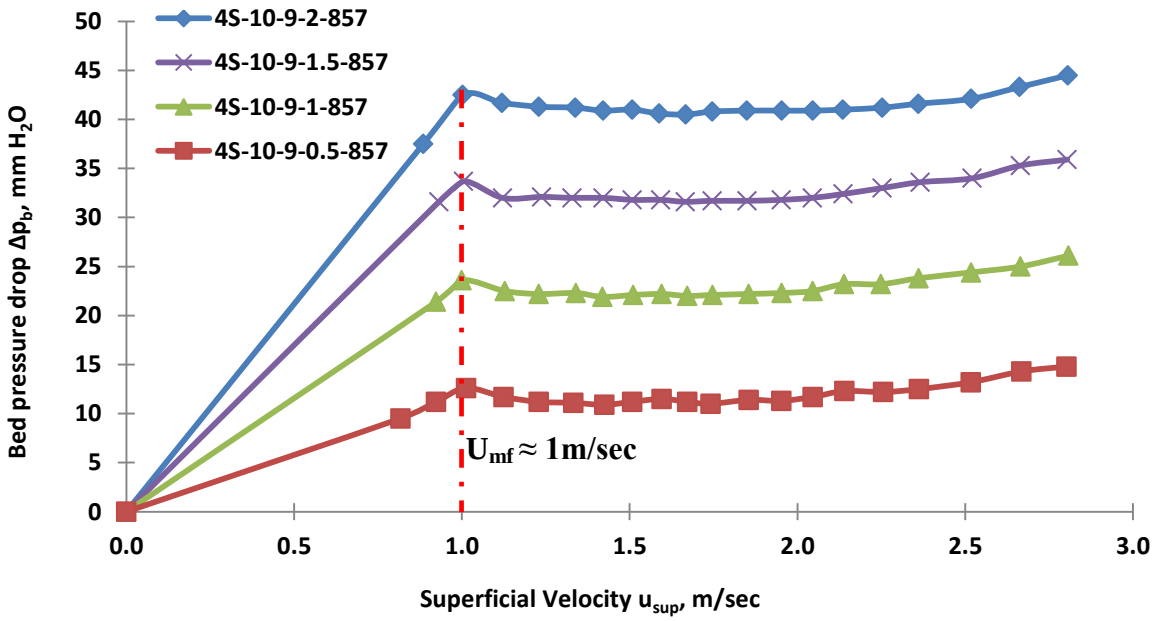

Figure 4.14: Bed pressure drop versus superficial velocity for various bed weights

Another fact to be noted is that the minimum fluidization velocity remains constant for all bed weights for given particles. This coincides with observations made by Gunn and Hilal [101] in a conventional gas-solid fluidized bed. As the fluid flows through the bed it exerts a drag on the particle which is responsible for

the fluidization when it equals the weight of the particle. Irrespective of the bed weight, for given particle size and density, the balancing of forces at minimum fluidization requires an identical drag force produced by an identical gas velocity.

4.5.7 Influence of Particle Density on Δp_b

Figure 4.15 depicts the variation of bed pressure drop with different shapes of particles. Two spherical particles, one with 2 mm diameter and high density and other 3 mm with low density along with two cylindrical and two non-spherical shaped particles used in the study were considered for the plot.

Because of simultaneous changes in diameter, density as well as shape, it was not possible to draw comparison s across the entire spectrum of particles used. Therefore the particles are compared on the basis of similarity of shapes. Thus there are three pairs of particles: non-spherical (elliptical and rice beads), cylindrical (short and long) and spherical.

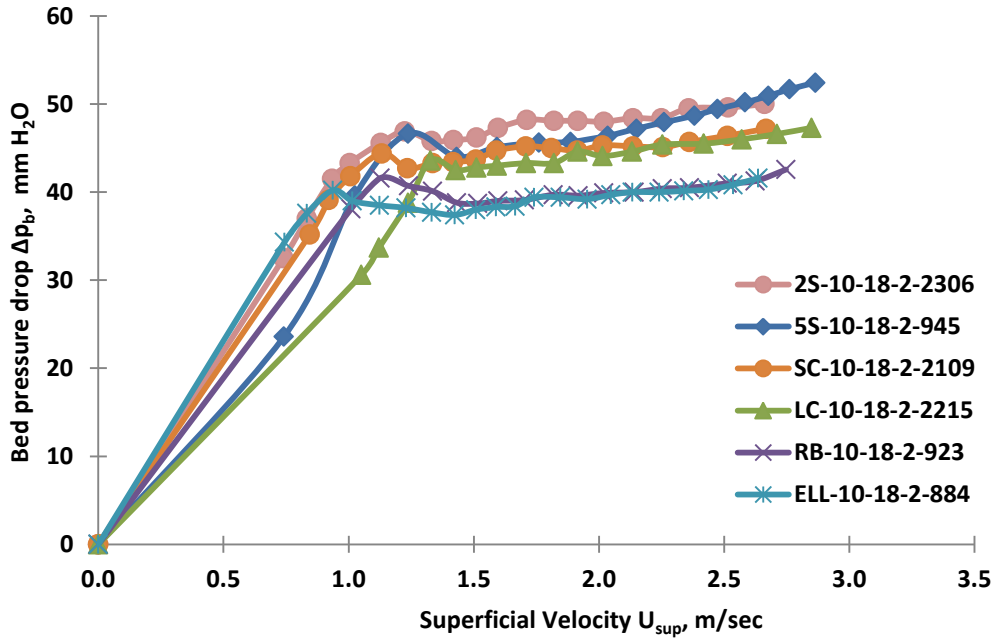

Figure 4.15: Bed pressure drop versus superficial velocity for particles with different densities

For the non-spherical and cylindrical particles, the minimum fluidization velocity varies with L/D ratio for similar particle diameter and density. This can be

understood to be a consequence of longer particles having a larger weight and hence a higher U_{mf}. This trend is well reflected in Figure 4.15. The rice bead particles with L/D of 2.0 fluidize later than the elliptical particles of L/D of 1.36. As for the cylindrical particles, short cylinders with L/D of 1.2 fluidize earlier than long cylinders with L/D= 4.1. In the case of the spherical particles, they appear to be proportional to ρd_p^2as stated earlier in section 4.5.4.Particles with the same size and different densities would have been ideal for this analysis. Since particles with required specifications cannot be obtained, those which are available in the market were used to perform the experiment.

4.6 Minimum Fluidization Velocity, U_{mf}

The minimum fluidizing velocity U_{mf} can be defined as the minimum superficial velocity at which the fluidization occurs i.e., the superficial velocity at which pressure drop through the bed is equal to the bed weight per unit area. There exist numerous empirical correlations for predicting U_{mf} in a conventional bed, but none exists in case of SFB. Hence U_{mf} has to be determined experimentally in the case of SFB.

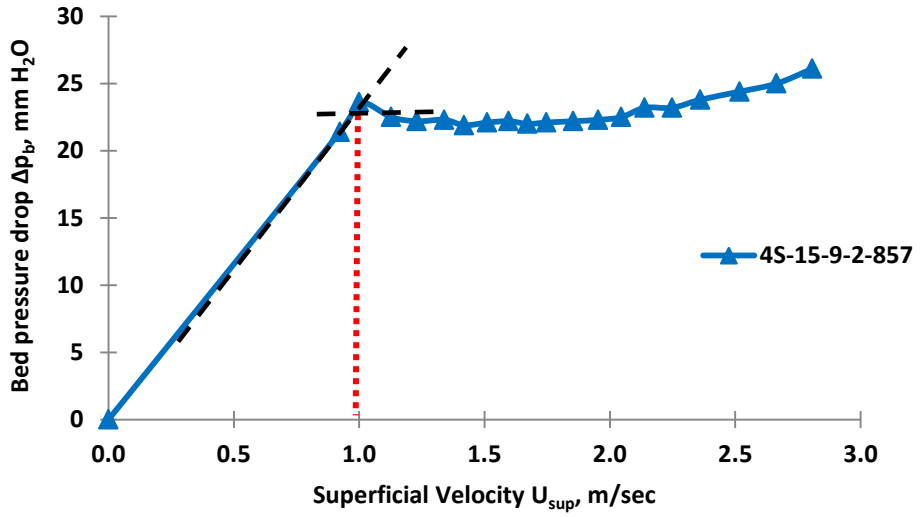

Figure 4.16: Bed pressure drop versus superficial velocity illustrating the method to find minimum fluidizing velocity, U_{mf}

U_{mf} can be determined from a graph with bed pressure drop plotted against superficial velocity as shown in Figure 4.16.The minimum fluidizing velocity, U_{mf}, corresponds to the superficial velocity at the intersection of two straight lines drawn fitting to the above graph. A linear trend line is drawn with a few points in the packed region and another horizontal one through the point right after the incipience of fluidization. Since previous studies [1] have shown that the graph in the packed bed region may be non-linear, as the flow may assume turbulent nature as the gas flows through the interstices, only a few points just before fluidization are considered. The method is illustrated in the figure above.

The study of minimum fluidization velocity, U_{mf} is another facet of bed hydrodynamics. It gives information on the gas flow required to fluidize the bed. As the bed operates at velocities higher than U_{mf}, usually specified as a ratio U_{sup}/U_{mf}, prediction of U_{mf} is useful for the design of a bed. The ratio of terminal velocity to minimum fluidization velocity, U_t/U_{mf} that decides the operating range of the bed also requires knowledge of U_{mf}.

The minimum fluidization velocity, U_{mf}, is an important factor as far as the fluidized bed is concerned. The effect of various aspects of the distributor as well as that of bed particles on minimum fluidization velocity is significant in view of reactor design.

Given below are various parameters, the effect of which on U_{mf} is investigated

1) Distributor blade inclination angle, θ
2) Distributor blade overlap angle, α
3) Size of the particle, d_p
4) Shape of the particle
5) Bed weight, W_b
6) Density of the particle, ρ_p

4.6.1 Influence of Blade Inclination Angle onU_{mf}

Figure 4.17 shows the variation of minimum fluidization velocity with Blade inclination, θ. Three different blade inclinations of 10^o, 15^o and 20^o were used in the study. It is seen from the plot that the minimum fluidization velocity is independent of blade inclination angle. Even though the angle of inclination affects the angle at which the fluidizing medium enters the bed, it has no effect on the minimum fluidization velocity. This can be explained thus: at minimum fluidization, the bed is still in a packed regime, though in a weightless state. There is no swirling yet and the gas stream entering the bed encounters stationary bed particles, gets dissipated by them and percolates upwards through the bed. The entire velocity is in the vertical direction and balances the bed weight irrespective of the blade inclination. For a given size of bed particles with given bed weight, the minimum fluidizing velocity is seen to remain the same.

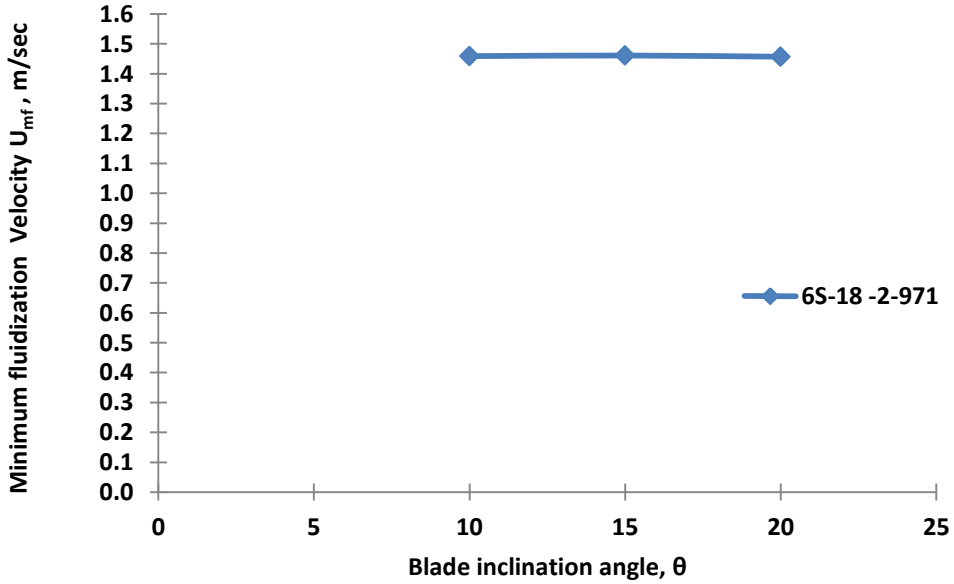

Figure 4.17: Minimum fluidizing velocity versus blade inclination angle

4.6.2 Influence of Blade Overlap Angle on U_{mf}

From Figure 4.18 depicting the variation of minimum fluidization velocity with change in blade overlap angle, we can observe that the longer the blade overlap

angle, the higher is the velocity required for fluidization. The longer the overlap of the blades, the smaller is the gas inlet angle. This leads both to a larger horizontal velocity component as well as a lower vertical velocity component. For a smaller overlap, the gas exits at a higher inclination leading to a larger vertical component, which enables fluidization at a lower velocity. As overlap increases, the vertical component decreases and the required velocity for fluidization increases progressively. The effect of overlap angle on minimum fluidization can be attributed to the flow development when the fluidizing air passes between the blades of the distributor. As the minimum fluidization concerns lifting of the particles against gravity and freeing them, a higher fluidizing velocity for a given bed particle size and given density simply means that the vertical velocity available for fluidization is less for a longer blade overlap.

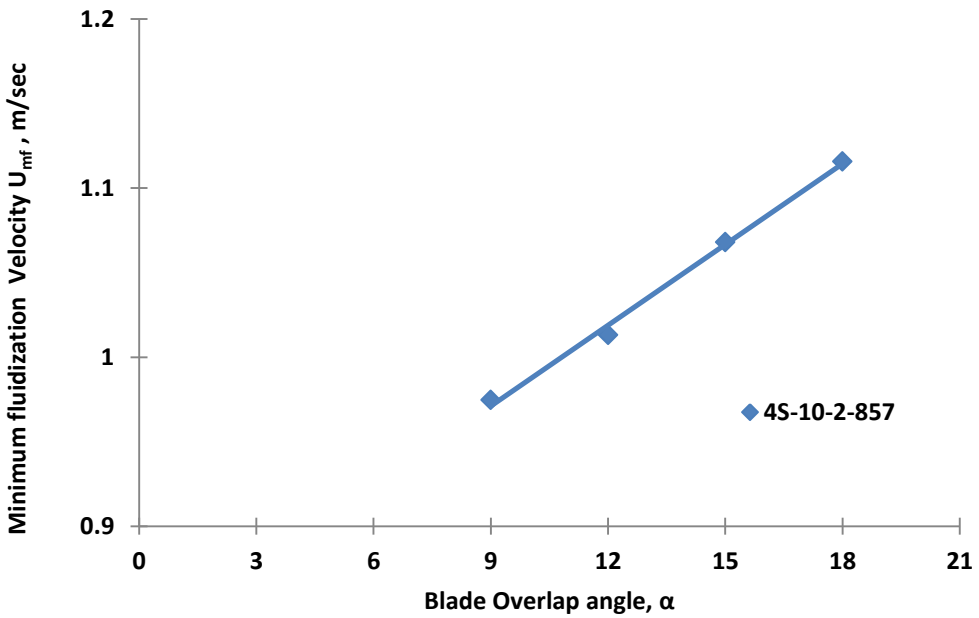

Figure 4.18: Minimum fluidizing velocity versus blade overlap angle

This can be compared to the flow between inclined flat plates. The longer the plate, the longer is the path and the more developed is the flow. In the case of smaller angle of overlap the flow path is shorter, hence the peak velocity of the fluid exiting the distributor is comparatively lower and the flow is underdeveloped. When the overlap angle increases, the width of the blade increases resulting in a longer flow path helping the fluid to develop more fully and exit at a higher peak

velocity. The trend in Figure 4.18 appears to be a consequence of flow development in the blade passage. The important conclusion here is that the minimum fluidization velocity is a function of overlap angle.

4.6.3 Influence of Particle Size on U_{mf}

The effect of bed particle diameter is demonstrated in Figure 5.19 from which we can see that the U_{mf} increases with an increase in the particle size/diameter. A similar observation is made in Figure 4.10. The larger the particle, the larger is its weight for a given particle density and the smaller its surface area per unit volume of the particle. Therefore to reach U_{mf}, more drag force i.e. higher velocity is required.

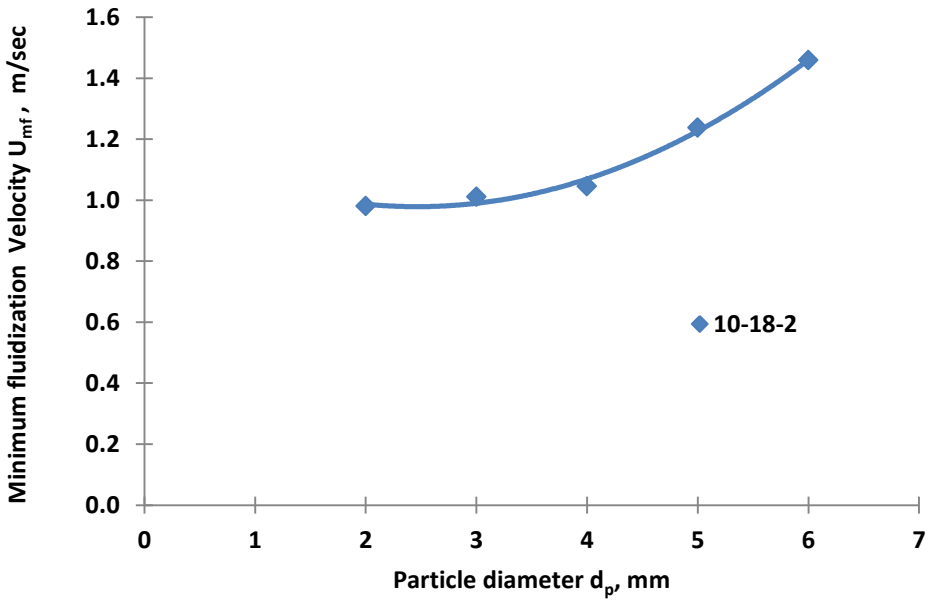

Figure 4.19: Minimum fluidizing velocity versus bed particle diameter

As the curve is extrapolated to lower d_p values, U_{mf} seems to approach an unlikely asymptotic limit. The explanation for this is available in the form of the Ergun equation, 2.1, which is repeated below.

$$\frac{\Delta p}{L} = k_1 \frac{(1-\varepsilon)^2}{\varepsilon^3}\frac{\mu U_{mf}}{d_p^2} + k_2 \frac{(1-\varepsilon)}{\varepsilon^3}\frac{\rho_m U_{mf}^2}{d_p} \tag{2.1}$$

The expression rewritten in terms of U_{mf} will have two terms, one being proportional to d_p and the second, to d_p^2. According to Geldart [99], dp>2 mm lies in the range of D-type particles, termed as 'large'. The d_p values of the present study fall in this range at which the quadratic term is dominant and the trend seen in Figure 4.19 appears. For the 'small' range of d_p values, the first term is dominant and U_{mf} will be proportional to d_p and the curve is not to be extrapolated to lower values of d_p.

4.6.4 Influence of Particle Shape on U_{mf}

Variation of the minimum fluidization velocity, U_{mf} with respect to the shape of bed particles represented in the form of L/D ratio is shown in Figure 4.20. Observing the plot we can conclude that with an increase in L/D ratio the minimum fluidization velocity increases. This behavior can be explained in the following way: as the L/D ratio increases, the mass of the particle increases proportionally to LD^2 and requires a higher velocity to fluidize it. However, the area on which the drag force acts is proportional to LD. While it shows a complicated relationship of L/D to U_{mf}, Figure 4.20 suggests an approximately linear functionality.

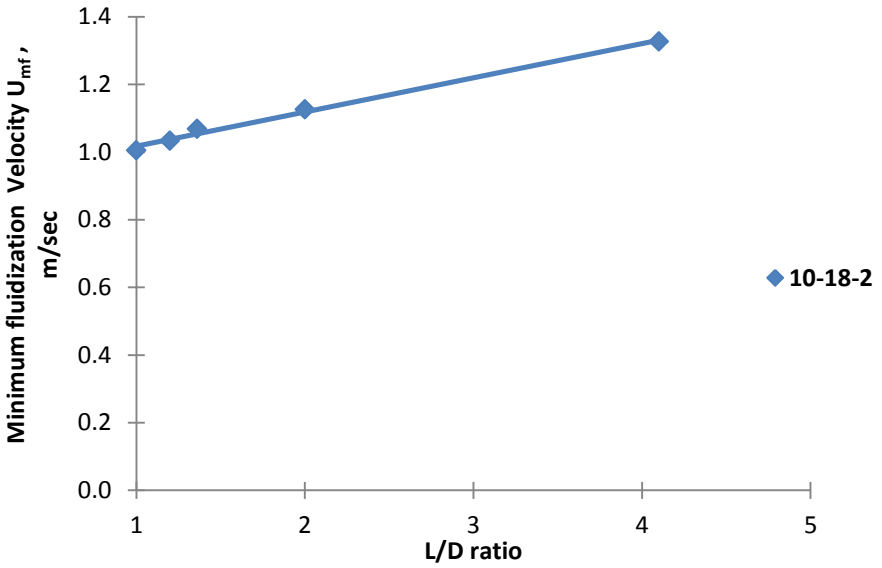

Figure 4.20: Minimum fluidizing velocity versus L/D ratio for particles of various shapes

4.6.5 Influence of Bed Weight on U_{mf}

The above plot in Figure 4.21shows the variation of minimum fluidization velocity U_{mf} with respect to a variation in bed weight. It can be seen from the plot that the minimum fluidization velocity remains a constant for a given set of aspects irrespective of the bed weight. The reason for this would be that in the fluidized state, the particles are freed from each other and behave as separate entities. The velocity required to produce the drag force required to balance the weight and thereby fluidize the bed is dependent on the individual particle size and shape and not on the bed weight of the assemblage of particles.

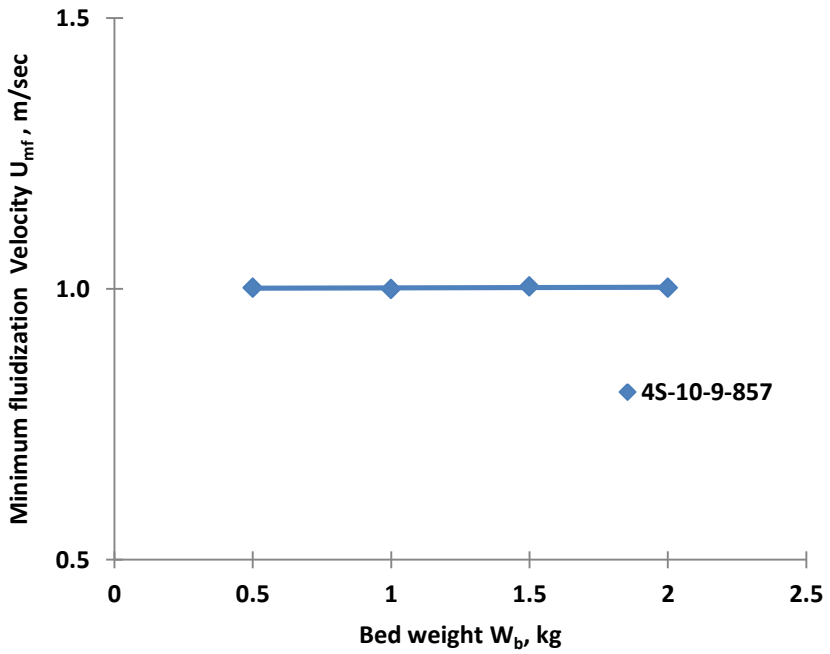

Figure 4.21: Minimum fluidizing velocity versus bed weight

4.6.6 Influence of particle density on U_{mf}

In the plot of U_{mf} as a function of d_p, Fig. 4.19, the density varied slightly from one particle size to another. As stated before, this variation occurs as a result of limitations in commercial availability of particles.

According to the explanation given earlier, the trend of U_{mf} versus d_p follows a direct proportionality. Similarly, if a sufficient range of particle density for each particle diameter were available, a plot such as U_{mf} against ρ would also have followed a direct proportionality. Evidence for these two dependencies comes from a number of correlations as set out in Table 2-1: Summary of various correlations for U_{mf} in terms of density and particle diameter.

In this case, the particles straddle the range from 2 mm to 6 mm, in the course of which the interstitial gas flow appears to undergo transition from laminar to turbulent. Accordingly, the U_{mf} dependence also changes character. As shown in Fig. 4.22 (a), the straightforward ρd_p^2 functionality of U_{mf} seems to hold for the lower values of ρd_p^2 and gradually yields to the empirical and more involved implicit form that has been given by Wen and Yu [83]. This can be seen from the difficulty of fitting a reasonable line to all the points. The plot of U_{mf} vs. ρd_p^2 is strictly expected to be linear only in the laminar region. The few points corresponding to the smaller particle sizes do seem to follow the expected linear trend. However, over the entire range, a linear variation does not seem to be valid.

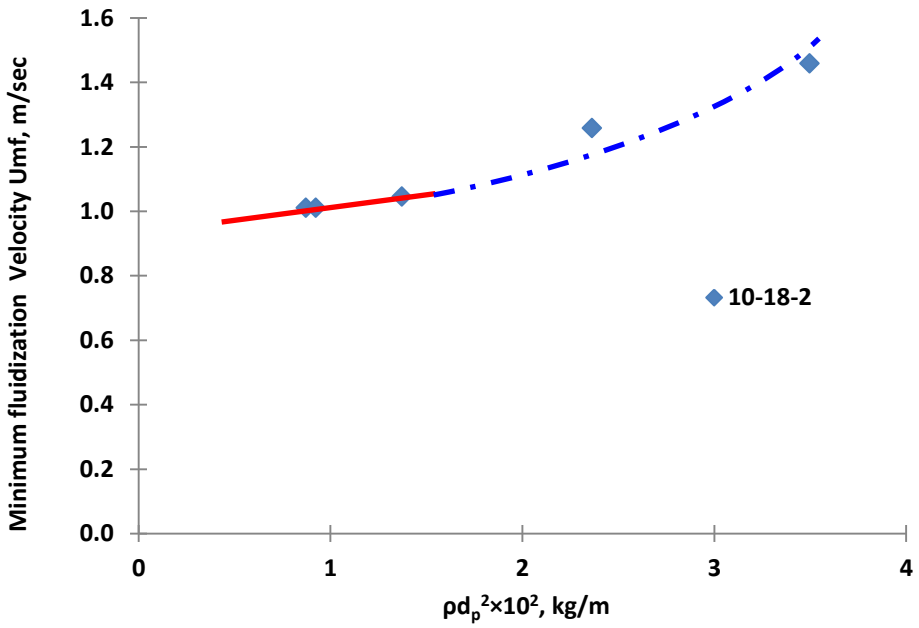

(a)

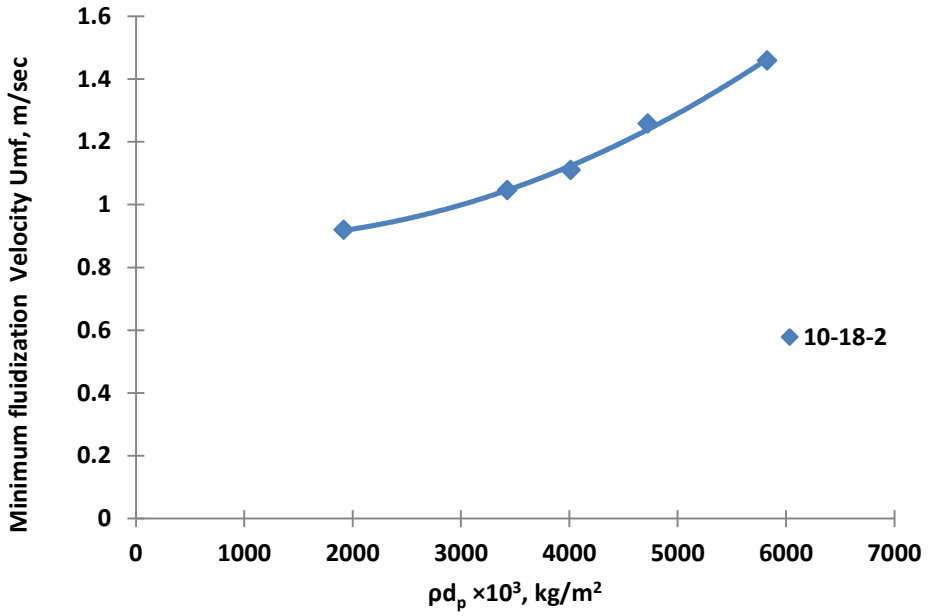

(b)

Figure 4.22: Minimum fluidizing velocity versus f (ρd_p)

(a) versus ρd_p^2 (b) versus ρd_p

As our aim in this work is to investigate the relationship between various parameters, between U_{mf} on the one hand and ρ and d_p on the other, a correlation is sought between this pair of variables. The most natural approach that suggests itself is the combined variable (ρd_p). Fig. 4.22 (b) appears to give a reasonably good correlation between U_{mf} and the combined variable ρd_p. Because of the complicated dependency of U_{mf} on ρd_p in view of the transition of flow in the region of the experiment, this result is considered adequate for revealing the qualitative propensity.

4.7 Bed Height, H_B

Bed height in the packed bed regime is called the static bed height and it depends on the bed weight and size of the particles. The conventional fluidized bed expands at and beyond minimum fluidization in aggregative fluidization as well as

particulate fluidization. The static bed height will be higher for an as-poured bed than a defluidized bed, as the particles collapse and get rearranged more tightly on defluidization. In the case of aggregative gas-solid fluidization the bed volume is the volume at minimum fluidization plus the volume of the gas bubbles passing through. In liquid-solid fluidization, there are no bubbles. The particles move apart to accommodate the increased flow of the liquid and the inter-particle distance increases. This is termed as particulate fluidization.

Even though it is a gas-solid system, it is remarkable that the swirling fluidized bed is bubble-free and exhibits a particulate-like behavior for all the cases considered here. Hence an increase in bed height with little fluctuations of the bed surface is seen in all the cases investigated in the work. This is because of the absence of gas bubbles in swirling fluidization.

The study of bed height as a part of hydrodynamics evolves from the need to know the degree of bed expansion and the expanded bed height in at least two practical situations. The first is in the design of heating/cooling coils enclosing the bed for heat addition or heat extraction. The second situation arises in continuously operated single-stage or multi-stage reactors where the outflow weir has to be appropriately positioned. Thus a study of the bed height is an important part of bed hydrodynamics.

Given below are various parameters, whose effect on H_B is investigated

1) Distributor blade inclination angle, θ
2) Distributor blade overlap angle, α
3) Size of the particle, d_p
4) Shape of the particle
5) Bed weight, W_b

4.7.1 Influence of Blade Inclination angle H_B

Figure 4.23 shows the variation of bed height in a swirling fluidized bed with respect to change in blade inclination angle. The results reveal that the bed height increases with an increase in blade inclination. In fluidized beds, expansion occurs when the superficial velocity exceeds U_{mf} and the flow rate is more than enough to support the weight of the bed. The extent of expansion depends on the superficial velocity of the fluidizing medium. In aggregative fluidization, the excess gas appears as bubbles inflating the bed. In particulate fluidization the excess fluid flows, not as bubbles but as interstitial gas that drives the particles apart and expands the bed. In this respect, the SFB behaves like a particulate bed. Depending on the depth of the bed and size of the bed particles, certain beds can undergo a high degree of expansion before elutriation sets in. To explain this effect, recourse has to be taken to the force diagram given earlier in Figure 4.1. A smaller angle introduces more vigorous swirling which in turn generates a higher centrifugal force. A corollary of this is that the downward frictional force is higher, restraining the bed expansion. The converse is true with the larger angles.

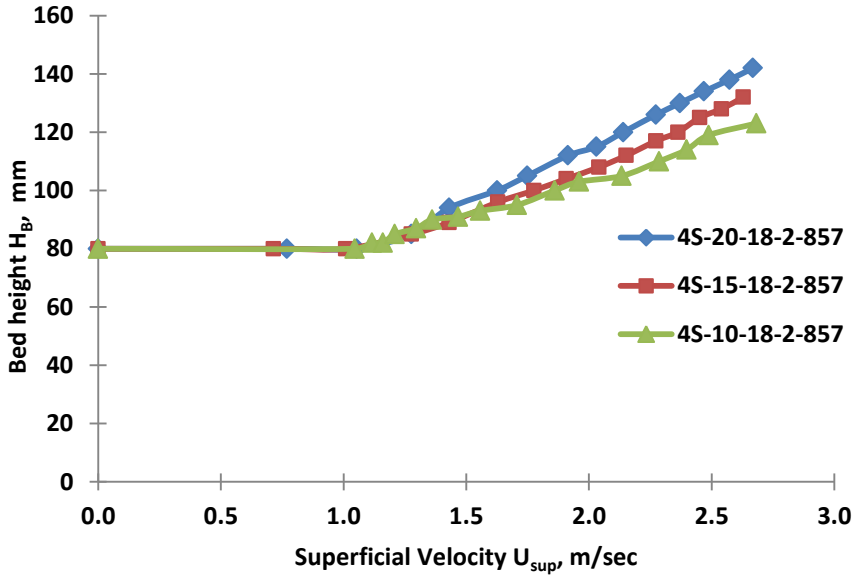

Figure 4.23: Bed height versus superficial velocity for different blade inclination angles

4.7.2 Influence of Blade Overlap Angle H_B

The variation of bed height in accordance with a change in blade overlap angle is depicted in Figure 4.24. This may also be explained with the aid of forces in the bed. Though the overlap angle varies from 9^o to 18^o, the actual exit angle varies by a far smaller extent as shown in Figure 4.1. The small changes of angle result in small changes in centrifugal force, in downward frictional force and finally in bed expansion. This is the trend seen in Figure 4.24. All the cases follow a similar trend where the bed height is only minimally sensitive to an increase in blade overlap angle.

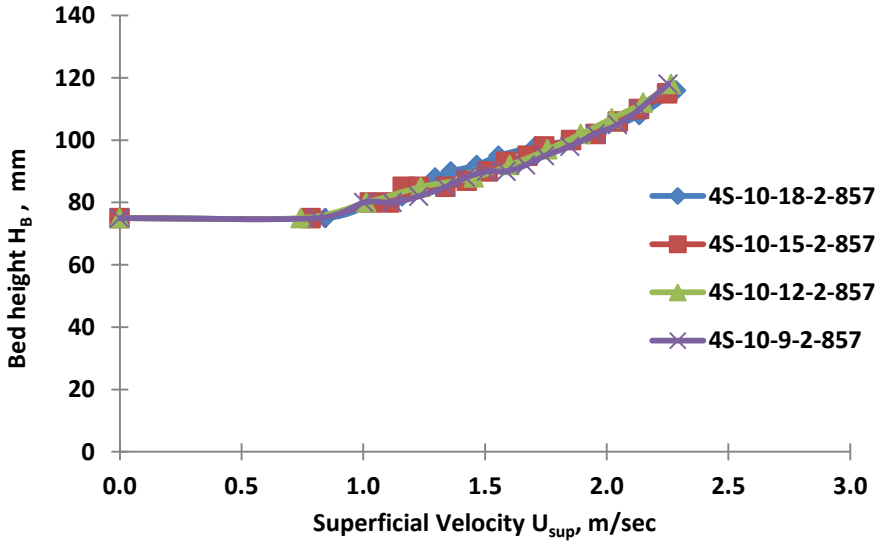

Figure 4.24: Bed height versus superficial velocity for different angles of overlap

4.7.3 Influence of Particle Size on H_B

The plot in Figure 4.25 represents the variation of bed height with respect to change in particle size. On observation, it is quite clear that the bed of smaller particles expands more. This effect is also explained by the force diagram (Figure 4.1). Smaller particles have a smaller mass, a smaller centrifugal force, a smaller downward frictional force and therefore, larger expansion.

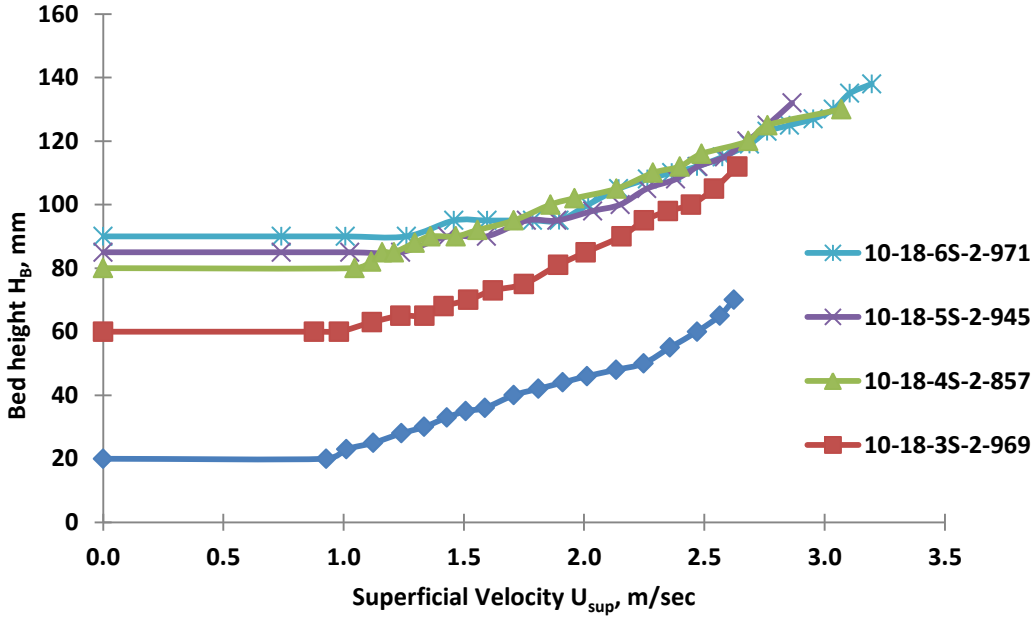

(a)

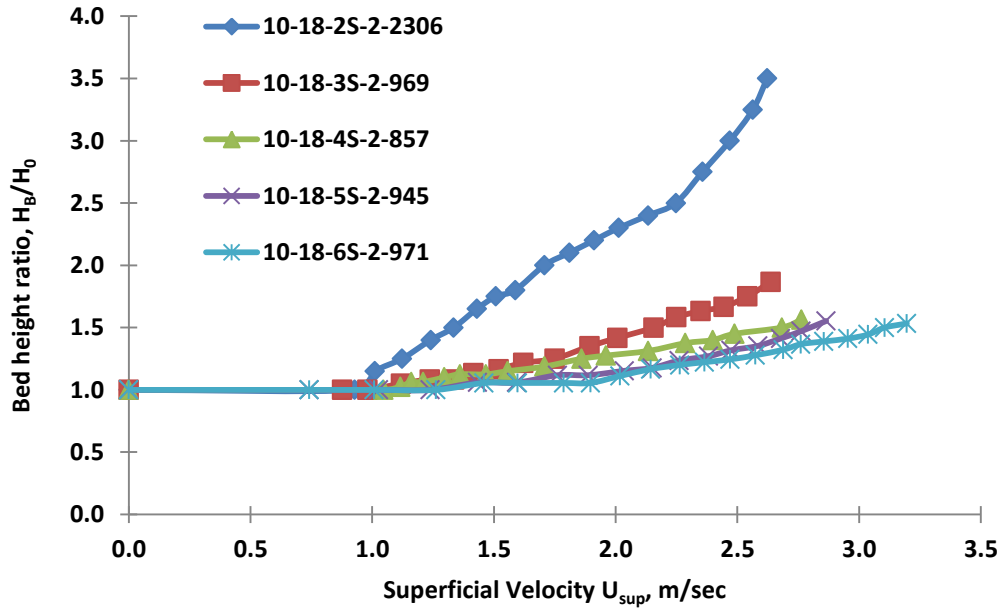

(b)

Figure 4.25: Bed height versus superficial velocity for different size particles

(a) Physical bed height, H_B (b) Bed height ratio, H_B/H_0

The smaller particles must swirl at a lower velocity than the larger particles. This premise stems from the following facts. The minimum fluidization velocity is

less for the smaller particles. Momentum transfer occurs from the gas to the particle. A precondition for this to happen is that the particle velocity be smaller than the gas velocity. The outcome of the above argument is that, for smaller size of particles, a combination of smaller weight and lower swirling velocity leads to larger bed expansion as can be seen from Figure 4.25 (a) and (b). The intersection of the 4S line with those for 5S and 6S is because of the lower density, by about 10%, of the 4S particles.

If we calculate the expansion ratio, defined as the ratio of the average height of a fluidized bed to initial static bed height, H_B/H_0 at a particular flow rate of the fluidizing medium above the minimum fluidizing velocity, the above result is brought out clearly. In the case of conventional beds also, the larger particles have a smaller expansion. For this result Singh *et al.* [102] found an explanation that, due to the larger weight, the bigger particles impose a larger downward force and restrict bed expansion. This explanation is incorrect and the scientific explanation lies in the weight being proportional to D^3 and the opposing drag being proportional to D^2.

4.7.4 Influence of Particle Shape on H_B

Figure 4.26 (a) and (b) represents the trend when bed height was plotted against superficial velocity for different shapes of particles keeping the bed weight constant. The bed of cylindrical particles had the highest density and lowest bed height. The rice bead particles had the highest bed expansion followed by the elliptical and spherical particles respectively.

Density seems to be the prominent aspect rather than shape in the case of the long cylinder. It has the least static bed height, with other lighter particles showing a comparatively higher bed expansion. As compared to spherical particles, elliptical particles and rice beads have smaller sphericity and lower bed compactness. Spherical particles could be expected to pack the closest, with smallest interstitial spaces. The smaller voidage in the packed state carries through to the fluidized

state. The smallest U_{mf} of elliptical particles generates the highest bed expansion.

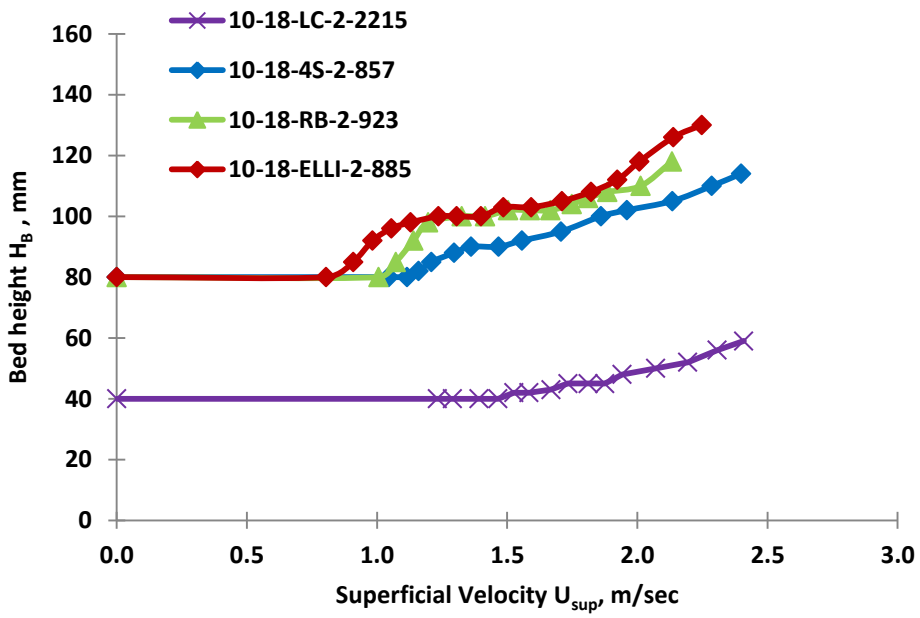

(a)

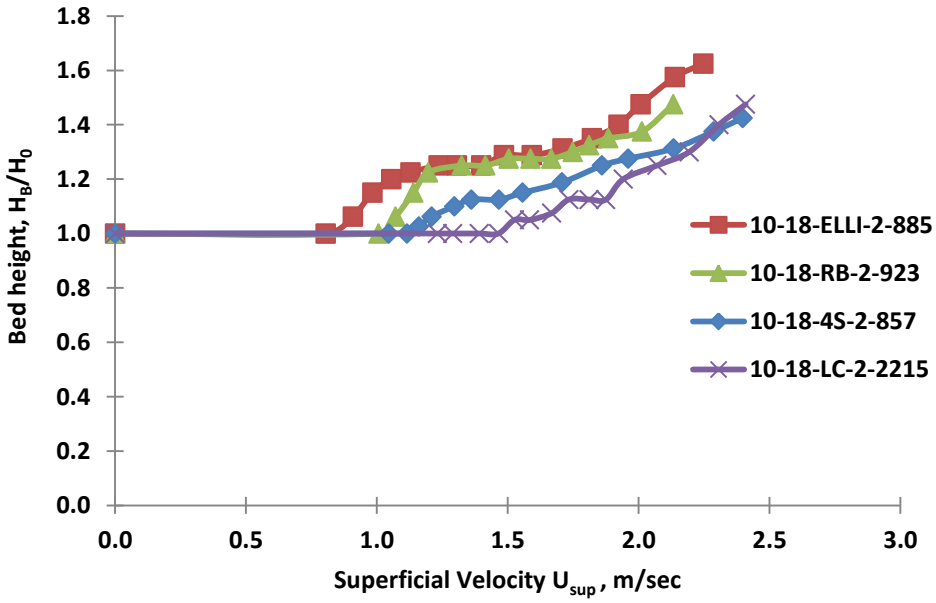

(b)

Figure 4.26: Bed height versus superficial velocity for particles of different shape (a) Physical bed height, H_B (b) Bed height ratio, H_B/H_0

4.7.5 Influence of Bed Weight on H_B

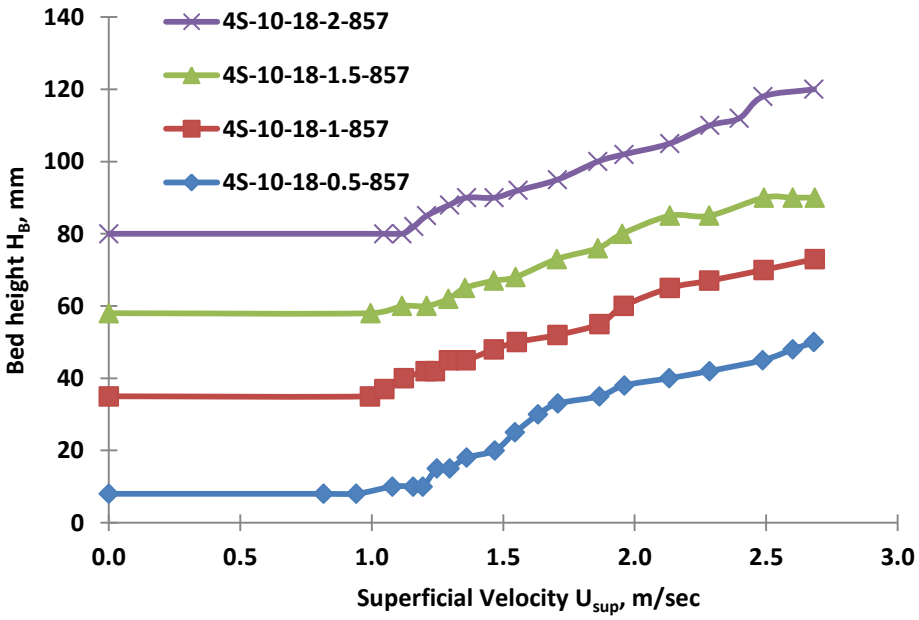

(a)

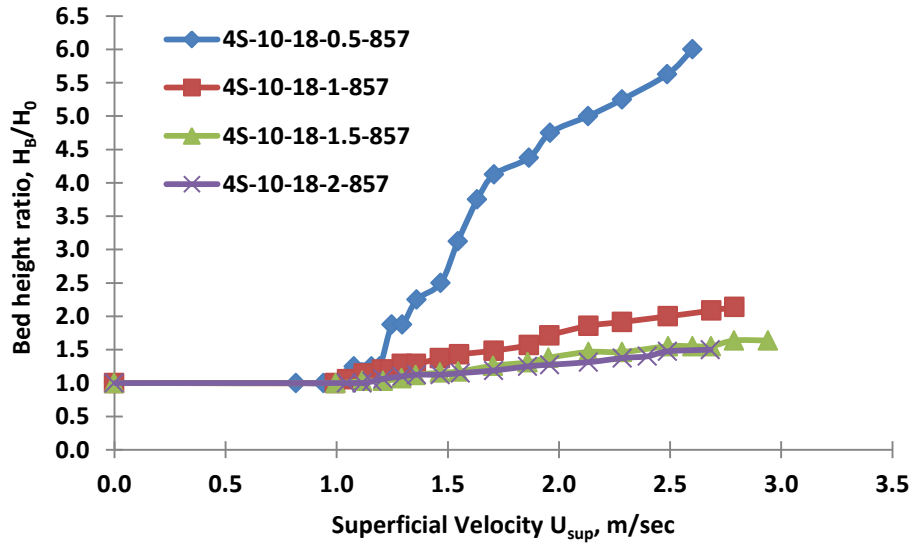

(b)

Figure 4.27: Bed height versus superficial velocity for different bed weights

(a) Physical bed height, H_B (b) Bed height ratio, H_B/H_0

The influence of bed weight on bed height is shown in Figure 4.27 (a) and (b). From the trend it is evident that with an increase in bed weight the bed height also

increases. But when we calculate the bed expansion ratio the trend is contrary. The highest bed expansion ratio is recorded at the lowest bed weight and vice-versa. The earlier argument of higher bed expansion for lower bed weight is in agreement with the observation. The justification of Singh *et al.* [102] that in conventional beds, a larger bed weight acts more strongly downwards and keeps the expansion lower is evidently untenable. The correct elucidation is based on the dependence on diameter given in 4.7.3.

4.8 Slug-Wave Regime

The slugging or wavy regime can be considered as a partially fluidized regime in which a part of the annular bed swirls while the rest of the bed is in a packed condition. Because of the dynamics of swirling, the moving part of the bed goes around the periphery at a certain periodicity and no part of the bed is stationary at all times. Slugging seems to occur when certain conditions are met: a low distributor pressure drop or a low bed weight. Fully swirling beds are ideal for kinetically controlled processes rather than diffusion controlled processes, for which a packed bed is more suited. As the swirling arc of the bed is ideal for kinetically controlled processes and the static arc of the bed is suitable for diffusion controlled processes, the slug-wavy regime can be thought to combine the beneficial features of both swirling beds and packed beds. Such beds have longer particle residence times as compared to fully swirling beds. Thus the slug-wavy regime represents a novel processing method that is economical on gas consumption and suitable for diffusion-controlled processes and hence, deserves greater attention. It is with this objective that the regime has been studied in the present work.

The slug-wavy regime owes its origins to imperfections in the distributor, in which there will always be non-uniformities. For example, if there is a slightly larger flow area in a particular blade passage, it will cause the neighboring blade passage to be narrower. The flow resistance of the particular imperfection can be expected to have a larger flow rate than the rest of the distributor. Thus a local gas

channel will be formed. The gas stream entrains nearby particles and the bed builds up at the channel and suppresses it. The process continues around the periphery of the annular path, giving rise to a slug like motion that can be described as a wave. Hence the term slug-wavy regime is given to it.

The mechanism of slug-wavy regime is quite complex and the governing physics is as yet poorly understood. Conventional wisdom has it that the slug-wavy regime is an undesirable mode of operation of the SFB and is to be eliminated in the design of a reactor. However, as pointed out earlier, the slug-wavy regime holds great promise for diffusion controlled reactions and economizing gas use and has much potential for practical application. There is a need to study this regime in greater detail. This is the rationale for the study of the slug-wavy regime.

When slugging occurs, it appears at a superficial velocity just beyond minimum fluidization and before full swirling. During the motion around the annular bed in this regime, the particles begin to pile up and later collapse, giving the impression to the onlooker as if a wave is moving along the annular path. This happens due a phenomenon similar to channeling in conventional beds. In an SFB, with an increase in flow rate the fluid will try to pierce its way through the resistance offered by the bed. There exists a point of low resistance from where the slugging always starts. The fluid pushes its way through the bed moving the bed particles forward. As the particles in that region begin a swirling motion, those behind them are free to move under the influence of the fluidizing medium as depicted in Figure 4.28. The momentum of the fluid at that particular flow will not be enough to carry the particle to a longer distance through the primarily stagnant bed, resulting in formation dunes/peaks. Thus the low resistance zone keeps on shifting and the dunes/ peaks move in a direction opposite to that of the swirling, resulting in what is designated as a slugging or wavy regime as shown in Figure 4.29. The packed bed transforms progressively into a slug-wavy bed with initiation of dunes as shown in the figure. The dune continues to grow, reaches a maximum, and then starts decaying until it reaches the initial stage of packed bed. This is referred to as a single slug-wave cycle and the time taken for this is the slugging time, t_S.

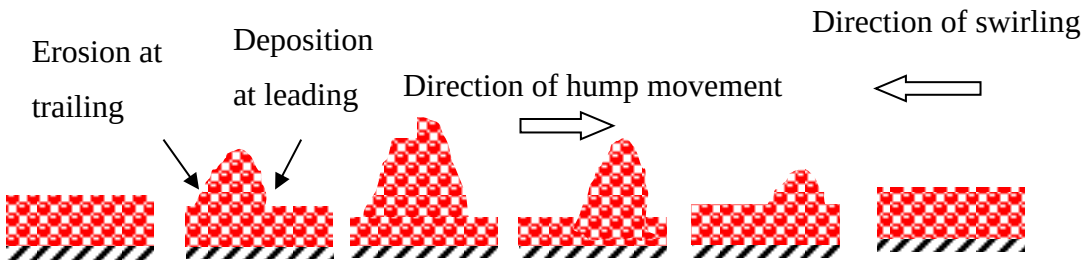

Figure 4.28: Different stages of the bed in a slug-wave regime

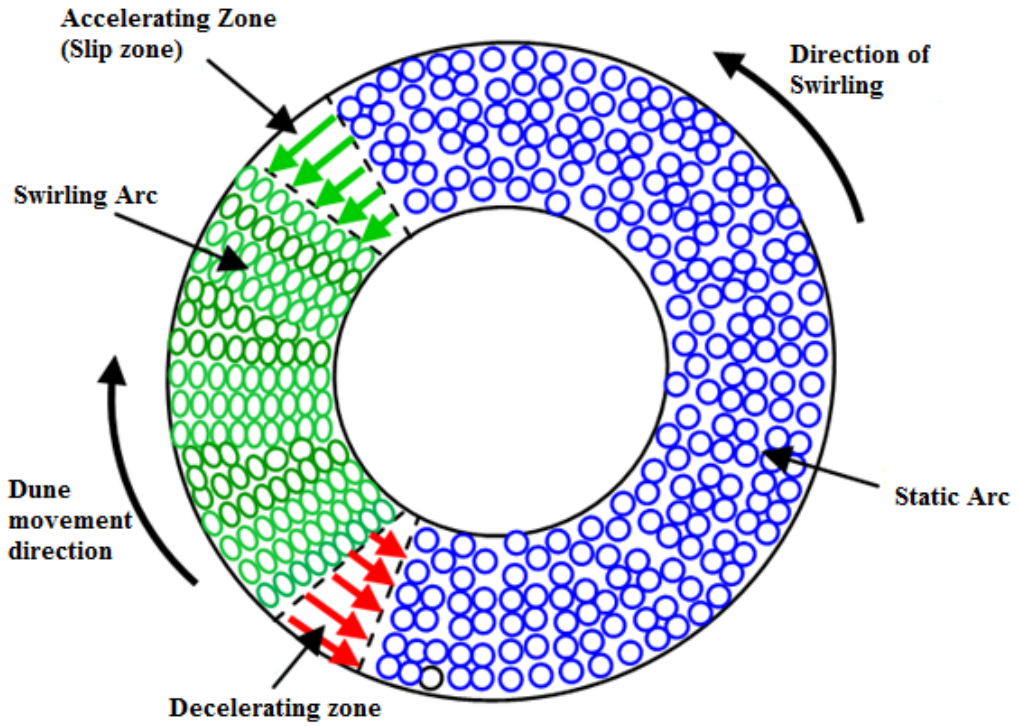

Figure 4.29: Top view of a swirling fluidized bed experiencing slug-wave

In relatively shallow beds, slug-wave sets in at a lower superficial velocity. The overall slugging velocity will be low as the peak is higher due to lack of momentum in the fluidizing air to push the particle. When the velocity increases, the height of the dune decreases and it becomes wider, giving an impression that it is moving faster. Deeper beds have a higher flow resistance and a lower tendency to slug. The behavior of the slug-wavy regime is investigated below as a function of several aspects.

4.8.1 The Time Taken for One Slugging cycle, t_S

The time taken for slugging is the duration of time required for a peak to travel around the circumference and reach the same point from where it started. The variation of slugging time with bed weight, particle shape, blade overlap, blade inclination and particle size seems to be prominent.

4.8.2 Influence of Bed Weight on t_S

Figure 4.30 shows the variation slugging time for various bed weights. With an increase in bed weight the minimum slugging velocity increases, slugging time decreases and the velocity range of slugging is similar. The explanation for this could be as follows: a smaller bed weight has a lower flow resistance and a greater susceptibility for instability. Thus the slugging sets in earlier. An earlier slugging initiation is synonymous with lower gas velocity. As particle velocity cannot exceed the gas velocity, the particles swirl slower and the slugging period t_s is longer.

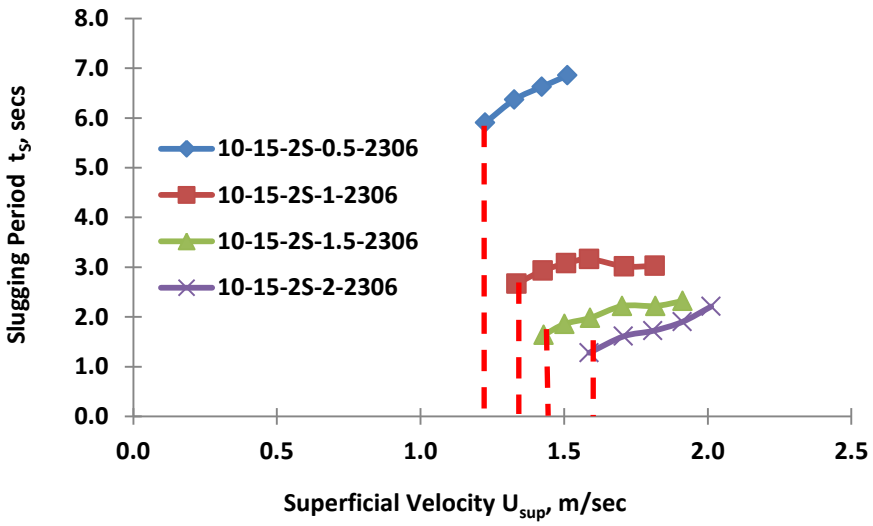

Figure 4.30: Plot of slugging time versus superficial velocity for various bed weights

4.8.3 Influence of Particle Shape on t_S

From Figure 4.31 showing the variation of slugging time with different shapes of particles, the slugging period is longer for spherical particle than the others. The minimum slugging velocity, i.e., the velocity at which the slug-wavy regime initiates, is independent of the particle shape.

There appears to be a distinct effect of sphericity here. Spherical particles have a sphericity of unity and pack more compactly. Their slugging period is longer though the velocity range of slugging is the same. As sphericity decreases, the particles undergo slugging more easily.

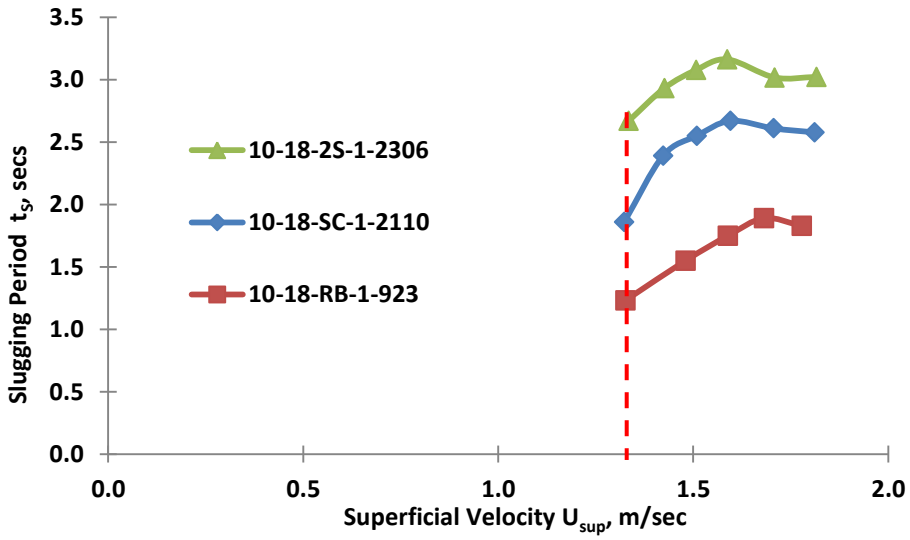

Figure 4.31: Plot of slugging time versus superficial velocity for different shapes of particles

4.8.4 Influence of Blade Overlap Angle on t_S

Figure 4.32 describes the variation of slugging time with respect to different blade overlap angles. Two effects are seen here. First, the slugging time increases with blade overlap angle. Secondly, the superficial velocities at which the slugging starts are seen to increase with blade overlap angle. As stated earlier, there is a relationship between slugging and resistance to flow of air, which might originate

from the distributor or the bed. The lowest distributor resistance corresponds to earlier setting in as well as more rapid slugging. As smaller overlap corresponds to lower distributor resistance, the observed behavior is well-interpreted. With an increase of flow resistance associated with an increase in blade overlap angle, a higher flow rate is required to supply the greater energy needed to initiate slugging.

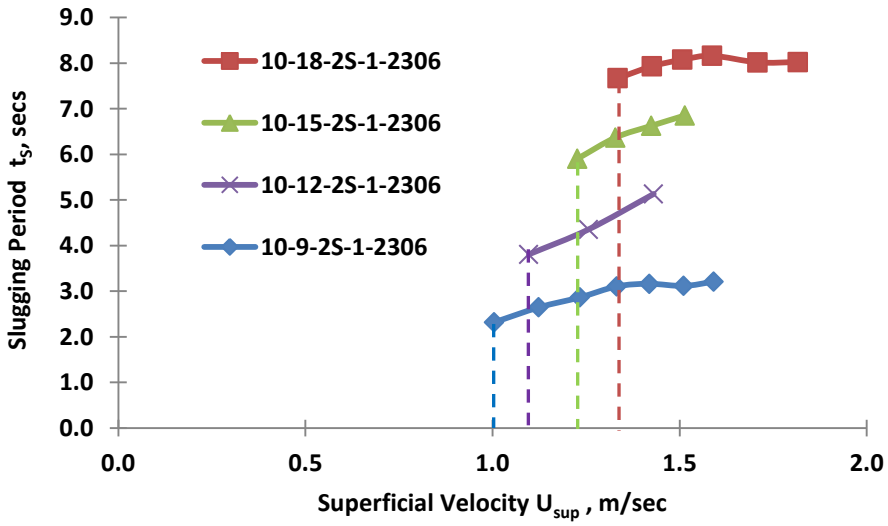

Figure 4.32: Plot of slugging time versus superficial velocity for different blade overlap angles

4.8.5 Influence of Blade Inclination on t_S

From Figure 4.33 it is evident that when blade inclination increases the slugging period increases. It can also be seen that, with increase of with blade inclination, the range of superficial velocities over which slugging occurs is broader. With an increase of blade inclination the resistance of the bed decreases which is favorable for occurrence of the slug-wave.

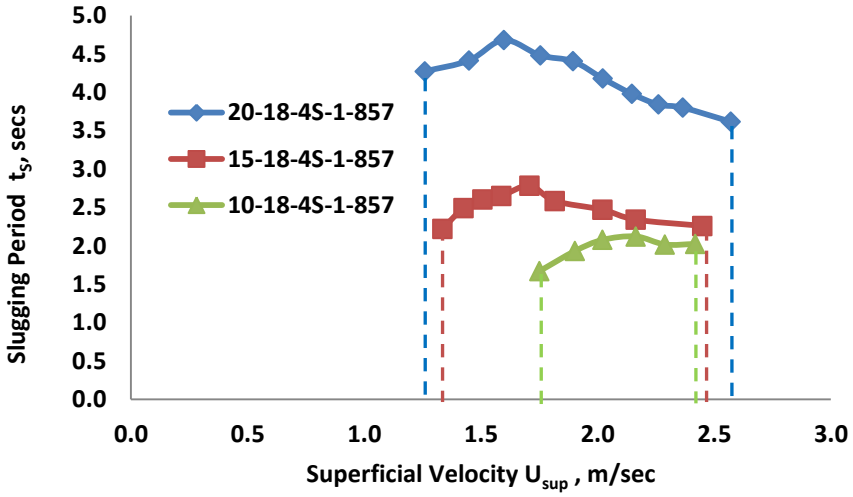

Figure 4.33: Plot of slugging time versus superficial velocity for different blade inclinations

4.8.6 Influence of Particle Size on t_S

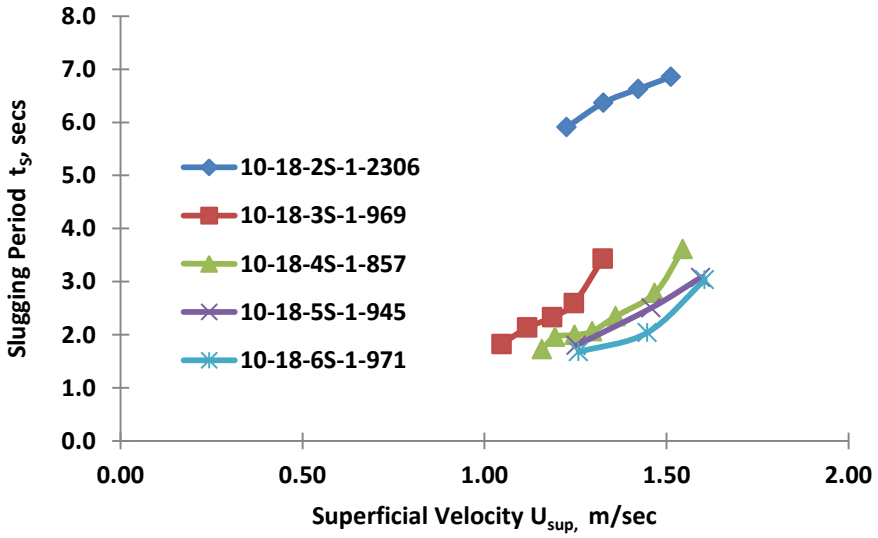

Figure 4.34: Slugging time versus superficial velocity for different particle sizes

Figure 4.34 refers to variation in slugging time for different sizes of particles. As observed in earlier cases, the superficial velocity at which the slugging starts increases with increase in size of the particles. It is also observed that the slugging

time decreases with increase in particle size. These results are in consonance with the bed resistance postulate and the evidence in Figure 4.10. The plot for 2 mm spherical particle lies distinctly because it has a density more than 2.2 times that of the other particles. However, the particle density effect on slugging has not been possible due to unavailability for custom-made particles.

4.9 Hysteresis Observed during Fluidizing and Defluidizing of the Bed (increase and decrease of air flow)

When the bed pressure drop is plotted against superficial velocity as the flow increases or decreases progressively, the trends followed are different, giving rise to hysteresis. In the direction of increasing velocity, additional energy is required for unlocking the particles in the packed bed to get them fluidized as shown in Figure 4.35.

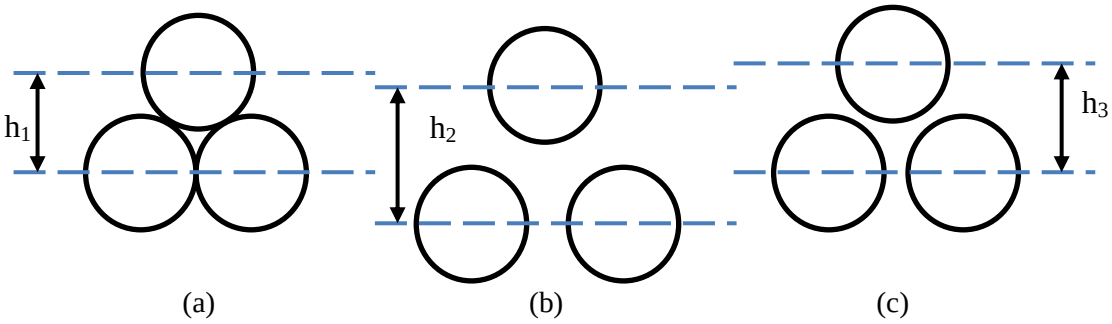

Figure 4.35: Illustration of hysteresis at minimum fluidization

Figure (a) corresponds to packed bed condition at incipience. The forces are in balance, drag D = weight W.

Figure (b) corresponds to the state just after incipience, when D > W and the higher drag D forces the particles apart and the inter-particle distance is increased. The lifting of the particles absorbs additional energy from the gas stream and is visible as a peak in the Δp curve.

The greater distance between particles in (b) causes the interstitial velocity to decrease and the force equilibrium D = W is again attained but at a larger gas flow rate than at incipience. This causes the particles to settle to a new position as shown in Figure (c).

i) The voidage varies as $\varepsilon_a < \varepsilon_b$, $\varepsilon_a < \varepsilon_c$ and $\varepsilon_b > \varepsilon_c$

ii) Between (a) and (b), the bed pressure drop increases. There is a decrease in pressure drop from (b) to (c).

iii) During defluidization, i.e., when the velocity is decreased, the particle arrangement goes from (c) to (a) directly.

iv) This is how the hysteresis appears.

This is similar to a trend observed by Botterill *et al.* [75] when they worked with Geldart D particles in a conventional fluidized bed. From a design point of view, the hysteresis peak is unimportant. However, the principle of hysteresis phenomenon affords an insight into the physics of fluidization that is helpful in other interpretations.

From Figures 4.36 to 4.38, it is observed that hysteresis occurs for all shapes of particles, spherical, cylindrical as well as rice beads. The hump appearing in each plot during the increase of fluid flow represents the additional energy required for unlocking the particles. Even though the extent or size of the hump is seen to vary in each case, the phenomenon is consistently seen in all cases investigated in the work.

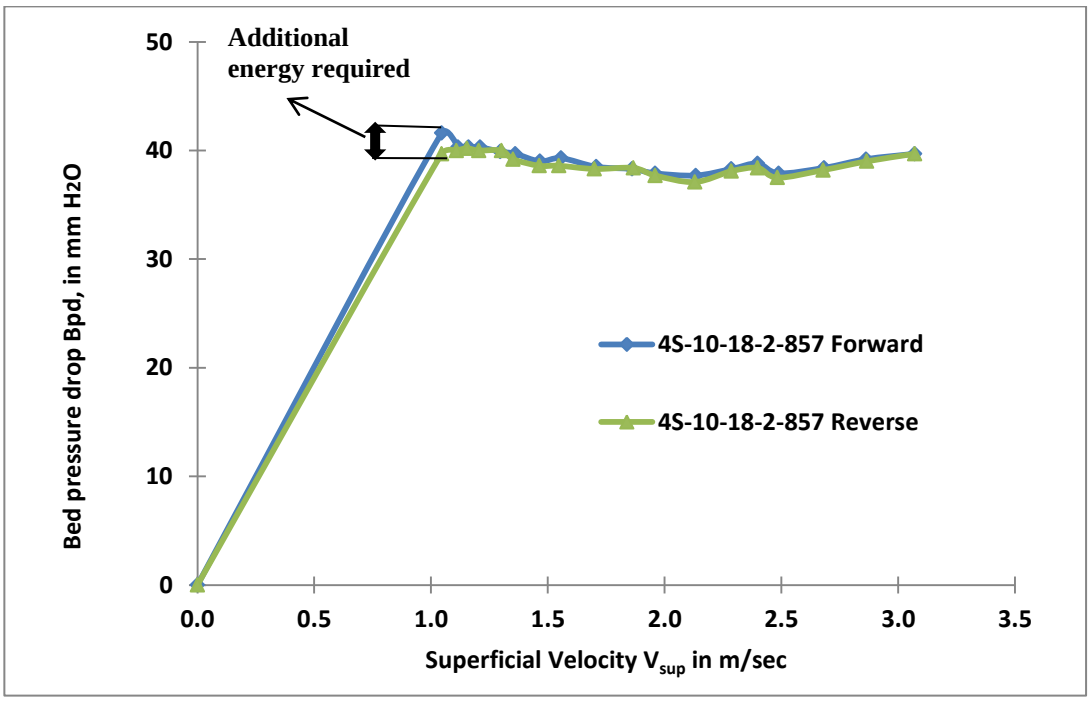

Figure 4.36: Plot demonstrating the hysteresis in 4 mm spherical type particle

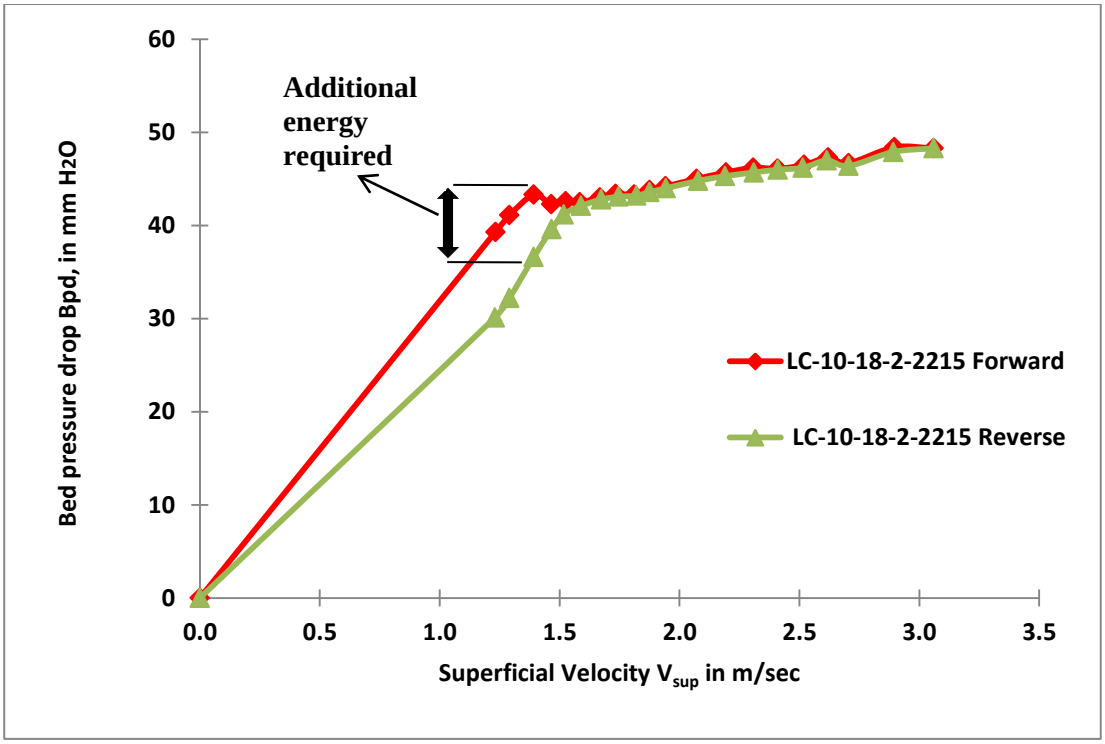

Figure 4.37: Plot of demonstrating the hysteresis in long cylindrical type particles

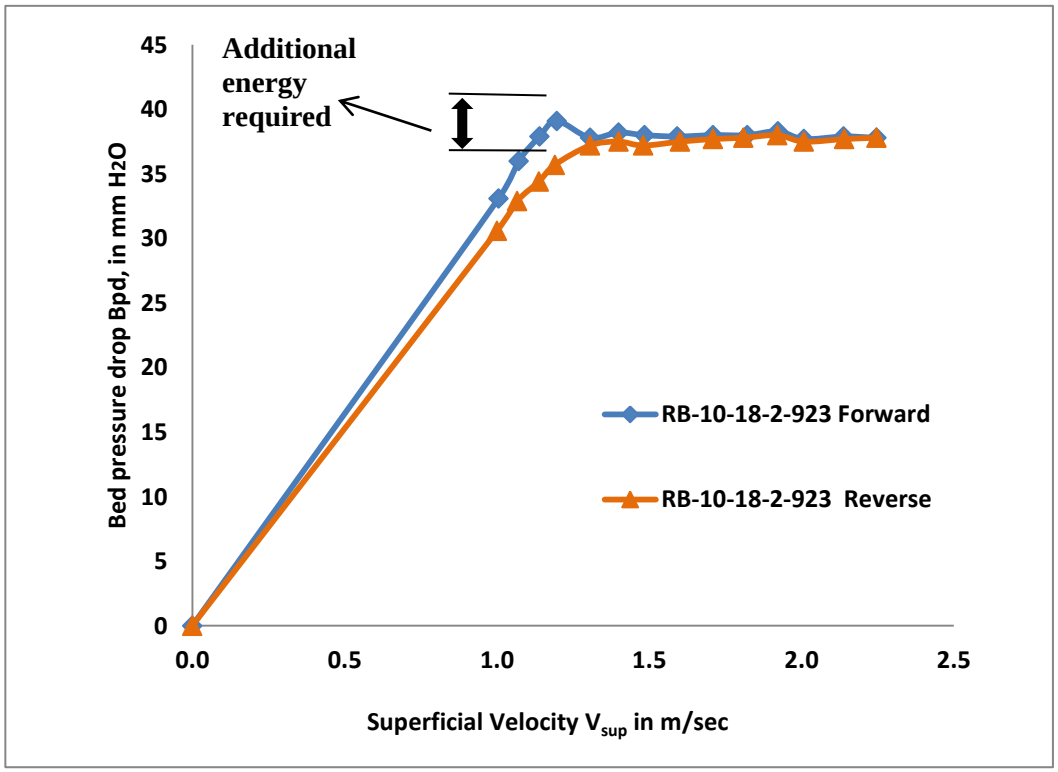

Figure 4.38: Plot demonstrating the hysteresis in rice bead type particles

4.10 Statistical Analysis and Data Reduction

To find a correlation a curve has to be found that fits the data which abide by the existing relationship between the variables and the physics of the system. The relationship that one would like to model may be a curve but whether it is exponentially growing, decaying or other non-linear relationship may be unknown. In such situations one makes use of general/non-linear regression.

In the case of swirling fluidized bed there is a set of independent variables of which, the dependent variable is a function. The most general model correlation which would abide by rules of physics would be

$$Y = Kx_1^a \times x_2^b \times x_3^c \times x_4^d \ldots. \quad (4.1)$$

where Y is the dependent variable and the x_1, x_2, x_3..., x_n are independent variables which affect Y.

To fit the curve and arrive at a relationship the equation is converted into linear form by taking logarithms of both sides and applying regression.

The aspects chosen in this study to affect the hydrodynamics of swirling fluidized bed were: (i) bed pressure drop, ΔP_b (ii) superficial air velocity, U_{sup} (iii) diameter of the bed particle, d_p (iv) density of particle, ρ_p (v) blade overlap angle, α (vi) blade inclination angle, θ (vii) bed weight, W_b. In order to normalize the parameters, certain other known parameters like minimum fluidization velocity (U_{mf}), mean diameter of the bed (D_m), density of air (ρ_a) and centrifugal weight (W_{cf}) were used. In the case of packed bed Re is used instead of U_{sup}/U_m for more meaningful representation.

In this case the following normalized relationship is obtained:

$$(\Delta P_b/0.5\rho_a (U_{sup})^2) = K (U_{sup}/U_{mf})^a \times (d_p/D_m)^b \times (\rho_p/\rho_a)^c \times (\alpha/90)^d \times (\theta/90)^e \times (W_b/W_{cf})^f \quad (4.2)$$

When converted to linear form, one gets

$$\log(\Delta P_b/0.5\rho_a (U_{sup})^2) = \log K + a\times \log (U_{sup}/U_{mf}) + b\times \log (d_p/D_m) + c\times \log (\rho_p/\rho_a) + d\times \log (\alpha/90) + e\times \log (\theta/90) + f\times \log (W_b/W_{cf}) \quad (4.3)$$

For simplicity each term in Eq. (4.3) was substituted by variables and re-written as

$$C_1 = \log K + a\times \log C_2 + b\times \log C_3 + c\times \log C_4 + d\times \log C_5 + e\times \log C_6 + f\times \log C_7 \quad (4.4)$$

where $C_1 = \log (\Delta P_b/0.5\rho_a U_{sup}^2)$, $C_2 = \log (U_{sup}/U_{mf})$, $C_3 = \log (d_p/D_m)$, $C_4 = \log (\rho_p/\rho_a)$, $C_5 = \log(\alpha/90)$, $C_6 = \log (\theta/90)$, $C_7 = \log (W_b/W_{cf})$. In the case of packed bed Re replaces U_{sup}/U_{mf}, hence $C_2 = \log (Re)$

The software Minitab was used for statistical analysis. Since the swirling fluidized bed has mainly two regimes viz. packed bed and swirling regime, the correlation for each regime is obtained separately.

4.10.1 Packed Bed Regime

For packed regime Reynolds number, Re is a factor chosen to represent velocity. Based on the nature of flow, Laminar and Turbulent, the correlation is split into two as in case or Ergun's equation [11] in conventional fluidized bed.

4.10.1.1 Summary of the analysis for the laminar region

The correlations obtained for Laminar region, Re ≤ 1990, is as follows

$$(\Delta P_b/0.5\rho_a(U_{sup})^2) = [19.84\times Re^{0.4559}\times d_p/D^{-0.834}\times \rho_p/\rho_a^{-1.106}\times \alpha/90^{0.0380}\times \theta/90^{-0.2223} \times W_b/W_{cf}^{0.917}] \quad (4.5)$$

Summary of model: S = 0.0809, R^2 = 92.26%

4.10.1.2 Summary of the analysis for the turbulent region

The correlations obtained for turbulent region, 2100≤ Re ≤3300, is as follows

$$(\Delta P_b/0.5\rho_a U_{sup}^2) = [3.219E{+}14 \times Re^{-0.7709} \times d_p/D_m^{-0.2734} \times \rho_p/\rho_a^{-3.817} \times \alpha/90^{-0.3029} \times \theta/90^{0.8375} \times W_b/W_{cf}^{1.165}] \quad (4.6)$$

Summary of model: S = 0.1499, R^2 = 87.55%.

As explained by Ergun [11], the total pressure is a consequence of both laminar and turbulent effects. Hence Combining Eqs. (4.5) and (4.6) for the entire region of Re numbers of interest a correlation for packed bed is obtained region as:

$$\left(\frac{\Delta P_b}{0.5 \times \rho_a \times \left(U_{sup}^2\right)}\right) = \frac{19.84 \times Re^{0.4559} \times \left(\frac{\alpha}{90}\right)^{0.0380} \times \left(\frac{W_b}{W_{cf}}\right)^{0.917}}{\left(\frac{d_p}{D_m}\right)^{0.834} \times \left(\frac{\rho_p}{\rho_a}\right)^{1.106} \times \left(\frac{\theta}{90}\right)^{0.2223}} + \frac{3.219 \times 10^{14} \times \left(\frac{W_b}{W_{cf}}\right)^{1.165} \times \left(\frac{\theta}{90}\right)^{0.8375}}{Re^{0.7709} \times \left(\frac{d_p}{D_m}\right)^{0.2734} \times \left(\frac{\rho_p}{\rho_a}\right)^{3.817} \times \left(\frac{\alpha}{90}\right)^{0.3029}} \quad (4.7)$$

Goossens [103] refers to an equation which is based on Ergun [11] and derived using Stokes and Newton's law, combining laminar and turbulent effects of the bed, as follows

$$Ar = 18Re + {}^{1}/_{3Re^2} \quad (4.8)$$

where Ar is Archimedes number and Re is Reynolds's number, also Re < 30, 0000.

Comparing Eqs. (4.7) and (4.8) we can see that dependence of Re is proportional in the laminar flow region and inversely proportional in turbulent flow region. This similarity affirms the presence of Re as a term in the correlation and its variation with laminar and turbulent flow. In case of diameter of particle, in both terms of the Eq. (4.7) diameter ratio is found to be in the denominator. This is in agreement with Eq. (2.1) from Ergun [11].

Except for density that features in the turbulent term of Eq. (2.1), all other aspects considered for obtaining correlation as in Eq. (4.8) are different, hence are

not a basis for comparison. The swirling fluidized bed has general similarities with conventional, but there are differences even at the packed bed level.

4.10.2 Swirling bed regime

In this regime the ratio of superficial velocity to minimum fluidization velocity, U_{sup}/U_m is chosen to represent the non-dimensional velocity.

For Swirling bed regime the following equation was obtained.

$$\left(\frac{\Delta P_b}{0.5 \times \rho_a \times \left(U_{sup}{}^2\right)}\right) = \frac{1427.22 \times \left(\frac{U_{sup}}{U_{mf}}\right)^{0.4826} \times \left(\frac{d_p}{D_m}\right)^{0.6357} \times \left(\frac{\alpha}{90}\right)^{0.1645} \times \left(\frac{W_b}{W_{cf}}\right)^{0.9053}}{\left(\frac{\rho_p}{\rho_a}\right)^{0.5361} \times \left(\frac{\theta}{90}\right)^{0.4875}} \quad (4.9)$$

Summary of model: S = 0.0787, R^2 = 96.27%,

In Eq. (4.9) the pressure drop is expressed in terms of all the SFB aspects considered in the study. It can be perceived from the above correlation that the bed pressure drop is proportional to a velocity term carrying a power more than 2, confirming the supralinear behavior observed during the experiments.

The regression analysis of swirling regime data is summarized in Appendix B. All the variables considered for the study showed a perfect fit as value of p = 0 during the analysis. A higher value of R^2 = 96.27% and very low value of S=0.0787 confirmed the high fit of the observed data to the regression model developed.

In the swirling regime, it can be seen that for analysis of variance, all the variables under consideration F-ratio has large value indicating a high quality fit of the data acquired during the experiment and also reiterates the significance of the coefficients obtained during the analysis. From the statistical analysis, provided in Appendix B, only 57 of the 1216 total observed data were observed to be out of fit and the data fit quality is better than the packed bed regime.

Swirling behavior of the bed is represented by the correlation (4.9). This is the first attempt to develop such a correlation. The exponents of the terms in the correlation justify the behavior as observed from the experimental results.

4.11 Chapter Summary

All the results obtained during the work are presented in this chapter and their detailed discussion leads to a conclusion that all the aspects considered in the work are relevant and have a significant effect on the hydrodynamics of the swirling fluidized bed.

With a statistical analysis of the acquired data and correlations between the aspects considered, the bed pressure drop could be predicted. The packed bed regime has a correlation which is a combination laminar and turbulent flow regions as in case of Ergun [11]. As for swirling regime, a single correlation is adequate to characterize the behavior.

CHAPTER 5

CONCLUSIONS AND FUTURE WORK

5.1 Chapter Overview

The important findings from the research work are reviewed and presented in this chapter. The achievement of objectives is also discussed here. The effect of various aspects on the hydrodynamics of swirling fluidized bed is highlighted. The chapter concludes with recommendations for future work.

5.2 Findings and Conclusions

A comprehensive study on the effects of various aspects of the distributor such as blade inclination and blade overlap, as well as several other parameters on the hydrodynamic behavior of a swirling fluidized bed has been conducted. It was seen that blade inclination has a significant effect on the bed hydrodynamics as it affects the distributor as well as the bed pressure drop. Overall, every objectives of the work was achieved.

The hydrodynamic study done in this work is a fundamental (cold bed) study to understand the physics of the system, the behavior of the bed and ways to control it. This is a necessary first step towards designing scaled-up swirling fluidized bed reactors and those which work at higher temperature and/or pressure. The cold bed studies can first lead to the study of lower temperature processes like drying, torrefaction etc. which could be further developed towards medium temperature apparatus for processes like gasification. A high temperature apparatus, as for processes like combustion, will need further studies. The scaling up of the prototype to industrial level would be the culmination of the work initiated here.

Findings of this research work could be summarized as follows:

1) Swirling fluidized beds, unlike other contemporary techniques, can handle and fluidize particles irrespective of shape and size. Especially Geldart D type particles, which are difficult to fluidize by conventional fluidization techniques, can be handled without any issues here.

2) Of the various aspects, velocity of the fluidizing medium is the most dominant factor which is evident from the correlation developed in this work, as bed pressure drop is related to velocity to the power of 2.4. Bed weight is the next which shows a power of 0.9 followed by the diameter of the particle having a power of 0.6. Blade inclination and density also show significant impact on the hydrodynamics. Even though other aspects affect the pressure drop, the effect is comparatively less.

3) The swirling fluidized bed has three major regimes viz. packed bed, slugging regime and swirling regime. The swirling regime itself can be divided into a slowly swirling regime and a vigorous swirling regime with an upper bubbling layer (two-layer regime).

4) The slugging period in the slugging regime of the Swirling fluidized bed is also affected by the all the hydrodynamic aspects considered in the study. The size of the particle, bed weight and inclination angle have a prominent effect on the slugging time while others like shape of the particles have a relatively minor effect.

5) Bed expansion in swirling fluidization shows a similar pattern irrespective of the changes in aspects considered. The bed height increased in a supra-linear fashion in all the observed cases.

6) The minimum fluidization velocity was seen to be independent of bed weight, bed height and bed particle size but other aspects seemed have an effect on it as it showed variation with changes in the aspect values.

7) A correlation was successfully derived with the help of a statistical software Minitab by means of nonlinear regression technique. The ANOVA results shows more than 90% fit in most cases which confirms the fidelity of the correlation.

The major points of departure of the swirling fluidization technique from conventional fluidization are summarized below:

No.	Features of swirling fluidization	Features of conventional gas-solid fluidization
1	Lower distributor pressure drop	High distributor pressure drop
2	Particulate fluidization though it is a gas-solid system	Aggregative fluidization
3	Bubbling is absent in swirling mode. The bed agitation is by virtue of inclined entry of gas	Bubbling is the most prominent regime and bed agitation is by virtue of bubbles
4	Better mixing due to tumbling motion. Good radial mixing due to toroidal movement of particles	Good degree of Mixing
5	No slugging or channeling in the conventional sense as swirling of the particles takes care of it.	Slugging and Channeling are potential problems
6	Can handle all shapes of particle	Irregular shapes of particles difficult to fluidize
7	Presence of 3 distinct regimes : packed bed, slug-wavy and swirling regime	Only packed bed and bubbling regime

8	Geldart D type particles fluidize well.	D type are poorly fluidized
9	Multi-staging can be effectively done.	Multi-staging is possible.
10	Best solid- fluid contact and highest shear at the solid-fluid interface.	Good solid-fluid interaction and shear at the solid-fluid interface.
11	Uniformity in temperature and concentration is excellent	Uniformity in temperature and concentration is good.
12	Partial fluidization is an excellent new processing technique	Partial fluidization is undesirable

5.3 Recommendations for Future Work

This particular research was a fundamental study done with an objective to understand the bed hydrodynamics and the effects of various factors affecting it. These effects could be studied further individually in detail and the predictive correlation could be improved.

Various regimes in the swirling fluidized bed are yet to be analyzed and understood well, hence there is a vast potential for research in this area especially in the slug-wavy regime. This regime as well as the two-layer bubbling regime can be the subject of a detailed study thereby understanding the physics of the occurrences.

A thorough study of the residence time distribution is essential for operating the bed in the continuous mode. Likewise, multi-staging studies will also be needed.

The relationship between the velocity of fluidizing medium, velocity of particle and the gas-particle transport coefficients are yet to be established, which is key in designing and controlling a reactor.

Lastly, the exploitation of the available area of the swirling bed still remains an unsolved problem, and its solution is indispensable in establishing the superiority of the swirling fluidized bed and its wide application to industry. Thus scaling up and establishing scaling laws, with due consideration of the order of the reactions offers much opportunity.

REFERENCES

[1] R. Howard, *Fluidized bed technology: Principles and applications*,Adam Hilger Publication, Bristol, U.K. 1989.

[2] C. Amonsirirat, B. Chalermsimsuwan, L. Mekasut, P. Kuchontara and P. Piumsomboon, "Experiment and 3D simulation of slugging regime in a circulating fluidized bed", *Korean J. Chem. Eng.*, 28(3), 686, 2011.

[3] C. T.Crowe, *Multiphase flow handbook*. Boca Raton, FL, CRC Press, 2006.

[4] R.Holdich, *Fundamentals of Particle Technology*, Loughborough University, Midland Information Technology and Publishing, 2002.

[5] L.G Gibilaro, *Fluidization-Dynamics*, Butterworth, Heinemann, 2001.

[6] C.K.Gupta and D.Sathiyamoorthy, *Fluid Bed Technology in Materials Processing*, CRC Press LLC., 1999.

[7] www.TORBED.com (Acessed on 10 January 2012)

[8] S. Binod, "Hydrodynamic and wall–bed heat transfer studies on a swirling fluidised bed", Masters Thesis, Department of Mechanical Engineering, IIT, Madras, 1995.

[9] P. C. Josephkunju, "Influence of Angle of Air Injection and Particles in Bed Hydrodynamics of Swirling Fluidized Bed", PhD Thesis, School of Engineering, CUSAT, Kochi, 2009.

[10] D. Kunii and O. Levenspeil, *Fluidization Engineering*, Wiley, New York, 1969

[11] S.Ergun, "Fluid Flow through Packed Columns". *Chemical Engineering Progress*, Vol. 48, pp. 89-94, 1952.

[12] J.M.D. Merry, 'Penetration of a horizontal gas jet into a fluidized bed', *Trans. Inst. Chem. Eng.*, 49, 189, 1971.

[13] L.T. Fan, C.C. Chang, and Y.S. Yu, "Incipient Fluidization Condition for a Centrifugal Fluidized Bed", *AIChE. Journal*, Volume 31, 999, 1985.

[14] D.G. Kroger, G. Abdelnour, E.K. Levy and J. Chen, "Flow Characteristics in Packed and Fluidized Rotating Beds", *Powder Technology*, Volume 24, 9-18, 1979.

[15] T.Takahashi, Z.Tanaka and A. Itoshima, "Performance of Rotating Fluidized Bed", *Journal of Chemical Engineering of Japan*, Vol 17, No.3, 333-336, 1984.

[16] Y.M. Chen, "Fundamentals of centrifugal fluidized bed", *AIChE. Journal*, Volume 33, No.5, 722, 1987.

[17] G.S. Lee, G.Y. Han and S.D. Kim, "Combustion Characteristics in a Circulating Fast Fluidized Bed", *Korean J. Chem. Eng.*, 1, 71-76, 1984.

[18] J.S. Lee and S.D. Kim, "The Vertical Pneumatic Transport of Cement Raw Meal", *HWAHAK. KONGHAK*, 20, 207, 1982.

[19] H. Weinstein, M. Meller, M.J. Shao, and R.J. Parisi, "The Efffect of Particle Density on Holdup in Fast Fluidized Bed" *AlChE Symp. Ser.*, 234. Vol. 80, 52, 1984.

[20] N.T. Cankurt, and J. Yerushalmi, *Fluidization*, Cambridge Univ., Press, p. 387, 1978.

[21] J. Yerushalrni, D.H. Turner and A.M. Squires, "The Fast Fluidized Bed", *Ind. Eng. Chem. Proc. Des. Dev.*, 15, 47, 1976.

[22] J. Yerushalmi, and N.T Cankurt, "High Velocity Fluid Bed", *CHEMTECH*, 10, 564, 1978.

[23] J.Yerushalmi, and A.M Squires, *AIChE Symp. Ser. 73*, 44, 1975.

[24] J.Yerushalmi and N.T.Cankurt, "Further Studies of the Regimes of Fluidization", *Powder Technology*, 24, 187, 1979.

[25] C.E.Capes and K. Nakamura, "Vertical Pnuematic Conveying: An Expereimental Study with Particles in Intermediate and Turbulant Region", *Can. J. Chem. Eng.*, 51, 31, 1973.

[26] L.S. Leung and R.J.Wiles, "A Quantitative Design Procedure for Vertical Pnuematic Conveying System", *Ind. Eng. Chern. Proc. Des. Dev*., 15, 552,1976.

[27] L.S. Leung, R.J.Wiles and D.J. Nicklin, "Correlation for Choking Flowrates in Vertical Pnuematic Conveying". *Ind. Eng. Chem. Proc. Des.Dev.*, 10, 183, 1971.

[28] G. Y. Han, G. S. Lee and S. D. Kim, "Hydrodynamic Characteristics Of A Circulating Fluidized Bed', *Korean J. of Chem. Eng*., 2(2), pp 141 –147, 1985.

[29] N. K. Sowards, U.S. Patent 4,075,935, 1978.

[30] C. S. Chyang, and M. C.Hsu, "Combustion of waste tyres in a pilot scale fluidized bed combustor", *Chung Yuan Journal*. Vol19, p: 30, 1990.

[31] C. Sobrino, J. A. Almendros-Ibañez, D. Santana and M. de Vega, "Fluidization of Group B particles with a rotating distributor", *Powder Technology*,181, 273–280, 2008.

[32] J. De Wilde and A. de Broqueville, "Rotating fluidized beds in a static geometry: experimental proof of concept", *AIChE J.* 53 (No. 4) 793–810, 2007.

[33] C.E. Dodson, Apparatus for processing matter in a turbulent mass of particulate material, US Patent 4,479,920, 1984.

[34] F. Ouyang and O. Levenspiel, "Spiral Distributor for Fluidized Beds", *Ind. Eng. Chem. Process Des. Dev.*, Volume 25, 504, 1986.

[35] J. Shu, V.I. Lakshmanan and C.E. Dodson, "Hydrodynamic Study of a Toroidal Fluidized Bed Reactor", *Chemical Engineering and Processing*, 39, 499-506, 2000.

[36] J.De Wilde and A. de Broqueville, "Experimental investigation of a rotating fluidized bed in a static geometry", *Powder Technology*, 183, 426–435, 2008.

[37] R. Kaewklum and V. I. Kuprianov, "Experimental studies on a novel swirling fluidized-bed combustor using an annular spiral air distributor", *Fuel*, *89*, 43–52, 2010.

[38] S. Harish Kumar and D.V.R. Murthy, "Minimum superficial fluid velocity in a gas–solid swirled fluidized bed", *Chemical Engineering and Processing*, 49, 1095–1100, 2010.

[39] B. Sreenivasan and V.R. Raghavan, "Hydrodynamics of a Swirling Fluidized Bed", *Chemical Engineering and Processing*, 41, 99-106, 2002.

[40] G. Vikram, V.R. Raghavan and H. Martin, "A model for the Hydrodynamics of Swirling Fluidized Beds", *4th International Conference*

for Conveying and Handling of Particulate Solids, Budapest, 2003,Volume 1, 7.1.

[41] V. R. Raghavan, M. Kind and H. Martin, "Modeling of the Hydrodynamics of Swirling Fluidized Beds", *4th European Thermal Sciences Conference 'EUROTHERM' & Heat Exchange Engineering Exhibition, Birmingham, UK*, 2004.

[42] D. Sathiyamoorthy and H. Masayuki, "On the Influence of Aspect Ratio and Distributor in Gas Fluidized Beds", *Chemical Eng. Journal*, vol.93, pp.151-161, 2003.

[43] W. Michael, P.S. Todd and T. Helen, "The Influence of Distributor Design on Fluidized Bed Dryer Hydrodynamics", *The 12th Int. Conf. On Fluidization Engineering, Canada*, 2007, pp. 100.

[44] D. Geldart and J. Baeyens, "The Design of Distributors for Gas-fluidized Beds", *Powder Technology*, 42, 67– 78, 1985.

[45] J. Werther, "Effect of gas distributor on hydrodynamics of gas fluidized beds", Ger. Chem. Eng.,1, 168,1978.

[46] J.C. Agarwal, W.L. Davis and D.T. King, "Fluidized bed coal dryer", *Chem. Eng. Prog.*, 58 (11), 85, 1962.

[47] D.R. Richardson, "How to design fluid flow distributors", *Chem. Eng.*, 68, 83, 1961.

[48] F. J. Zuiderweg, "Session report", *Proceedings of Int. Symp. on Fluidization*, ed. A. A. H. Drinkenburg Neth. Univ. Press, Amsterdam, p. 739,1967.

[49] S.A. Gregory, "The distributor plate problem", *Proceedings of Int. Symp. on Fluidization*, ed. A. A. H. Drinkenburg Neth. Univ. Press, Amsterdam, p. 751, 1967.

[50] A. B. whitehead, "Problems in Large Scale Fluidized Beds", in J. F. Davidson and D. Harrison(eds.), *Fluidization*, Academic Press, London, chap. 19,1971.

[51] F. A. Zenz, "Bubble formation and grid design", *P Fluidization: I.Chem.E.Symposium Series No. 30*, pp. 136-139, 1968.

[52] J.W. Hiby, "Critical minimum pressure drop of gas distribution plate in fluidized bed units", *Chem. Ing. Techn.*, 36, 328, 1964.

[53] J.F. Richardson and W.N. Zaki, "Sedimentation and fluidization", *Trans.Instrum. Chem. Eng.*, 32, 35, 1954.

[54] Y.F. Shi and L.T. Fan, "Effect of distributor to bed resistance on uniformity of fluidization", *AIChE J*., 30, 860, 1984.

[55] S. Fakhimi and D. Harrison, "Multi-orifice Distributors in Fluidized Beds—A Guide to Design in Chemeca-70", *Proceedings of the Institution of Chemical Engineers Symposium Series*, vol. 33, London,p. 29,1970.

[56] D. Sathiyamoorthy and Ch.S. Rao, "Gas distributors in fluidized bed", *Powder Technology*, 20, 47, 1978.

[57] D. Sathiyamoorthy and Ch.S. Rao, "Multi-orifice distributors in gas fluidized beds—a model for design of distributors", *Powder Technology*, 24, 215, 1979.

[58] D. Gidaspow, *Multiphase flow and fluidization: Continuum and kinetic theory description*, Academic Press, Boston, 1994.

[59] A.P. Baskakov, V.G. Tuponogov and N.F. Philippovsky, "Uniformity of fluidization on a multi-orifice gas distributor", *Can. J. Chem. Eng.*, 63, 886, 1985.

[60] P. Mazumdar, U. P. Ganguly, "Effect of aspect ratio on bed expansion in particulate fluidization", *Can. J. Chem. Eng.*, 63, 850, 1985.

[61] A. E. Qureshi and D. E. Creasy, "Fluidised Bed Gas Distributors", *Powder Technology*, 22, 113 – 119,1979.

[62] D. Geldart and J.R. Kelsey, The influence of the gas distributor on bed expansion, bubble size and bubble frequency in fluidized beds. *Fluidization: I.Chem.E.Symposium Series No. 30*, 114-125 1968.

[63] J. S. M. Botterill, *Fluid Bed Heat Transfer*, Academic press, London, 1975.

[64] S. C. Saxena, A. Chatterjee and R.C.Patel, "Effect of distributors on gas-solid fluidization", *Powder Technology*, Vol. 22, pp 191- 198, 1979.

[65] C.S. Chyang and C.C. Huang, "Pressure drop across a perforated plate distributor in a gas-fluidized bed", *J. Chem. Eng. Jpn.*, 24, 249, 1991.

[66] R. A. Otero and C. R. Munoz, "Fluidized Bed Gas Distribution of Bubble Cap Type". Powder Technology, Vol 9. pp 279-287, 1974.

[67] D. Sathyamoorthy and C. H. Rao, "The choice of distributor to bed pressure drop ratio in gas fluidized beds", *Powder Technology*, Vol. 30, pp 139- 143, 1981.

[68] S. Fakhimi, S. Sohrabi and D. Harrison, "Entrance effect of a multi-orifice distributor in gas fluidized beds", *The Canadian Journal of Chemical Engineering*, Vol. 61, pp 364-369, 1983.

[69] C.Y.Wen, R. Krishnan, R. Khosravi and S. Dutta, "Dead zone height near the grid of Fluidized bed in fluidization", *Cambridge University Press*, pp 32, 1978.

[70] N. Upadhyay, S. C. Saxena and F. T. Ravello, "Performance characteristics of multijet tuyere distrbutor plate", *Powder Technology*, Vol. 30, pp 155-159, 1981.

[71] R. H. Birk, G.A. Camp and L.B.Hutchinson, "Design of an agglomeration resistant gas distributor", *All India Chemical Engineering Symposium*, 1990, Vol. 86, pp 16-21.

[72] J. P. Sutherland, "The measurement of pressure drop across a gas fluidized bed", *Chemical Engineering Science*,Vol 19, pp 839-841, 1964.

[73] J. H. de Groot and N.J. Hasset, "Scaling up of gas fluidized bed reactors" *Proceedings of International Symposium on Fluidization*, Endhoven, Vol. 24, pp 32-35, 1967.

[74] J. S. Yang, Y.A. Liu and A .M. Squires, "Pressure Drop across Shallow Fluidized Beds: Theory and Experiment", *Powder Technology*, Vol 53, pp 79-89, 1987.

[75] J. S. M Botterill., Y.Teoman and K.R.Yuregir, "The effect of operating temperature on the velocity of minimum fluidization, bed voidage and general behaviour", *Powder Technology*, Vol. 31, pp 101-110, 1982.

[76] A. Mathur, S. C. Saxena and Z. F. Zhang, "Hydrodynamic Characteristics of Gas Fluidized Beds over a Broad Temperature Range", Powder Technology, Vo147, pp 247-256, 1986.

[77] M. Nakamura, Y. Hamada and S. Toyama, “An Experimental Investigation of Minimum Fluidization Velocity at Elevated Temperatures and Pressure”, *Can. J. Chem. Eng.*,Vol 63, pp 8–13, 1985.

[78] N. I. Gelperin, V. G. Einstein and K. Zaikovski, *Khimicheskoe Mashinostroenic No.3,1. Printed at the Autumn Meeting of The Society of Chemical Engineers*, Japan at Nagoya, October 1982.

[79] R. Bouratoua, Y. Molodtsuf and A. Koniuta, “Hydrodynamic characteristics of a pressurized fluidized bed”, *Proceedings of the 12thInternational Conference on Fluidized bed Combustion*, San Diego, California, 1993, pp 63-70.

[80] N. Ellias, H. T. Bi, C. J. Lim and J. R. Grace, “Hydrodynamics of turbulent fluidized beds of different diameters”, *Powder Technology*, Vol. 98, pp 124-136, 2004."

[81] Y. K.Mohanty, K.C. Biswal, G.K.Roy and B. P. Mohanty, “Effect of promoters on dynamics of gas-solid fluidized bed-statistical and ANN approaches”, *China Particuology*, Vol.5, pp 401-407, 2007.

[82] R. Kaewklum and V.I. Kuprianov, “Theoretical and experimental study on hydrodynamic characteristics of fluidization in air–sand conical beds”, *Chemical Engineering Science*, 63, pp 1471 – 1479, 2008.

[83] C.Y.Wen and Y.H. Yu, "A generalised method for predicting the minimum fluidization velocity", *Chemical Engineering Journal*, Vo1.12, pp 610-612, 1966.

[84] S. Y. Wu and J. Baeyens, “Effect of operating temperature on minimum fluidization velocity”, *Powder Technology*, 67, pp 217-220, 1991.

[85] D. C. Chitester, R. M. Kornosky and L. S. Fan, “Characteristics of fluidisation at high pressure”, *Chem. Eng. Sci*., 39, pp 253–261,1984.

[86] R. Moreno and R. Rios, "Study on sawdust drying techniques in fluidized bed", *Biosystems Engineering*, Vol. 82, pp 321-329, 2002.

[87] R. Kaewklum,V. I. Kuprianov and P. L. Douglas, “Hydrodynamics of air–sand flow in a conical swirling fluidized bed: A comparative study between tangential and axial air entries”, *Energy Conversion and Management*, 50, pp 2999–3006, 2009.

[88] M. Faizal, V. V.Kumar and V. R. Raghavan, "Experimental Studies on a Swirling Fluidized Bed with Annular Distributor", *Int. Conference on Plant, Equipment and Reliability, Malaysia*, 2010, pp 106-111.

[89] M. F. Mohideen, S. M. Seri, V.V. Kumar and V. R. Raghavan, "Effect of radial inclination of the distributor in a swirling fluidized bed", *HEFAT 2010 7th International Conference on Heat Transfer, Fluid Mechanics and Thermodynamics, Turkey*, 2010.

[90] M. Wormsbecker, T. Pugsley and H. Tanfara, "Influence of Distributor Design on Dryer Hydrodynamics", *The 12th International Conference on Fluidization - New Horizons in Fluidization Engineering* , 2007, Vol. RP4, Article 100.

[91] M. F. M. Batcha, M. F. A. Rahman, F. Jaafar and V. R. Raghavan, "Performance of various distributor designs in a Gas- Solid Fluidized Bed", *Proceedings of International Conference on Applications and Design in Mechanical Engineering (ICADME)*, 2009, pp. 13A 1 - 13A 6.

[92] C.S. Chyang and Y.C. Lin, "A Study in the Swirling Fluidizing Pattern," *J. Chem. Engg. of Japan*, vol. 35, no. 6, pp. 503-512, 2002.

[93] B. Wang, T. Li, Q. W. Sun, W. Y. Ying and D. Y. Fang, "Solid Concentration in Circulating Fluidized Bed Reactor for the MTO Process", *Inl. Jn. of Chem. and Bio. Engg.* 3:2, 2010.

[94] V. V. Kumar, M. Faizal and V. R. Raghavan, "Study of the Fluid Dynamic Performance of Distributor Type in TORBED Type Reactors", *Engineering e-Transaction*, Vol. 6, No.1, pp 70-75, 2011.

[95] S. Othman and A. A. Wahab and V. R.Raghavan, Numerical study of the plenum chamber of a swirling fluidized bed. *In: Proceedings of International Conference on Mechanical & Manufacturing Engineering (ICME2008), Malaysia*, 2008, 21-23 May.

[96] MS ISO5167-2:2005, "Measurement of fluid flow by means of pressure differential devices inserted in circular crosssection conduits running full – part 2: Orifice plates (ISO 5167-2:2003, IDT)", *ICS: 17.120.10, Department of standards*, Malaysia, 2005.

[97] M. M.Paulose, “Hydrodynamic study of Swirling fluidized bed And the role of distributor”, PhD Thesis, School of Engineering, CUSAT, Kochi, 2006.

[98] M. F. M. Batcha and V. R. Raghavan, “Experimental Studies on a Swirling Fluidized Bed with Annular Distributor”, *Journal of Applied Sciences*, vol. 11(11), pp. 1980-1986. 2011.

[99] D. Geldart, “Types of gas fluidization”, *Powder Technology*, 7, 285-292,1973.

[100] A. Bejan, *Shape and Structure, from Engineering to Nature*, Cambridge University Press, Cambridge, UK, 2000.

[101] D. J. Gunn and N. Hilal, “The expansion of gas-fluidised beds in bubbling fluidisation”,*Chemical Engineering Science*, 52(16): 2811-2822,1997.

[102] R. K.Singh, A Suryanarayana and G. K. Roy, “Prediction of Bed Expansion Ratio for Gas-solid Fluidization in Cylindrical and Non-cylindrical Beds”, *IE (I) journal-CH*, Vol 79,pp 51-54, 1999.

[103] W.R.A Goossens, “Classification of particles by archimedis number”, Powder Technology, 98, 45-53, 1998.

[104] K. A. Kobe and R. E. Lynn, “The Critcal Properties of Elements and Compounds”, *Chemical Review*, 52, 1, pp. 117–236,1953.

[105] Z. D. Husain, “Theoretical uncertainty of orifice flow measurement”, *Daniel measurement and control Inc.*, 2010, pp 1-7.

LIST OF PUBLICATIONS

Journals

1) V. K. Venkiteswaran, S. A. Sulaiman and V. R. Raghavan, "Comparative study of the hydrodynamic performance of shorter and longer blades in a Swirling fluidized bed"**,** *Advanced Materials Research*, Vol. 772, pp 560-565, 2013.

2) T. C. Sheng, S. A.Sulaiman, V. Kumar, "One-Dimensional Modeling of Hydrodynamics in a Swirling Fluidized Bed", *International Journal of Mechanical & Mechatronics Engineering (IJMME-IJENS)*, Vol:12, No:06, pp 13-22, 2012.

3) V. K. Venkiteswaran, G. J. Jun, C. Y. Sing, S. A. Sulaiman and V. R. Raghavan, "Variation of Bed Pressure Drop with Particle Shapes in a Swirling Fluidized Bed", *Journal of Applied Sciences*, 12, 2598-2603, 2012.

4) V.V. Kumar, M. Faizal and V. R. Raghavan, "Study of the Fluid Dynamic Performance of Distributor Type in Torbed Type Reactors", *Engineering e-Transaction (ISSN 1823-6379)*, 6, No 1, 2011.

Conferences papers

5) V. K. Venkiteswaran, S. A. Sulaiman and V. R. Raghavan**, "**Comparative study of the hydrodynamic performance of shorter and longer blades in a Swirling fluidized bed", *FEMR*, Singapore, 2013.

6) V. K. Venkiteswaran, G. J. Jun, C. Y. Sing, S. A. Sulaiman and V. R. Raghavan, "Effect of Particle Shape on Bed Pressure Drop in a Swirling Fluidized Bed", *Proceedings of the 3rd International Conference on production, Energy and Relaibility (ICPER'2012)*, Malaysia, 2012.

7) V. V Kumar , M. Jeevaneswary, V. R. Raghavan, "Experimental Studies on the Effect of Blade Overlap Angle on Bed Pressure Drop in a Swirling

Fluidized Bed", *Proceedings of the 3rd (2011) CUTSE International Conference*, Malaysia, 2011, pp 799- 917.

8) V. V Kumar and V. R. Raghavan, "Developments in fluidized bed technology -A Review", Paper ME-011, NPC'11, UTP, Malaysia, Sept 19-20, 2011.

9) M. F. Mohideen, S. M. Seri, V. Kumar and V. R. Raghavan, "Experimental Studies on a Swirling Fluidized Bed with Annular Distributor", *Proceedings of Int. Conference on Plant, Equipment and Reliability (ICPER'2010)*, Malaysia, , 2010, pp 106-111.

10) M. F. Mohideen, S. M. Seri, V. Kumar and V. R. Raghavan, "Effect of Radial Inclination of the Distributor in a Swirling Fluidized Bed", *Proceedings of 7th International Conference on Heat Transfer, Fluid Mechanics and Thermodynamics (HEFAT)*, TURKEY, 2010.

11) V.V. Kumar, M. Faizal and V. R. Raghavan ,'Study of the Fluid Dynamic Performance of Distributor Type in Torbed Type Reactors', *Proceedings of International Conference for Technical Postgraduates (TECHPOS)*, 2009, Malaysia, 2009.

Appendix A

DETAILS OF EXPERIMENTAL SETUP DESIGN CALCULATIONS

Details of experimental setup design calculations

Minimum fluidization velocity:

The minimum fluidization velocity is considered one of the most important factors to design the swirling fluidized bed, and it can be calculated from the following equation

$$\frac{d_p\, U_{mf} \rho_g}{\mu} = \left[(\llbracket 33.7 \rrbracket)^2 + 0.0408 \, \frac{{d_p}^3 \, \rho_g (\rho_s - \rho_g)\, g}{\mu^2} \right]^{0.5} - 33.7$$

It is clear from the equation, that diameter of the particles and their densities are two variables which control the minimum fluidization velocity, so the specifications used to design the swirling fluidized bed are:

Maximum diameter of the particles is 10 mm

The maximum density of the particles is 1000 kg/m^3

The values of the absolute gas viscosity and gas density are taken at standard conditions (temperature = 20°C and pressure = 101.325 kPa). By substituting these values in the minimum fluidization velocity equation

$$\frac{0.01 \times U_{mf} \times 1.2041}{1.91258 \times 10^{-5}} = [(33.7)^2 + 0.0408 \, \frac{(0.01)^3 \times 1.2041 \times (1000 - 1.2041) \times 9.81}{(1.91258 \times 10^{-5})^2}]^{0.5} - 33.7$$

the value of the minimum fluidization velocity, U_{mf} is got as 1.77 m/s

The design factor for the system is taken equal to 2, to be able to control and increase the flow rate in the system.

Hence, the maximum velocity can be applied by the system is 3. 54 m/s

Volume flow rate:

The volume flow rate required to reach the maximum velocity in the system can be calculated from the continuity equation.

$$Q = Av$$

Now bed area for a swirling fluidized bed with inner and outer diameter 200 mm and 300 mm respectievely. Substituting this in the equation of area we have

$$A = \pi(D_o^2 - D_i^2) = \ 0.13 \text{ m}^2$$

So by substituting in the continuity equation by the values of bed area (already designed) and the value of the maximum velocity or minimum fluidization velocity respectively, it is found that

$$Q = 0.13 \ \times \ 3.54 = 0.46 \text{ m}^3/\text{s}$$

Maximum flow rate in the system is 0.46 m^3/s = 1656 m^3/hr

$$Q = 0.13 \ \times \ 1.77$$

Volume flow rate to fluidize 10 mm diameter particles is 0.23 m^3/s = 828.4 m^3/hr.

The blower will be selected to provide a volume flow rate of 1700 m^3/hr

Pressure drop:

The pressurized flow generated in the blower passes through many components in the system before it reaches the particles; these components affect the pressure of the flow and cause a pressure drop. The pressure drop across the system is equal to:

$$\Delta p_{total} = \Delta p_{line} + \Delta p_{plenum} + \Delta p_{distributor} + \ \Delta p_{bed}$$

The pressure drop along the pipes is referred to as ΔP_{line}, and it occurs due to the friction with the pipes walls. It can be calculated from Darcy law:

$$\Delta p = \frac{4flv^2}{2\ d}$$

By using Moody's chart, the value of friction factor "f" for PVC pipes is equal to 0.016, and the diameter is equal to 100 mm, so by substituting in Darcy law:

$$\Delta p_{line} = \frac{0.016 \times 6 \times 3.54^2}{2 \times 9.81 \times 0.10}$$

The pressure drop along the swirling fluidized bed pipeline is equal to 0.61 Pa

Pressure drop of the pressurized flow also occurs when it passes through the plenum and distributor. Based on the experimental data, it is found not to exceed 200 Pa and 150 Pa respectively.

The last pressure drop occurs, when the pressurized flow reaches the bed column and, it can be calculated from the equation below:

$$\Delta p_b = g\ (bed\ height \times \rho_{bulk})$$

where the bed height is designed to be 20 cm and the ρ_{bulk} is assumed to be 70% of the particle density. The pressure drop in the plenum is equal to 1373.4 Pa. The total pressure drop across the system is found to be1724 Pa ≈ 175 mm of water.

Motor power:

To determine the theoretical motor power required to activate the blower, the equation below is used:

$$P = Q \times \Delta p$$

The theoretical power was found to be equal 1288.5 Watt.

The actual power can be calculated by considering the efficiency of the blower fan and the motor, for which reasonable values of 0.7 and 0.8 assumed respectively.

$$Actual\ power = \frac{Power}{\eta_{motor} \times \eta_{fan}}$$

From the equation, it is found that the actual efficiency of the motor will be equal to 2300 Watt ≈ 3.1 hp. The motor will be selected to have a power of 5hp, being standard motor power rating available close the calculated value.

Appendix B

DETAILS OF STATISTICAL ANALYSIS (NON LINEAR REGRESSION)

CONDUCTED

Details of statistical analysis (non linear regression) conducted

Packed bed

Laminar region

Regression Equation

C1 = 1.29744 + 0.455861 C2 - 0.839968 C3 - 1.10625 C4 + 0.0380349 C5 -

0.222364 C6 + 0.916919 C7

Coefficients

Term	Coef	SE Coef	T	P
Constant	1.29744	1.13870	1.1394	0.259
C2	0.45586	0.23540	1.9366	0.057
C3	-0.83997	0.16658	-5.0423	0.000
C4	-1.10625	0.14900	-7.4245	0.000
C5	0.03803	0.09425	0.4036	0.688
C6	-0.22236	0.13204	-1.6840	0.097
C7	0.91692	0.03884	23.6103	0.000

Summary of Model

S = 0.0809326 R-Sq = 92.26% R-Sq(adj) = 91.58%

PRESS = 0.578863 R-Sq(pred) = 89.95%

Analysis of Variance

Source	DF	Seq SS	Adj SS	Adj MS	F	P

Regression	6	5.31244	5.31244	0.88541	135.175	0.000000
C2	1	0.07972	0.02456	0.02456	3.750	0.056956
C3	1	1.27318	0.16654	0.16654	25.425	0.000004
C4	1	0.26699	0.36107	0.36107	55.124	0.000000
C5	1	0.00014	0.00107	0.00107	0.163	0.687808
C6	1	0.04108	0.01858	0.01858	2.836	0.096762
C7	1	3.65133	3.65133	3.65133	557.447	0.000000
Error	68	0.44541	0.44541	0.00655		
Total	74	5.75784				

Normplot of Residuals for Packed bed laminar region

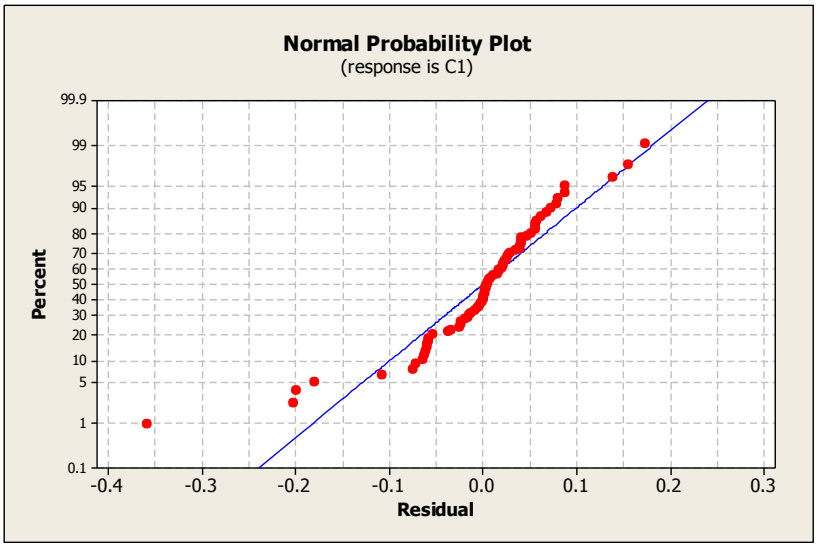

Fits and Diagnostics for Unusual Observations

Obs	C1	Fit	SE Fit	Residual	St Resid	
28	0.97414	1.17313	0.0291974	-0.198989	-2.63623	R
49	0.96835	1.16939	0.0231938	-0.201038	-2.59276	R

59 1.23922 1.41856 0.0269612 -0.179338 -2.35013 R

62 1.20896 1.03478 0.0307673 0.174177 2.32682 R

63 1.21405 1.05796 0.0299592 0.156084 2.07604 R

65 0.91525 1.27349 0.0315565 -0.358239 -4.80684 R

R denotes an observation with a large standardized residual.

Turbulent region

Regression Equation

C1 = 14.5077 - 0.770853 C2 - 0.273349 C3 - 3.81656 C4 - 0.302891 C5 + 0.83753 C6 + 1.16513 C7

Coefficients

Term Coef SE CoefT P

Constant 14.5077 5.96733 2.4312 0.019

C2 -0.7709 0.40788 -1.8899 0.064

C3 -0.2733 0.61215 -0.4465 0.657

C4 -3.8166 1.74179 -2.1912 0.033

C5 -0.3029 0.28631 -1.0579 0.295

C6 0.8375 0.23290 3.5962 0.001

C7 1.1651 0.06895 16.8972 0.000

Summary of Model

S = 0.149957 R-Sq = 87.55% R-Sq(adj) = 86.12% PRESS = 1.51947

R Sq(pred) = 83.83%

Analysis of Variance

Source	DF	Seq SS	Adj SS	Adj MS	F	P
Regression	6	8.22533	8.22533	1.37089	60.964	0.000000
C2	1	0.62491	0.08032	0.08032	3.572	0.064348
C3	1	0.06069	0.00448	0.00448	0.199	0.657061
C4	1	0.01900	0.10797	0.10797	4.801	0.032943
C5	1	0.16069	0.02517	0.02517	1.119	0.294990
C6	1	0.93968	0.29081	0.29081	12.932	0.000718
C7	1	6.42037	6.42037	6.42037	285.515	0.000000
Error	52	1.16932	1.16932	0.02249		
Total	58	9.39466				

Normplot of Residuals for C1 packed bed Turbulent region

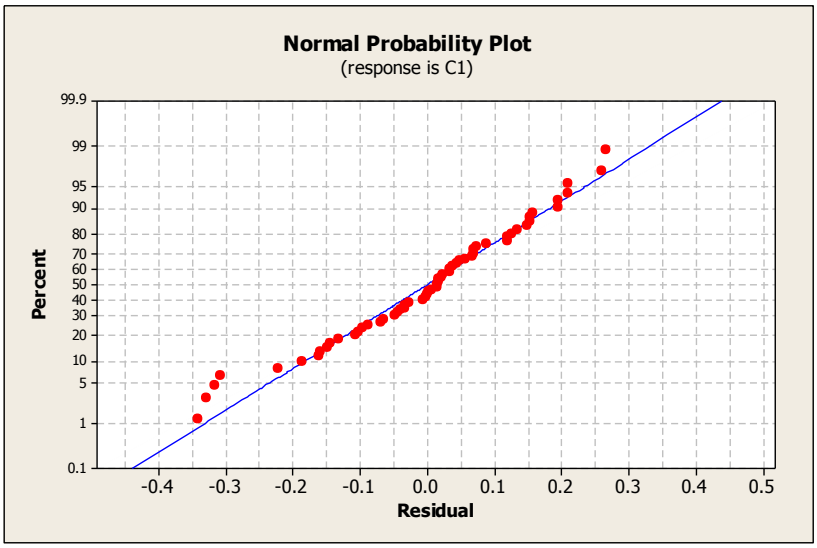

Fits and Diagnostics for Unusual Observations

Obs	C1	Fit	SE Fit	Residual	St Resid

13 1.87150 1.84958 0.139734 0.021918 0.40276 X

26 0.66236 0.97803 0.055200 -0.315675 -2.26408 R

28 1.02100 1.34985 0.049579 -0.328857 -2.32369 R

46 1.82496 2.16639 0.065204 -0.341429 -2.52838 R

56 1.28501 1.59206 0.055098 -0.307049 -2.20158 R

R denotes an observation with a large standardized residual.

X denotes an observation whose X value gives it large leverage.

Swirling regime

Regression Equation

C1 = 3.15449 + 0.482607 C2 + 0.635652 C3 - 0.536084 C4 + 0.164511 C5 -

0.48747 C6 + 0.905278 C7

Coefficients

Term	Coef	SE	CoefT	P
Constant	3.15449	0.0536055	58.846	0.000
C2	0.48261	0.0211640	22.803	0.000
C3	0.63565	0.0286488	22.188	0.000
C4	-0.53608	0.0261472	-20.503	0.000
C5	0.16451	0.0239814	6.860	0.000
C6	-0.48747	0.0257665	-18.919	0.000
C7	0.90528	0.0083445	108.488	0.000

Summary of Model

S = 0.0786605 R-Sq = 96.27% R-Sq(adj) = 96.25%

PRESS = 7.60733 R-Sq(pred) = 96.22%

Analysis of Variance

Source	DF	Seq SS	Adj SS	Adj MS	F	P
Regression	6	193.547	193.547	32.2578	5213.4	0.0000000
C2	1	96.380	3.217	3.2174	520.0	0.0000000
C3	1	17.221	3.046	3.0461	492.3	0.0000000
C4	1	4.258	2.601	2.6009	420.4	0.0000000
C5	1	1.637	0.291	0.2912	47.1	0.0000000
C6	1	1.226	2.215	2.2146	357.9	0.0000000
C7	1	72.825	72.825	72.8250	11769.7	0.0000000
Error	1213	7.505	7.505	0.0062		
Total	1219	201.052				

Normplot of Residuals for C1 Swirling regime

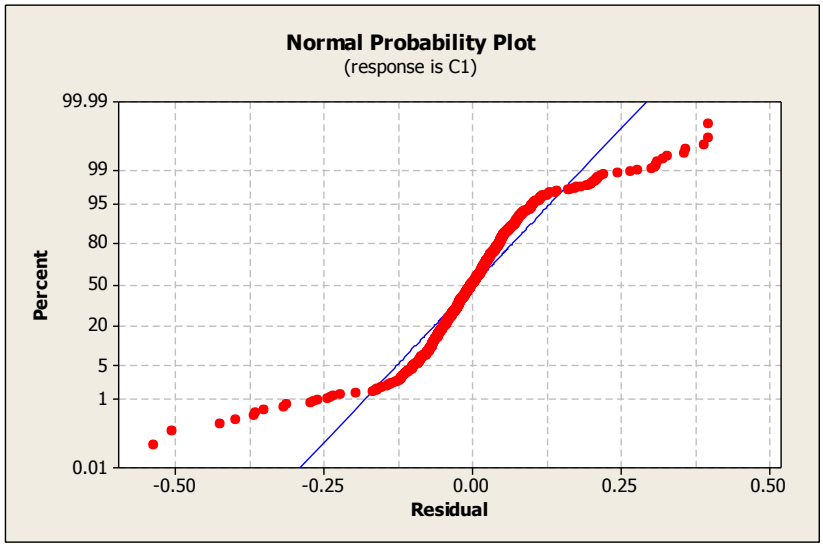

Fits and Diagnostics for Unusual Observations

Obs	C1	Fit	SE Fit	Residual	St Resid	
79	1.87098	2.03249	0.0058301	-0.161507	-2.05888	R
80	1.92667	2.08983	0.0059011	-0.163161	-2.08010	R
651	1.43023	1.62814	0.0062407	-0.197907	-2.52392	R
652	1.39788	1.66550	0.0060531	-0.267624	-3.41239	R
653	1.34680	1.71405	0.0058197	-0.367252	-4.68166	R
654	1.43803	1.78964	0.0054829	-0.351611	-4.48088	R
655	1.52172	1.84070	0.0052764	-0.318986	-4.06438	R
656	1.49636	1.89559	0.0050761	-0.399235	-5.08602	R
657	1.40183	1.94073	0.0049300	-0.538898	-6.86444	R
658	1.71433	2.02834	0.0047008	-0.314010	-3.99911	R
659	1.81642	2.07790	0.0046061	-0.261479	-3.32986	R
676	2.74104	2.58018	0.0046000	0.160864	2.04855	R

677	2.86686	2.65543	0.0047516	0.211431	2.69282	R
678	2.89765	2.69308	0.0048494	0.204570	2.60562	R
679	2.95927	2.74411	0.0050034	0.215157	2.74081	R
689	2.90879	2.72536	0.0054767	0.183429	2.33758	R
690	2.96208	2.76849	0.0055377	0.193596	2.46728	R
691	2.99934	2.79986	0.0055929	0.199482	2.54242	R
692	3.03744	2.83753	0.0056709	0.199903	2.54796	R
693	3.09885	2.89035	0.0058008	0.208492	2.65777	R
715	2.39502	2.20311	0.0062718	0.191910	2.44752	R
716	2.49255	2.27267	0.0063046	0.219882	2.80436	R
717	2.60981	2.33243	0.0063656	0.277377	3.53786	R
718	2.68919	2.38006	0.0064352	0.309126	3.94310	R
719	2.74865	2.42729	0.0065222	0.321359	4.09951	R
720	2.82869	2.46993	0.0066154	0.358764	4.57714	R
721	2.86956	2.51237	0.0067214	0.357185	4.55752	R
722	2.93811	2.54820	0.0068208	0.389911	4.97563	R
723	2.98126	2.58524	0.0069325	0.396011	5.05410	R
724	3.01495	2.61702	0.0070354	0.397928	5.07916	R
734	2.87827	2.71441	0.0057140	0.163859	2.08864	R
735	2.92984	2.75764	0.0058669	0.172202	2.19529	R

736	2.96684	2.79628	0.0060145	0.170568	2.17478	R
737	3.03775	2.83131	0.0061567	0.206439	2.63251	R
738	3.08335	2.87178	0.0063299	0.211578	2.69851	R
739	3.09765	2.89641	0.0064398	0.201243	2.56699	R
740	1.78884	2.02294	0.0057256	-0.234104	-2.98405	R
755	1.87414	2.14822	0.0055409	-0.274074	-3.49294	R
770	1.42691	1.64909	0.0090269	-0.222181	-2.84334	R
776	2.50032	2.32596	0.0075484	0.174359	2.22688	R
777	2.59505	2.38604	0.0075629	0.209011	2.66949	R
778	2.68282	2.43876	0.0075968	0.244062	3.11730	R
779	2.75434	2.48893	0.0076472	0.265407	3.39014	R
780	2.82817	2.52583	0.0076953	0.302336	3.86209	R
781	2.87206	2.56631	0.0077587	0.305755	3.90607	R
782	2.91536	2.60660	0.0078325	0.308758	3.94480	R
783	2.95122	2.63884	0.0078991	0.312372	3.99132	R
784	2.99646	2.66950	0.0079685	0.326954	4.17802	R
785	1.55545	1.92346	0.0078132	-0.368014	-4.70176	R
786	1.95150	2.11982	0.0071211	-0.168325	-2.14871	R
804	1.64960	2.07536	0.0075688	-0.425757	-5.43782	R
805	2.02978	2.26872	0.0068492	-0.238942	-3.04922	R

824 1.66339 2.16966 0.0075773 -0.506265 -6.46615 R

825 2.14943 2.39323 0.0067845 -0.243806 -3.11107 R

894 2.02999 2.19095 0.0039842 -0.160959 -2.04888 R

R denotes an observation with a large standardized residual.

Appendix C

FLOW CHART AND EXPERMENTAL PROCEDURE

Flow chart

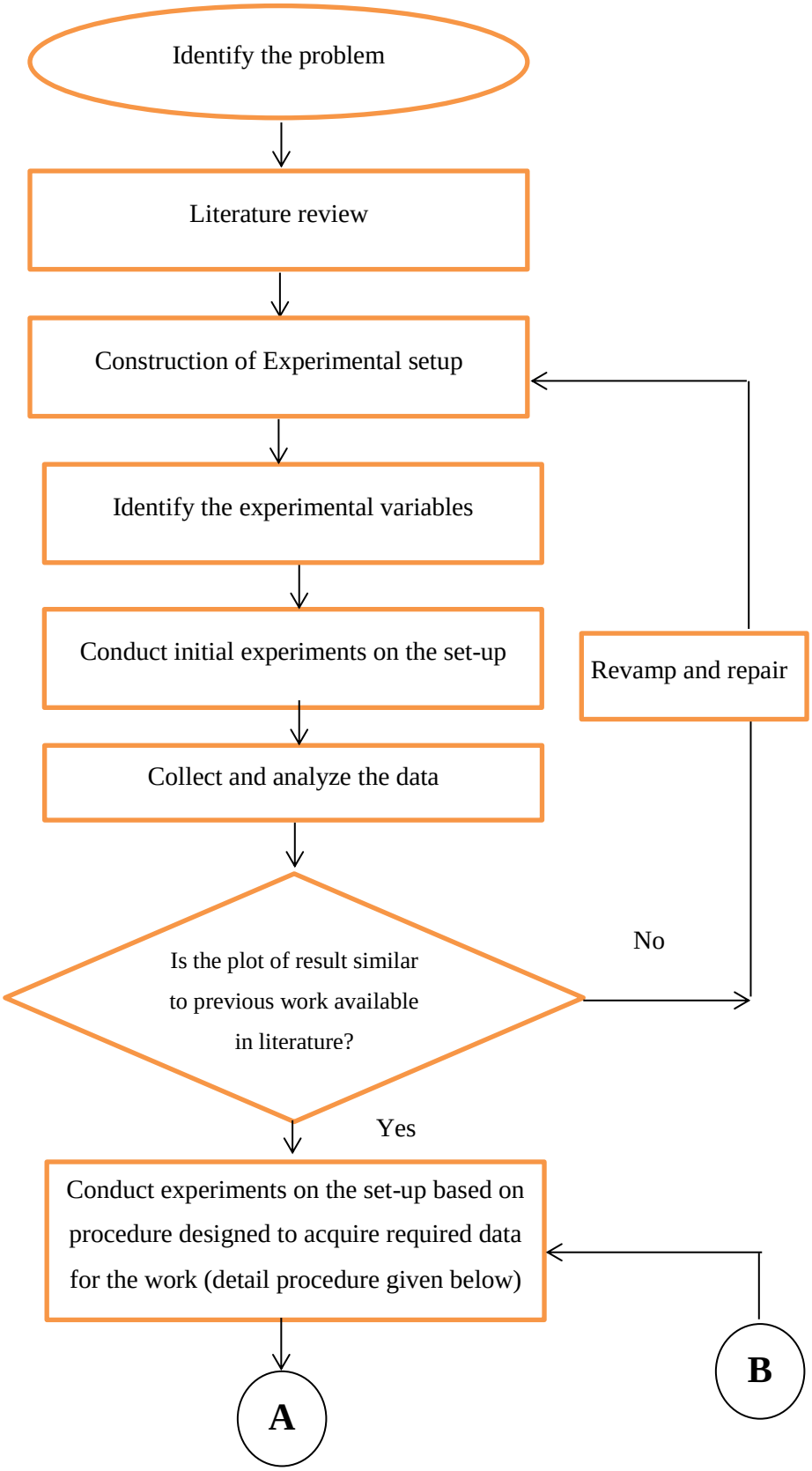
Identify the problem
Literature review
Construction of Experimental setup
Identify the experimental variables
Conduct initial experiments on the set-up
Collect and analyze the data
Is the plot of result similar to previous work available in literature?
No
Revamp and repair
Yes
Conduct experiments on the set-up based on procedure designed to acquire required data for the work (detail procedure given below)
A
B

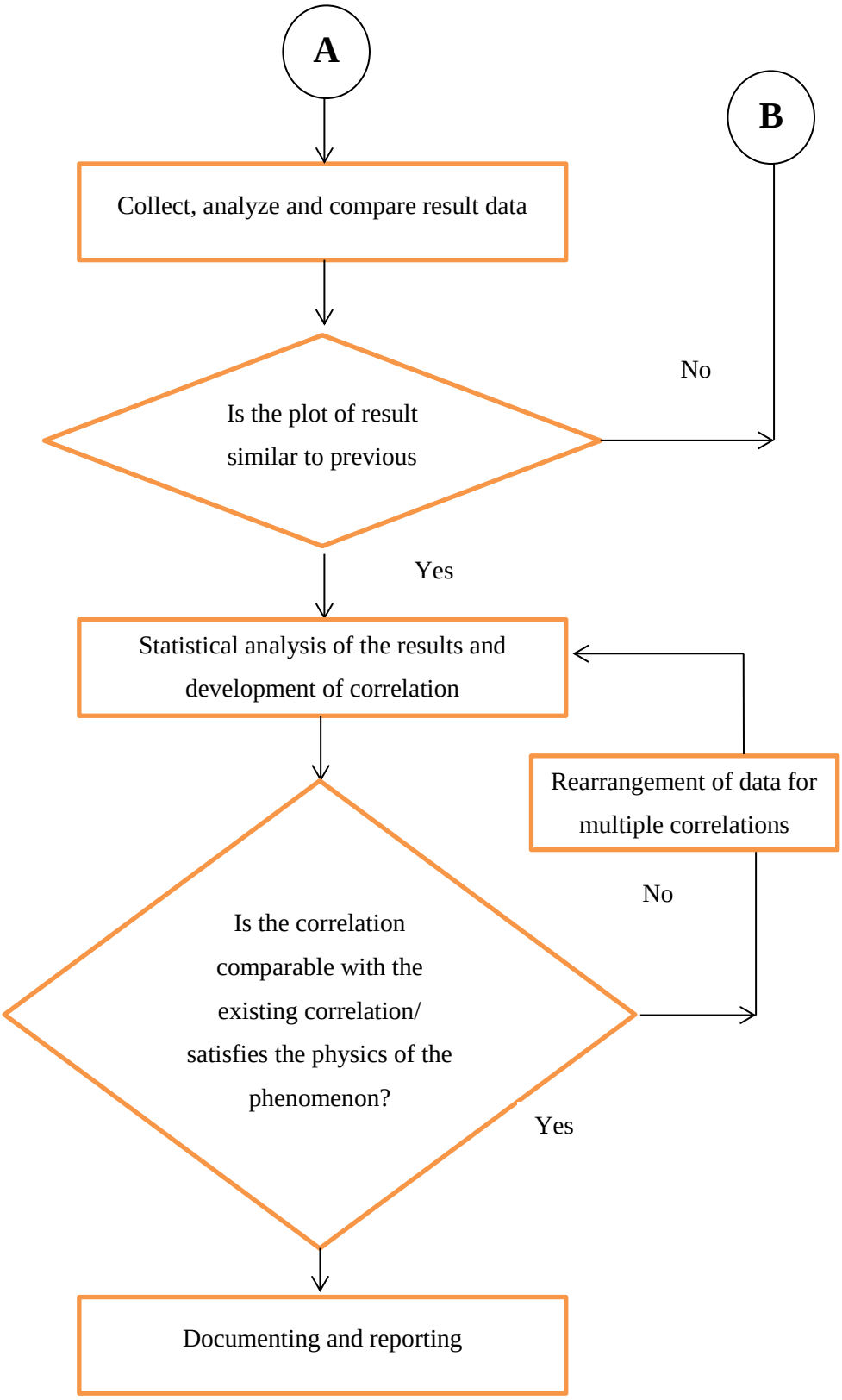
A
B
Collect, analyze and compare result data
Is the plot of result similar to previous
No
Yes
Statistical analysis of the results and development of correlation
Rearrangement of data for multiple correlations
No
Is the correlation comparable with the existing correlation/ satisfies the physics of the phenomenon?
Yes
Documenting and reporting

Experimental Procedure

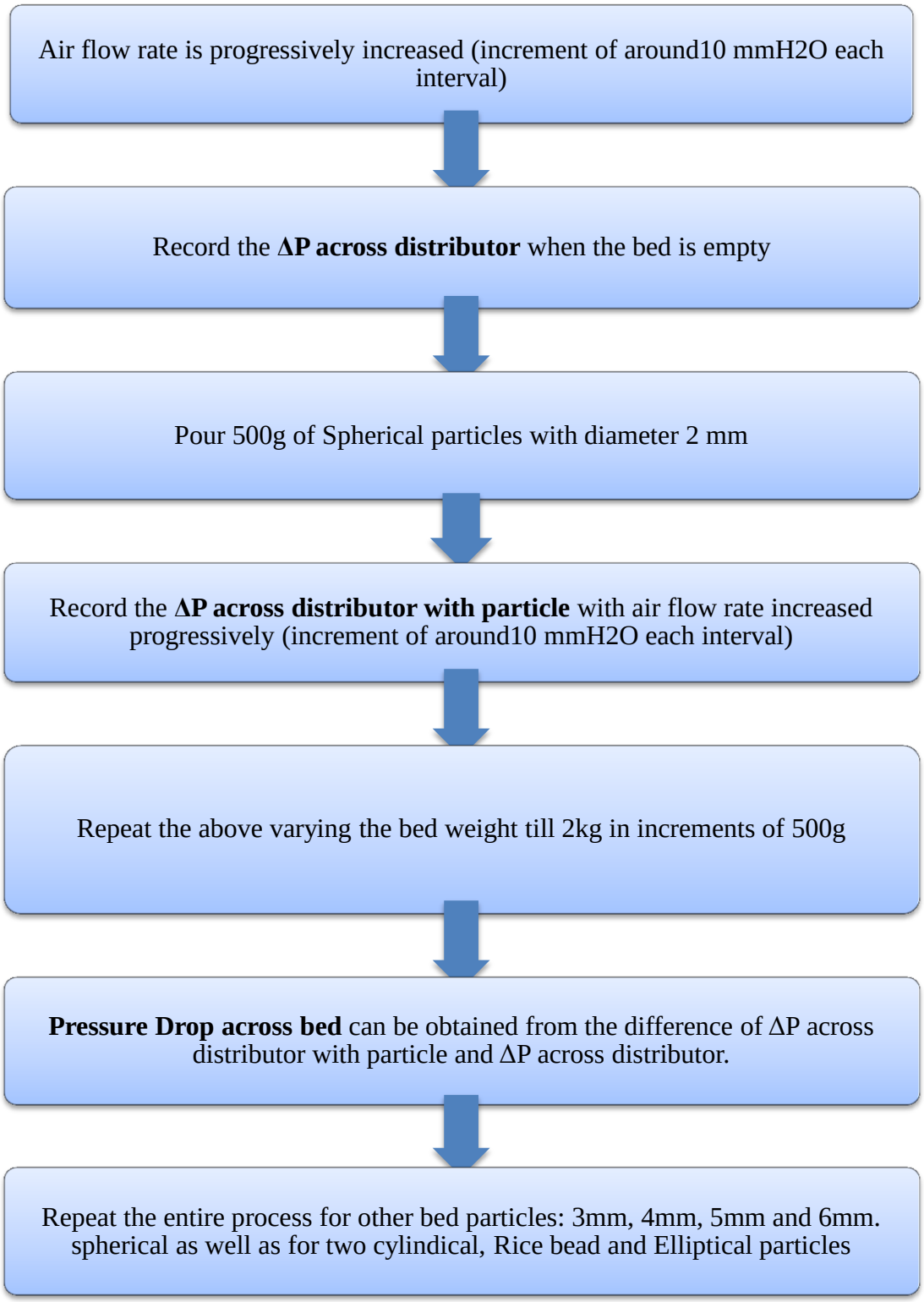

Appendix D

DESIGN DRAWINGS

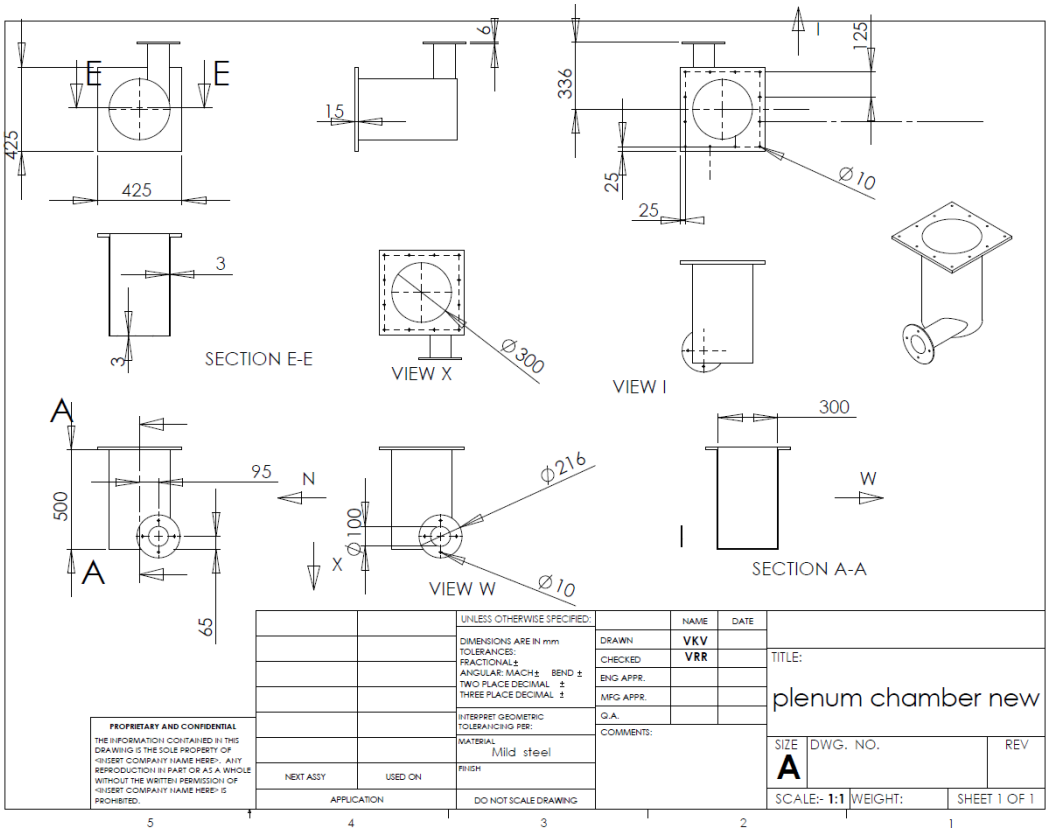

Figure D.1: Plenum chamber design drawing

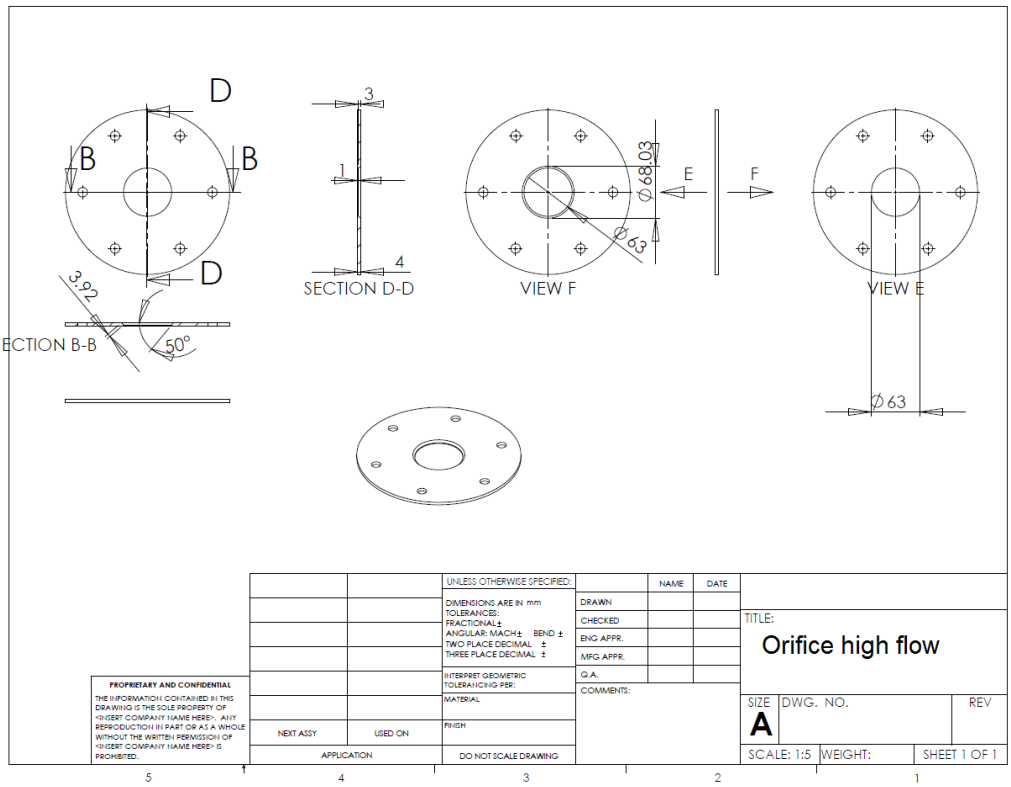

Figure D.2: Design drawing of high flow orifice plate

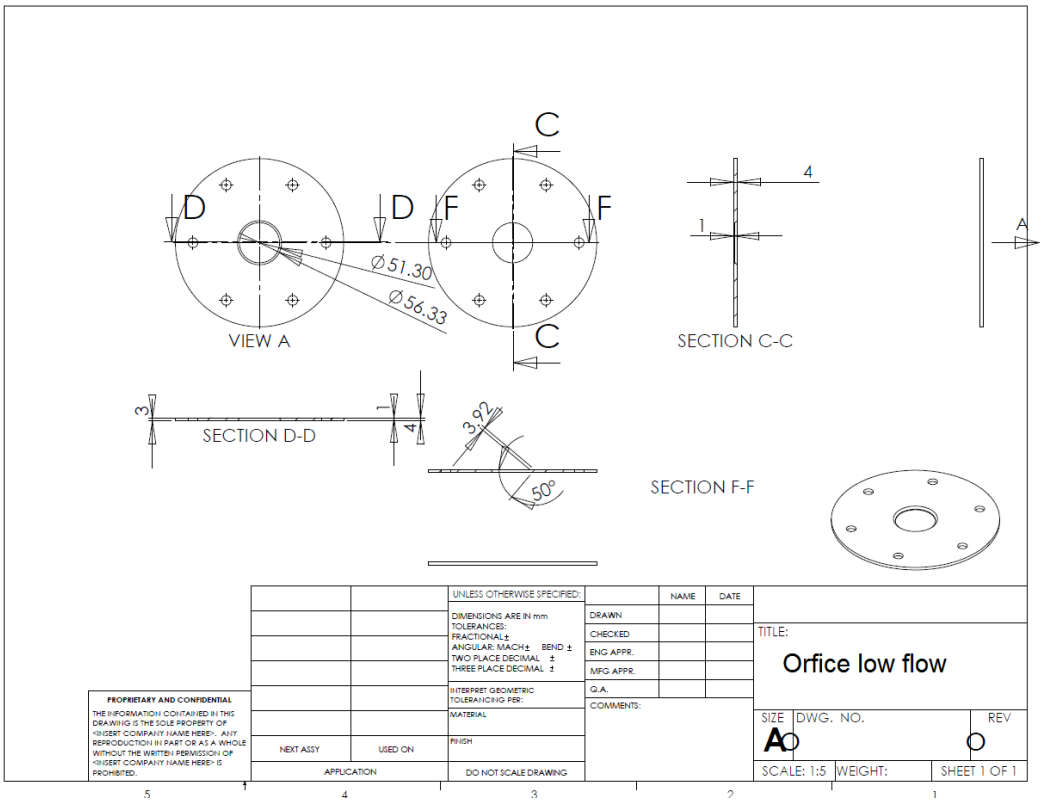

Figure D.3: Design drawing of low flow orifice plate

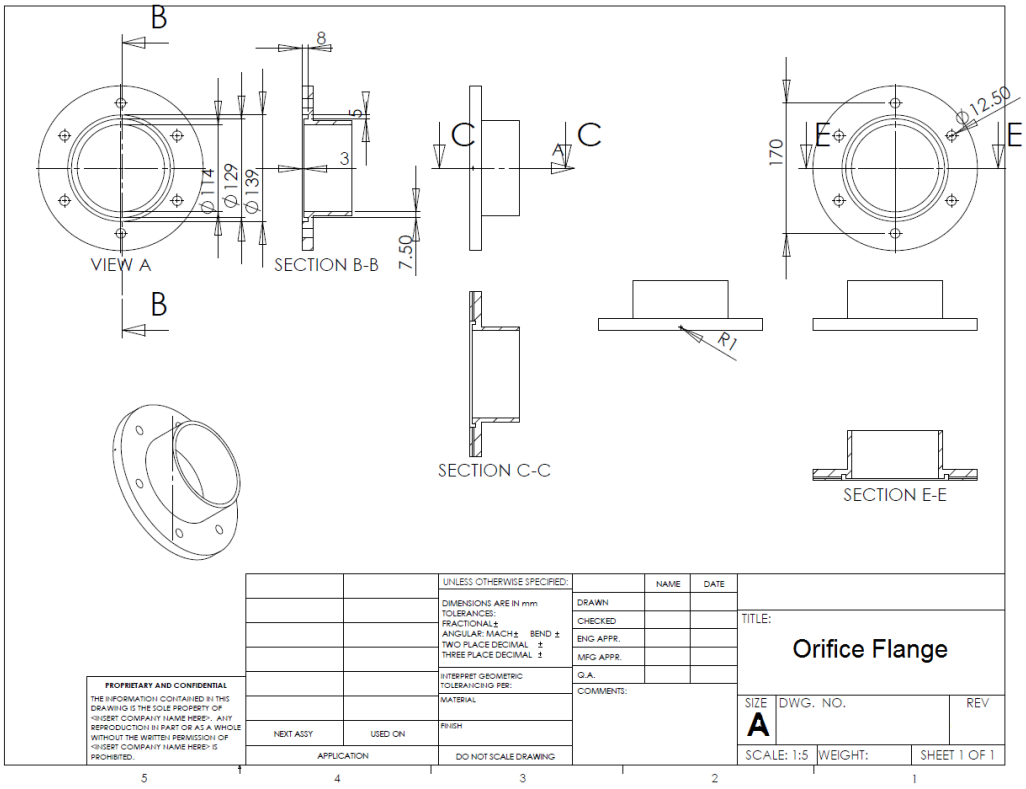

Figure D.4: Design drawing of flanges for orifice meter

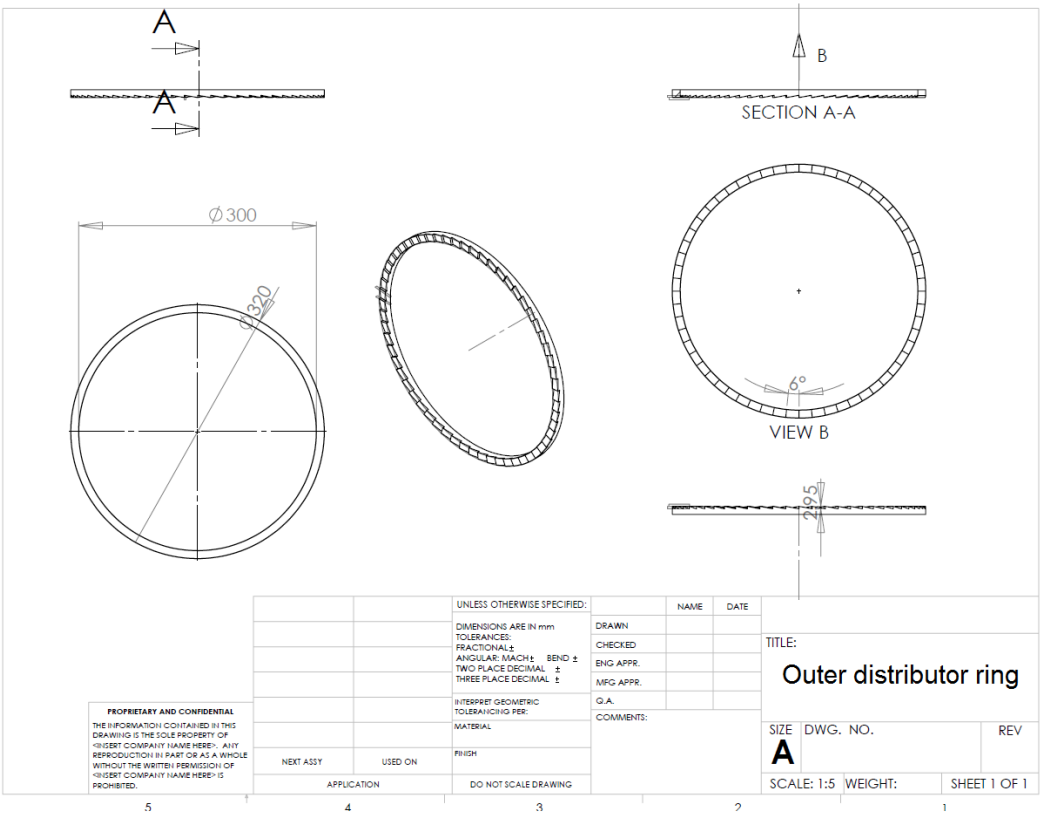

Figure D.5 : Design drawing of outer ring of annular spiral distributor

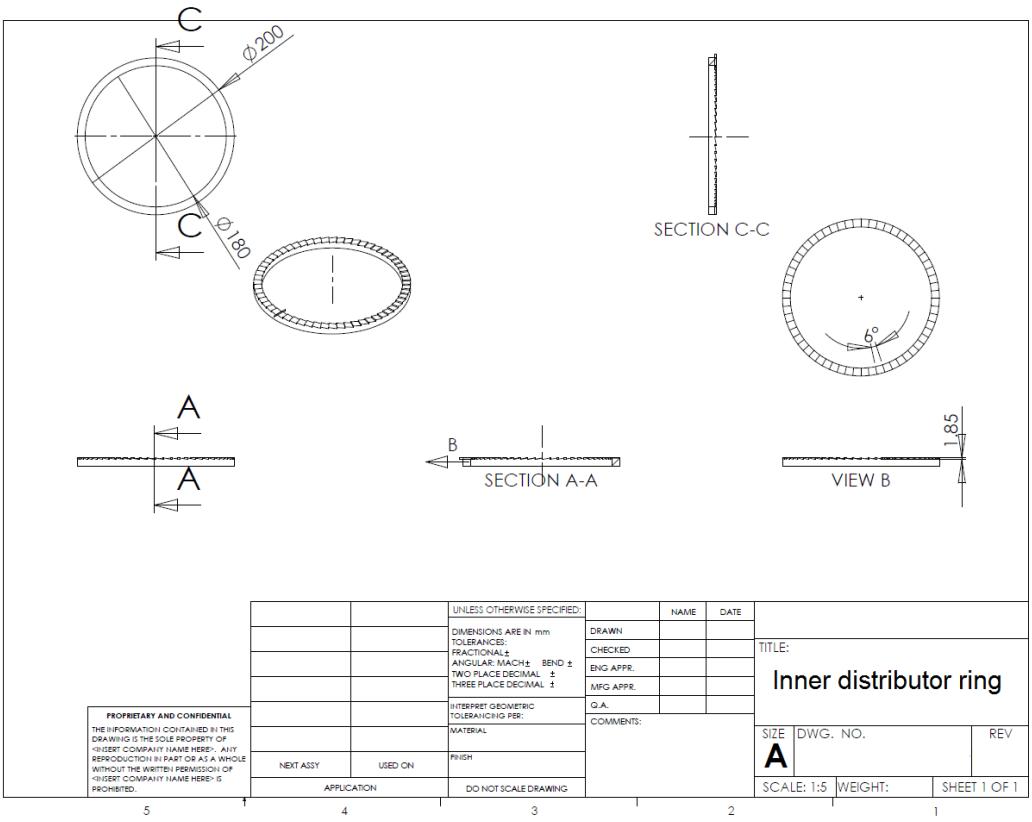

Figure D.6: Design drawing of inner ring of annular spiral distributor

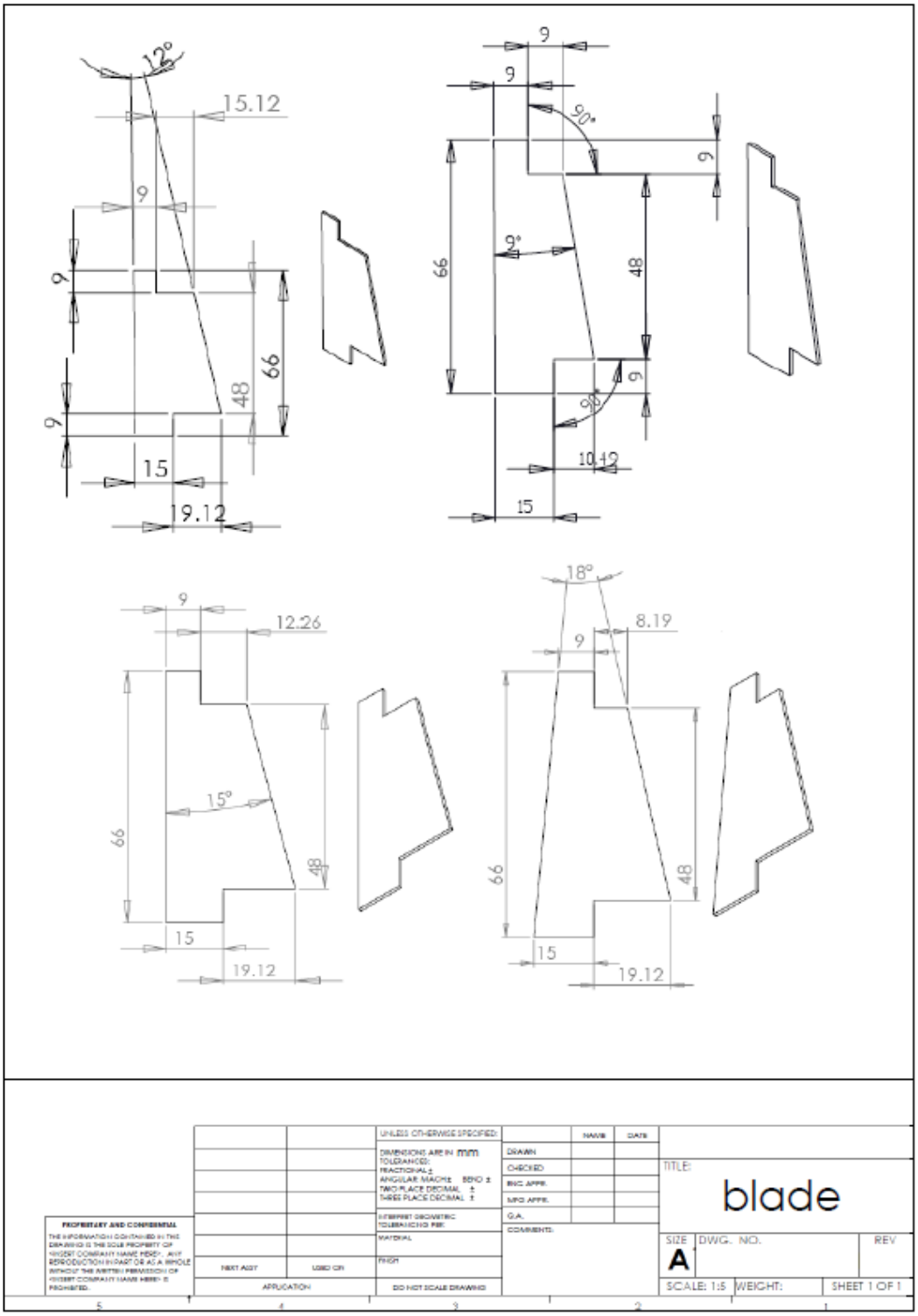

Figure D.7: Design drawing of blades with angles of overlap varying from 9 degrees to 18 degrees

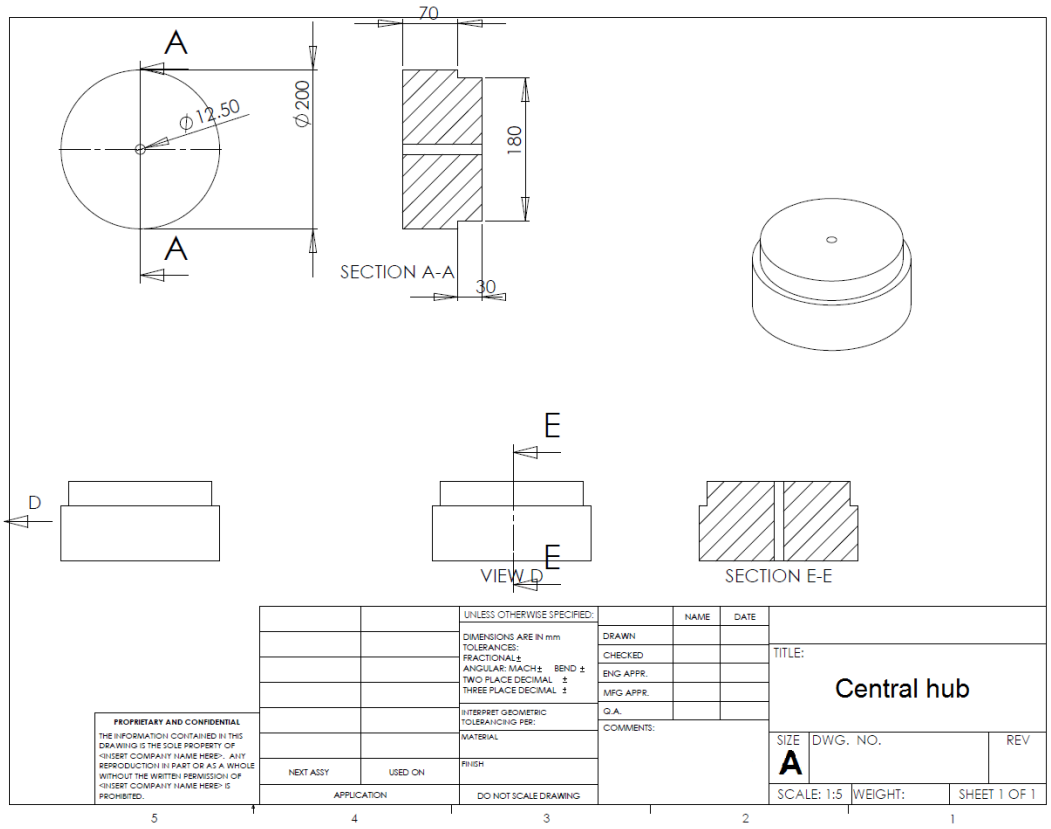

Figure D.8: Design drawing of central hub of annular spiral distributor

Appendix E

PROCEDURE FOR CALCULATING DENSITY OF THE BED PARTICLES AND TABULATION

Procedure for calculating desity of bed particles:

Mass of pycnometer = M_{py} (E.1)

Mass of pycnometer with particle = M_{py+p} (E.2)

Mass of pycnometer with water and particle = M_{py+p+w} (E.3)

Mass of pycnometer with water = M_{py+w} (E.4)

Mass of particles (M_p) in the pycnometer = (M_{py+p}- M_{py}) (E.5)

Volume of pycnometer, V_{py} = (M_{py+w} -M_{py}) /ρ_w (E.6)

where, ρ_w is density of water

Volume of void space V_o = (M_{py+p+w}-M_{py+p})/ ρ_w (E.7)

Volume of particle V_p = (V_{py}- V_o) (E.8)

Density of particle ρ_p = (M_p/ V_p) (E.9)

Table E-1: Observations for determining particle density

Type of particles	Mass of pycnometer = M_{py}	pycnometer with particle = M_{py+p}	Mass of pycnometer with water and particle = M_{py+p+w}	Mass of pycnometer with water = M_{py+w}	Mass of particles(M_p) in the pycnometer = (M_{py+p}- M_{py})	Volume of pycnometer V_p = (M_{py+w} - M_{py}) /ρ_w where, ρ_w density of water	Volume of void space V_o = (M_{py+p+w}- M_{py+p})/ ρ_w	Volume of particle V_p = (V_{py}- V_o)	Density of particle ρ_p = (M_p/ V_p)in kg/ m3
6S	212	348	458	462	136	0.25	0.11	0.14	971.43
5S	212	350	454	462	138	0.25	0.104	0.146	945.21
LC	212	500	620	462	288	0.25	0.12	0.13	2215.38
RB	212	332	452	462	120	0.25	0.12	0.13	923.08
Elli	212	350	444	462	138	0.25	0.094	0.156	884.62
2S	212	558	658	462	346	0.25	0.1	0.15	2306.67
4S	212	332	442	462	120	0.25	0.11	0.14	857.14
3S	212	338	458	462	126	0.25	0.12	0.13	969.23
SC	212	520	624	462	308	0.25	0.104	0.146	2109.59